INTERACTION STUDIES OF CHIRAL NON-STEROIDAL ANTI-INFLAMMATORY DRUGS WITH HSA PROTEIN USING CAPILLARY ELECTROPHORESIS FRONTAL ANALYSIS AND ELECTROKINETIC CHROMATOGRAPHY

By

Sinegugu Khulu

Submitted in fulfillment of the requirements of the degree of Master of Applied Science in Chemistry in the Faculty of Applied Sciences at the Durban University of Technology.

March 2015

Declaration

I, Sinegugu Khulu declare that this thesis is submitted for the degree of Master of Applied Science in Chemistry at the Durban University of Technology, and has not been submitted to any other university and no portion of this or any other closely related work is under consideration for publication elsewhere in any medium. All the work was done by the author, and all sources used or quoted to have been indicated and acknowledged by complete references.

Signed: [redacted] Date: 16/03/15

Student

Signed: [redacted] Date: 18/3/15

Supervisor

Signed: [redacted] Date: 16/03/15

Co-supervisor

Acknowledgements

To God - our father, all the glory belongs to him. I wish to extend my deepest gratitude to him for making this study a success, and for all the dedication and patience that I as a person developed during the course of the study.

My deepest gratitude also goes to my supervisor Prof. K. Bisetty, my co-supervisors Dr. P. Singh and Dr K. Suvardhan. Special thanks go to Mr. M.I. Sabela. Thank you for all the support, guidance and patience throughout my studies. Thank you for sharing your experiences in the field of computational and experimental sciences. To the electo-analytical laboratory technician Mrs Xhakaza, thank you for providing a friendly research foundation.

To my family, especially my parents, my fiancé, and my friends; thank you for all the love, moral support, motivation and always believing in me, which kept me going through the difficult times of the study.

Finally, my gratitude goes to all the sponsors, Durban University of Technology, National Research Foundation, Centre of High Performance Computing (CHPC) and the Omnia group for their financial support throughout the research.

Dedication

This dissertation is dedicated to my daughter Zibusiso Ntuli, my parents (Mr. Bhekinkosi J. Khulu and Mrs. Sibongile M. Khulu) who have always been my pillar of strength and support, my late sister Zanele Shabangu and my late aunt S'khumbuzo Shabangu, who took very good care of me during my early childhood, and my sister Nompumelelo Shabangu, who has always been my role model and source of inspiration; God bless you.

Abstract

Human Serum Albumin (HSA) predominantly found in the blood plasma proteins, acts as a carrier for many drugs. In the present work binding interactions of eight arylpropionate non-steroidal anti-inflammatory drugs (NSAIDs) were studied with Human Serum Albumin HSA using Capillary Electrophoresis (CE) under physiological conditions. The concentration of HSA was kept constant (525 μM) whereas the drug concentrations were varied between 50-300 μM in each case. The Frontal analysis (FA) and Capillary Zone Electrophoresis (CZE) modes of CE were applied together with a mathematical modelling of the experimental results with a view to obtaining pharmacokinetic properties of each drug. The binding order of the drugs to HSA were established with the three methods together with the mathematical approach. Our studies revealed the presence of more than one binding sites for some of the available drugs. Additionally, molecular docking studies were conducted to establish the binding conformations of drugs in the binding pocket of the HSA. A very good correlation between the computed binding energies (docking) and the experimental binding constants were observed throughout this study. The logK values for all eight drugs were ranging from 3.37 - 4.56 for FA, 3.16 – 4.39 for CZE, and 3.48 – 5.30 for computational studies.

LIST OF CONTENTS

APPENDICES

List of Tables

List of Figures

Research Outputs

Poster Presentation

Durban University of Technology

Institutional Research Day

November **2012**

Study of NSAIDs interactions with Human Serum Albumin by Capillary Electrophoresis Frontal Analysis and molecular docking.

Oral presentation

Durban University of Technology

Institutional Research Day

November **2014**

Robust evaluation of interactions between NSAIDs and HSA: Experimental and Computational approaches.

Publications under review

1. S. Khulu, K. Bisetty, P. Singh, M.I. Sabela and K. Suvardhan, Estimation of pharmacokinetic properties of NSAIDs to HSA protein using Capillary Electrophoresis Frontal Analysis and Capillary Zone Electrophoresis. *Talanta.*

2. S. Khulu, K. Bisetty, P. Singh, M.I. Sabela and K. Suvardhan, Conformational Changes on HSA, upon binding with NSAIDs: Computational and Experimental approaches. *Electrophoresis.*

CHAPTER 1

INTRODUCTION

1.1 Background of the study

Several therapeutic drugs with one or more chiral centres are administered and marketed as racemic mixtures owing to difficulties in their purification and stereoselective synthesis. In a stereospecific environment, the enantiomers show different pharmacological and pharmacokinetic properties. Therefore, considerable attention has been directed in the study of drug binding to proteins. It is one of the most significant studies in biomedical, biological and pharmaceutical sciences, where the protein is considered to play a vital role in binding with drugs (Millot 2003; Pîrnău and Bogdan 2008). What intrigued the drug-protein interaction study mostly is, its importance in the determination of the activity and outcome of a pharmaceutical drug entering the body. In order for one to be able to optimize the therapeutic dosage of an agent it is important to understand and know the extent of its drug-protein (Jia et al. 2002). Human serum albumin (HSA) protein is the most widely studied protein because it is the principal protein in the blood plasma occupying about 60% of the plasma. Due to its ease of isolation and purification, HSA has proven to be the most useful protein model for studies involving ligand-protein interactions. Additionally, HSA-drug interactions are known to control the drug delivery to the tissue receptors thus preventing the drug from being metabolized rapidly. Structural characterization and binding energies of the complexes are therefore the main features in the understanding of biological and pharmaceutical properties, since interactions happen *via* the binding sites of HSA (Deschamps-Labat et al. 1997; Pîrnău and Bogdan 2008; Wybranowski et al. 2008).

In binding studies, the binding constants of non-covalent molecular interactions are considered to be the most vital property, e.g. in drug development studies where measurements of binding constants between a drug and plasma are important. The free (unbound) drug concentration shows a good correlation to the pharmacological activity of the drug, and its concentration is also used in the determination of pharmacokinetic properties such as metabolism, renal excretion, and distribution volume (Shibukawa et al. 1999; Tanaka and Terabe 2002). However, it is essential to conduct in vitro drug-protein studies with a specific plasma protein component for a thorough interpretation of drug distribution in a particular protein since drugs are capable of simultaneously interacting and binding to different proteins.

1.2 Problem statement

Most patients who benefit from non-steroidal anti-inflammatory drugs (NSAIDs) suffer a few side effects e.g. gastrointestinal bleeding, though not clearly understood it tends to be associated with the dosage. It is therefore desirable to take the lowest effective dose to minimize the side effects, and studies of drug-protein interactions help in obtaining the concentration of an unbound drug which shows a good correlation to the pharmacological activity (Shibukawa et al. 1999). In drugs marketed as racemates the side effects are associated with the enantiomer that is not involved therapeutically (Somasundaram 1997). Enantiomeric separation studies therefore help in the separation of a racemic mixture and the pharmacokinetic properties of each enantiomer measured after interaction with the protein.

1.3 Study hypothesis

A variety of approaches have been applied over the years in drug-protein studies in biomedical and pharmaceutical sciences. However, Capillary Electrophoresis (CE) remains a unique technique, due to its powerful ability in determining the binding constants (Østergaard and Heegaard 2003). CE uses several application modes, and its separation is based on various physico-chemical properties. The separation depends on differences in migration of solutes in an electric field, with the driving forces being electrophoretic migration and electro-osmotic flow (EOF). In this study the different modes of CE will be employed because of its relative simplicity, high and unique separation efficiency, flexibility, short analysis times, small sample requirements and low consumption of reagents (low cost) (Artuki 1998; Blanco et al. 1998; Martínez-Gómez et al. 2007; Koppenhoefer et al. 1995; Suntornsuk 2010). In CE information such as unbound concentrations which can be extracted from experimental data help in the calculation of the binding affinities of drugs towards HSA. In this study binding constant “K” will be calculated for each drug using the data generated by both frontal analysis (FA) and capillary zone electrophoresis (CZE). NSAIDs occur as racemic mixture or pure enantiomers due to an asymmetric α-carbon that they bear (Blanco 1998). An Electrokinetic chromatography (EKC) method for separation of the enantiomers will be developed since the enantiomers tend to show different pharmacological and toxicological properties (Główka Karaźniewicz 2004). This will aid in obtaining pharmacokinetic data for each enantiomer.

On the other hand, computational chemistry has become an advantageous way in predictions of structural properties, and to give a better understanding of experiments. Accordingly, computational chemistry which applies chemical, mathematical and computer skills to find a solution to interesting chemical problems will also be implemented in this study. This work will include calculation of binding constants, binding energies, as well as in the prediction of the binding sites of HSA that NSAIDs bind to, and their extent of binding. Literature suggests that these drugs have high affinity towards site II, followed by site I of the HSA (Deschamps-Labat et al. 1997)

1.4 Aims and Objectives

Aim:

- The aim of this work was to study the binding of non-steroidal anti-inflammatory drugs with HSA protein.

Objectives of this study were to:

- investigate the interaction of some commercially available NSAIDs with HSA protein using Frontal Analysis and Capillary Zone Electrophoresis.
- develop an analytical method for the resolution of racemic drugs using Electrokinetic chromatography with cyclodextrin derivatives.
- perform docking and mathematical modeling of the experimental results with the view to obtaining pharmacokinetic properties.

1.5 Scope and overview of the dissertation

Chapter 1 is literature review containing a background on drug-protein interactions as well as chiral separation.

Chapter 2 describes the principles of capillary electrophoresis including instrumentation, electro-osmosis, electrophoretic mobility, factors affecting resolution and different modes of electrophoresis.

Chapter 3 discusses the mechanism of chiral separation in capillary electrophoresis using chiral selectors such as crown-ethers, antibiotics, proteins, micelles and cyclodextrins.

Chapter 4 covers a discussion of the binding of drugs to plasma proteins and the pharmacokinetic properties involved. The different types of proteins in which drugs can bind to along with their different binding sites with emphasis on the HSA protein, are also discussed.

Chapter 5 describes the experimental procedures, outlining the specifications for all instruments along with details of the chemicals and reagents used in this work.

Chapter 6 covers results obtained for the interaction of non-steroidal anti-inflammatory drugs with human serum albumin, including data generated by computational work, the three main sections are capillary electrophoresis-frontal analysis; capillary zone electrophoresis; and the molecular simulations of drug-protein interactions.

Chapter 7 presents a summary of the project with key results highlighted.

References are presented at the end of chapter 7

Appendices contain raw data on the experimental designs and calibration results including physical constants.

1.6 Drug –Protein interactions:

Non-steroidal anti-inflammatory drugs (NSAIDs) which are the drugs of interest for this study are widely marketed and applied as racemates. In general, binding of racemic drugs to HSA is stereo-selective due to the chirality of the protein itself. The stereo-selectivity may be due to the enantiomers of the racemic mixture preferring one of the binding sites of HSA as opposed to the others or both enantiomers having a high affinity toward the same binding site (Ohnishi et al. 2002; Zhivkova and Russeva 1998). The binding properties of enantiomers in a racemic drug differs, thus causing differences in their pharmacokinetic behaviour. In drug development studies, more emphasis is in studying the drug-protein binding interactions of each enantiomer to ensure safety in its clinical use. This interaction is however, a rapid and reversible interaction which should be analyzed in an environment that will not disturb the binding equilibrium. A variety of methods have been developed for this study over the years with some shortcomings (Shibukawa et al. 1999). Zvetanka and co-workers studied the binding of each enantiomer of ketoprofen (an aryl propionic acid NSAID) with HSA on site I&II as the major binding sites of HSA. High-Performance Liquid-Affinity Chromatography (HPLAC) based on the immobilized HSA chiral stationary phase was used for their study, where they reported both enantiomers of ketoprofen to have high affinity towards site I as compared to site II (Zhivkova 1998). In another study by Chuang and colleagues, interactions of ketoprofen with HSA were investigated using equilibrium dialysis and characterized by spectroscopic (UV absorption, fluorescence, and NMR) techniques. According to this study, the binding specificity of the aryl propionic acid switched from site II to site I upon esterification of the carboxyl group, as indicated by the inability of the methyl arylpropionate to displace the site II fluorescent probe, dansyl sarcosine (Chuang et al. 1999) and showed that ketoprofen tends to have high affinity for site I of the HSA. On the other hand lipophilicity is considered to be one of the physicochemical parameters contributing to the binding of drugs to protein. Deschamps-Labat and co-workers studied a relationship between lipophilicity and binding of 11 aryl propionic acid NSAIDs (Alminoprofen, carprofen, fenbufen, fenoprofen, flurbiprofen, ibuprofen, ketoprofen, piprofen, suprofen, and tiaprofenic acid) to HSA and their binding properties were studied by equilibrium dialysis *in vitro*, with the lipophilic factor being studied by reversed phase HPLC and results represented by a capacity factor (k').

A Scatchard plot was plotted for the compounds studied in consideration of the two binding sites characterized as high and low affinity constants K_1 and K_2 respectively. Their results showed that the hydrophobic interactions played an important part in the binding of NSAIDs with HSA, since a linear relationship was observed between lipophilicity and the binding parameters for all 11 drugs studied (Deschamps-Labat et al. 1997). Amongst other techniques applied in drug development micro-dialysis technique plays a unique role, especially in pharmacological, physiological and behavioural studies. By far, the technique has been successfully combined with HPLC for the interaction studies of drugs with HSA with the view to obtain binding parameters. Theory suggests that drug-protein interactions revealed that competitive binding of drugs exists when more than two drugs are used simultaneously. Hyphenation of micro-dialysis with HPLC makes it possible to do studies of competitive binding of drugs to HSA (Hailin et al. 1997). Qi and co-workers also showed that drug-protein interaction studies can be performed by spectroscopic methods (Qi et al. 2008). The investigation was based on the binding of rofecoxib (an NSAID) with HSA protein under physiological conditions using UV-vis absorbance and fourier transfer infrared (FT-IR) spectroscopy. The complexation of rofecoxib-HSA resulted in fluorescence quenching of HSA by rofecoxib and allowed for the determination of binding constants. The FT-IR spectra and UV-vis absorbance revealed that the change in protein secondary structures resulted from the drug binding to a number of amino acids found on the hydrophobic pockets of HSA. Furthermore, from the results obtained the thermodynamic parameters such as entropy change (ΔS) and enthalpy change (ΔH) were calculated. The latter and spectroscopic measurements showed that van der Waals interactions and hydrogen bonds were the driving forces that stabilized the rofecoxib-HSA complex. Lastly, the study also revealed the possibilities of the binding site of rofecoxib with HSA to be the same as that for warfarin's site I of HSA (Qi et al. 2008). High-performance liquid affinity chromatography with the aid of a zonal elution technique could also be used to identify the different binding characteristics of drugs with HSA. This is normally achieved by a stationary phase based on an immobilized HSA, especially in the studies of stereo-selective binding. In that case site markers could be used to determine the binding sites in which each enantiomer binds to the HSA. With the aid of zonal elution and mathematical approaches it is possible to determine the high and low affinity binding sites. This method is however not limited to HSA but could also be used to identify the binding sites of ligands on proteins as well (Hage et al. 1995; Zhivkova and Russeva 1998).

Ultracentrifugation, calorimetry, surface plasmon resonance etc., could be used for drug-protein binding studies. These techniques bear some disadvantages, for example in equilibrium dialysis ligands tend to be adsorbed on the dialysis membrane. Also, with ultra-filtration the binding equilibrium may be subjected to change during the separation process due to changes in the sample concentration during filtration, thus altering the free drug concentration. On the other hand ultracentrifugation and ultra-filtration have a similar problem of causing errors in the measurements of free drug. In ultracentrifugation this is due to back diffusion and sedimentation taking place during the equilibrium process. Calorimetry measurements unlike the other two provide sufficient information including enthalpy and entropy of the interaction, binding sites, and binding constants. However, it has major shortcomings in drugs with poor aqueous solubility since they have to match with the buffer (Jia et al. 2002; Shibukawa et al. 1999). Recently, chromatographic methods were widely used but affinity chromatography makes it difficult to measure compounds with more than 95% affinity and compound with less than 50% affinity.

CE however, remains a method of choice as it is more cost effective than the above mentioned methods, and uses less protein and smaller volumes of drugs resulting in higher sample throughput than HPLC (Jia et al. 2002).

1.7 Chiral Separation:

Many synthetic compounds such as drugs and biological compounds are chiral in nature. About 50% of these are marketed as racemic mixtures but usually only one enantiomer is responsible for the therapeutic action although in some cases both enantiomers, in a correct ratio, have the therapeutic effect. Due to some regulations on the purity of drugs by the food and drug administration, enantioselective synthesis and enantioseparation have become of great importance (Verleysen and Sandra 1998). Over the past decades, liquid chromatographic enantiomer separation was one of the most necessary research areas for the development of chiral drugs. Reversed phase enantiomer separation being the most convenient for biological samples of plasma or serum as compared to normal phase (Huang et al. 2009; Nagori et al. 2011). HPLC, CE and hyphenated systems have been also applied for analysis of such complex mixtures. These are however, generally based on UV detection or an expensive combination of spectrometry with nuclear magnetic resonance (NMR), infra-red (IR), and mass spectrometry (Huanga et al. 2003).

For separation of chiral compounds in HPLC various stationary phases which are normally bonded to silica are used and those usually include macrocyclic glycopeptides, cyclodextrins (CD), cellulose/amylase, and protein. The order of elution depends on the formation of temporary diastereoisomers caused by interaction with the stationary phase. A less diastereomer formed is eluted first, followed by stronger diastereomers. Additives, solvents and alteration of parameters like temperature and pH plays a significant role in increasing the resolution between the chiral compounds (Mannschreck and Kiesswetter 2005). Ye and co-workers developed a method for the enantioseparation of some chiral NSAIDs, using reversed phase-HPLC with hydroxypropyl-β-cyclodextrin (HP-β-CD) as a chiral mobile phase additive. In this study different parameters such as concentration of the CD, composition of the mobile phase and the pH effect were used to enhance the enantioseparation. NSAIDs as acidic analytes are strongly affected by the pH of the mobile phase, at lower pH they tend to have better resolution and longer retention times, and decreased retention times with an increase in pH (Ye et al. 2009).

CE was developed from the principles of the other traditional separation techniques including gel electrophoresis, gas chromatography (GC) and HPLC. In the case of CE, separation is based on the mobility difference of the analytes under an electric field occurring in a fused silica capillary capable of employing up to 800V/cm voltage. Fused capillary provides effective heat dissipation due to properties like large surface area to volume ratio. CE bears an advantage of requiring small samples and smaller amounts of background electrolyte (BGE) due to the small capillary dimensions. Furthermore, the technique has an on-column detection, a variety of operating modes and a very high separation efficiency with a theoretical plate being greater than 10 000 (Sunfornsuk 2007). CE bears the advantage of enantiomer determination directly from compound mixtures in aqueous solution. Specifically capillary zone electrophoresis (CZE) and micellar electrokinetic chromatography (MEKC) are most widely used methods for enantioseparation in CE (Lin et al.1998). CE separations have been successfully performedwith suitable chiral selectors such as protein and cyclodextrins (CDs). A pair of enantiomers have identical electrophoretic mobilities (μ_s) hence, Wren in 2001 proposed a model using CD as chiral selector and resulting in the formation of diastereomeric inclusion complexes with almost identical electrophoretic mobilities (μ_{CD}).

$$A(\mu_s) + CD \leftrightarrow ACD(\mu_{CD}) \qquad K_1 = \frac{[ACD]}{[A][CD]} \qquad 1.1$$

$$B(\mu_s) + CD \leftrightarrow BCD(\mu_{CD}) \qquad K_1 = \frac{[BCD]}{[B][CD]} \qquad 1.2$$

For enantioseparation to occur, it is important that the electrophoretic mobilities for both A and B inclusion complexes has different values as well as K_1 and K_2 (Tanaka and Terabe 2002). Normally to achieve the separation of chiral drugs, both neutral and charged cyclodextrins are employed as chiral selectors since they were found to be the most powerful and versatile selectors with a broad spectrum (Schmitt et al. 2009). This is due to their physico-chemical properties such as low absorption in the UV region, having good solubility in aqueous buffers, commercial availability in native and derivatized forms (Abushoffa et al. 2002; Aturkiet al. 1998). This has however been achieved by a direct method in which the chiral selector is added to the background electrolyte. These are cyclic oligosaccharides consisting of 6, 7, or 8 D-(+) glucose units, linked by α 1,4 bonds include γ, and β-cyclodextrin. CDs play a key role in chiral resolution. In order to improve their poor solubility and to alter their enantioselective capacity methyl, carboxymethyl or hydroxypropyl derivatives are used with derivatization in the 2, 3, or 6 positions. Enantioselective recognition is explained by interactions between CDs (which have chiral centers) and the guest enantiomer (Główka and Karaźniewicz 2004).

CHAPTER 2

PRINCIPLES OF CAPILLARY ELECTROPHORESIS

In this section an overview of CE and its principle of operation is presented. The important instrumental aspects along with the different modes of detection relevant to analytical considerations are highlighted.

2.1 Introduction to electrophoresis

Capillary electrophoresis (CE) was developed from a group of related techniques such as HPLC and gel electrophoresis. It is a highly influential analytical technique with a major importance in drug discovery because of its unique resolving mechanism, efficiency, speed, versatility, rapid method development and simplicity (user friendly) (AbouI-EneinandAli 2000; Chankvetadze 1997; Marín and Barbas 2004; Suntornsuk 2010). The CE separations depend on the difference in migration of solutes in an electric field caused by the usage of relatively high voltages thus generating an electro-osmotic flow (EOF), and an electrophoretic flow of a BGE ionic species within the narrow-bore background electrolyte filled capillaries (Beckman Coulter 2011). The high electrical resistance provided by the silica capillary provides transparency in the UV region, allows the usage of high electric fields (100 to 500V/cm) with very low heat generation. The use of high electric fields results in shorter analysis times and higher efficiency and resolution. In addition, the large surface area-to-volume ratio and good thermal conductivity provided by the capillary effectively provides heat dissipation transparent in the UV region (Tagliaro et al. 1998). It is evident that components of CE play a critical role in micro-separations.

2.2 Instrumentation

A basic scheme of the CE instrumentation is shown in Figure 2.1 consisting of an autosampler, two electrodes (the anode and a cathode), a fused-silica capillary (20–100 mm I.D., 20–100 cm length) consisting of a viewing window aligned to the detector, a voltage power supply (up to 30 kV) operated in either positive or negative polarity, two buffer reservoirs, an online detection system (ultraviolet (UV)/diode-array, or fluorometric or electrochemical detector) or external detectors such as the mass spectrometer (MS), and a data output and handling device.

Each end of the capillary is placed in the buffer reservoirs which contain the same BGE filled in the capillary; the electrodes at each end of the capillary (anode on the injection side and cathode on the other) function to make an electrical contact between the high voltage and the capillary (Beckman Coulter 2011; Suntornsuk 2007; Tagliaro et al. 1998).

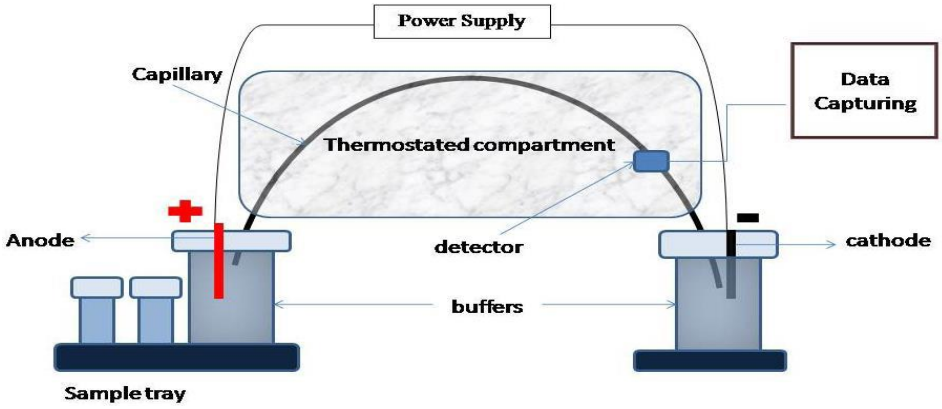

Figure 2.1: Scheme of Capillary Electrophoresis system

2.2.1 Principles of operation

The sample is introduced into the capillary filled with BGE usually at the anode by either hydrodynamic or electrokinetic injection. With buffer reservoirs on each end, an electric field is applied which results in a separation based on the migration of solutes. The solute migrations depend mainly on their sizes, degree of ionization, their charges as well as the dielectric constant of the BGE. As soon as the analytes are introduced into the capillary, voltage is applied causing them to move through the capillary by the electrophoretic mobility and electro-osmotic flow (EOF). Optical detection is done at the opposite end of the capillary which has an optical window aligned with the detector (Suntornsuk 2007; Tagliaro et al. 1998).

2.2.2 Basic components

2.2.2.1 Capillary

At present, the fused silica capillaries are widely used due to the essential properties which include high temperature conductance and transparency over a wide range of an electromagnetic spectrum. A small portion of the silica coating is chipped off to form a detection window aligned to the detector. Another advantage of using fused silica is that it is easy to use, with small diameters of few micrometres (typically 50 μm internal diameter) which help in facilitating heat control.

Capillary lengths vary with different applications, with the effective length ranging from 20-50 cm. In most cases it is essential to regenerate the surface by preconditioning the capillary before analysis (Sanchez-Vega 2005).

2.2.2.2 Detector

The CE instrument uses UV detection either by means of a scanning UV detector or Diode Array Detector–DAD (UV detector which provides a spectrum). UV detection is widely used as a universal detector due to its universal detection nature. For peptides and carbohydrates the use of phosphate and borate buffers are necessary, since they nominally absorb in the UV range making it possible for these compounds to be detected (Laurer and Rozing 2010). However, CE also provides separation of analytes that do not absorb in the UV region, in such cases an indirect method is employed whereby a UV absorbing species (chromophore) is added to the buffer. The chromophores are added in equal amounts to provide constant absorbance. Alternatively, a fluorescence detector is used for the non UV-absorbing species (Suntornsuk 2010). Species that neither absorb fluorescent nor UV radiation, may be derivatized so that they are in a detectable or UV action form (Suntornsuk 2007).

2.2.2.3 Power supply

Commercially available CE has a direct current power supply which entails a ramp-up power mode to help provide a smooth baseline. It takes a few seconds to reach the desired voltage. The current power supply can reverse polarity, by switching from cathode to anode. This is a user friendly approach for sample introduction on the cathodic end as it is done without changing the on-line detector. In general, the power supply can provide high voltages up to 30 kV, which generates electro-osmosis and electrophoretic flow of charged species and electrolytes through the capillary. For good reproducibility of migration times, it is recommended that the same voltages are applied for the entire analysis (Beckman Coulter 2011; Zaidi 2011).

2.3. Injection modes

In CE, small amounts of a sample ranging to nanoliters are injected. The sample is injected into a capillary either by hydrodynamic injection or electrokinetic injection. Electrokinetic injection is done by replacing the buffer vial at the injection end of the capillary with a sample vial and applying a voltage for a certain period.

Normally, the injection volume is about 3-5 times lower than the separation voltage. In this type the injection the sample enters the capillary through a pumping action and the migration of the EOF. Hydrodynamic injection is the most commonly used method for injection into the capillary. It could be performed in three ways, either by applying pressure at the injection point of the capillary, applying vacuum at the exit end of the separation capillary, or by siphoning action described as the elevation of the sample vial (inlet) relative to the exit vial. (Laurer and Rozing 2010; Suntornsuk 2007). Figure 2.2 below illustrates the above explained methods of sample injection in CE.

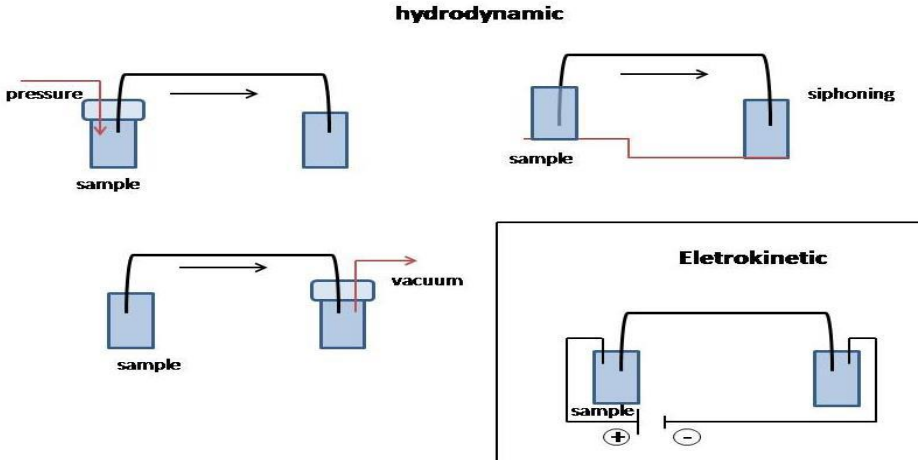

Figure 2.2: Sample injection methods (Laurer and Rozing 2010)

Electrokinetic injection is an important aspect in Capillary Gel Electrophoresis, whereby the polymeric sample becomes too viscous to be introduced via hydrodynamic injection, and thus requires a high voltage in order to be migrated through the capillary (Laurer and Rozing 2010).

2.4 Analytical Considerations

Capillary Electrophoresis (CE) provides both qualitative and quantitative information about the analytes. In qualitative analysis, analyte peak identification is done on the electropherogram. The easiest way to identify the peak(s) is to compare the migration times of the unknown peaks with that of a known compound (standard); however this is not always a reliable way for peak identity and purity.

A confirmation of this method includes comparing the ratio of the absorbances at different wavelengths in the sample with the ratio in suspected compounds (Xu 1996).

On the other hand, quantitative analysis provides information about the analyte concentration in a sample. Quantification in CE requires some parameters to be optimized for excellent resolution and separation. These parameters include capillary dimensions, voltage supplied, ionic strength, pH effects, sample matrix effect, sample preparation, estimation of impurities, limit of detection, internal calibration, external calibration and the range of linearity and reproducibility (Xu 1996). Factors affecting resolution are discussed in details in section 2.7.

2.5 Electro-osmosis

Electrophoresis is defined as the difference in the migration of electrically charged species when dissolved in an electrolyte through which an electric field is passed (Xu 1996; Zaidi 2011). The rate of migration as well as the direction of migration is determined by their charges. As the ions migrate towards the outlet of the separation capillary, cations are attracted towards the negatively charged electrode (cathode) while anions are attracted by the positively charged electrode (anode), and neutrals not attracted by either of the electrodes (Xu 1996). A fundamental process that drives CE is electro-osmosis; this is a phenomenon that results from the surface charge on the wall of the capillary. Capillaries normally used in the CE are made of fused silica thus resulting in the inner walls of the capillary yielding the ionization of silanol groups. The silanol groups (-SiOH) produces hydrogen ions (H^+) into the background electrolyte leaving the inner walls negatively charged (SiO^-) even at low pH; the positive ions in the electrolyte are attracted to the walls thus causing double ionization and forming a double layer. At low pH, the ionization is low and at high pH the ionization is high, the same goes for the EOF. Controlling the EOF can considerably influence the efficiency and selectivity of a separation, since EOF is a main driving force in CE. EOF however, has some factors that affect it such as the electric field, pH, and concentration/ionic strength of the BGE, additives, temperature, and capillary coatings (e.g. silanol groups). The EOF enables the simultaneous analysis of cations, anions, and neutral species in the same analysis (Suntornsuk 2007).

The magnitude of electro-osmosis flow (EOF) can be defined by:

$$v_{eo} = \frac{\epsilon\zeta}{4\pi\eta} E \qquad 2.1$$

Where ϵ is the dielectric constant, η is the viscosity of the buffer, and ζ isthe zeta potential measured at the plane of shear close to the liquid-solid interface.

Zeta potential is dependent mainly on the electrostatic nature of the capillary walls where there is a build-up of counterions near the surface to maintain charge balance from a diffuse double-layer. To a small extent, it is dependent to the pH of the electrolyte. From the neutral to alkaline pH range, the EOF is sufficiently stronger than the electrophoretic migration such that all species are swept towards the cathode. The elution order of migration for a positive polarity system are cations, neutrals and then anions. Cations travel the fastest because the electrophoretic attraction favours the cathode and also the EOF is towards the cathode, neutrals are carried by the velocity of the EOF, and the anions migrate slowly because they are attracted to the anode but are still migrating towards the cathode due to the EOF. At lower pH where the EOF is very low, both cations and anions can still be measured but they are unlikely to be measured in the same run. For anions, the polarity needs to be reversed so that the anode could be behind the detection window (Frazier et al. 2000; Tagliaro et al. 1998; Xu 1996).

In order to ensure complete ionization the electrolyte pH should be at least two units above or below the *pKa* of the analyte. However, at high pHs the EOF is great and migration is fast and this could result in incomplete separations. In electrically driven systems, the driving force of the EOF is equally distributed along the entire length of the capillary, as a result there is no pressure drop and the flow velocity is the same across the entire tubing diameter except very close to the wall where the velocity again approaches zero as can be seen in Figure 2.3.

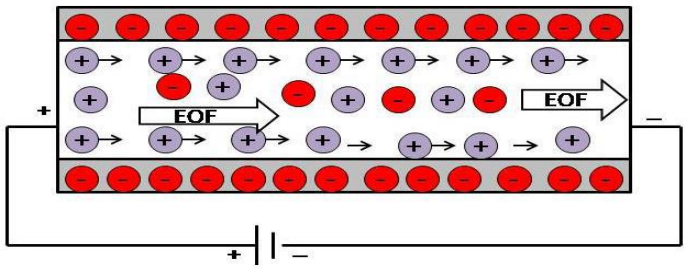

Figure 2.3: Illustration of an EOF upon application of an electric field

The velocity profile of EOF is normally said to be independent of the diameter of the capillary; however it can be disturbed if the internal diameter is too wide. This is because the surface tension then becomes inadequate to evenly pull the middle portion of the liquid at the velocity generated on the walls.

2.6. Electrophoretic mobility

The CE system's efficiency, especially CZE uses the following fundamental principles of electrophoresis and electro-osmosis:

(I) The basis of CE said to be on the difference in the solutes migration velocity when an electric field is applied. The migration velocity, v_{ep}, described as:

$$v_{ep} = \mu_{ep} E = \mu_{ep} \frac{V}{L} \qquad 2.2$$

Where μ_{ep} is the electrophoretic mobility of an ion, *E* being the applied electric field, V being the applied voltage and L is the effective length of the capillary.

(II) The mobility of an ion is related to the electric field experienced by a charged molecule or particle when it is frictionally dragged through a medium. The electrophoretic mobility is described as:

$$\mu_{ep} = \frac{q}{6\pi\eta r} \qquad 2.3$$

where q is the charge of an ion and r the radius of a hydrated ion. This equation however proves that the highly charged analytes have high mobilities.

(III) The time it takes for an ion to reach the detector is referred to as migration time, t, and is defined as:

$$t = \frac{L}{v_{ep}} = \frac{L^2}{\mu_{ep} V} \qquad 2.4$$

It is however a quotient of migration distances and velocity.

(IV) Peak dispersion σ^2, which results from the molecular diffusion which takes place as the solute migrate through the capillary, is calculated as:

$$\sigma^2 = 2Dmt = 2Dm \frac{L^2}{\mu_{ep} V} \qquad 2.5$$

Where Dm = the solute's diffusion coefficient cm^2/s.

(V) The efficiency is given as:

$$N = \frac{\mu_{ep} V}{2Dm} \qquad 2.6$$

Equation 2.6 shows that macromolecules with smaller diffusion coefficient, D, have a higher number of theoretical plates. Moreover, the use of higher voltages will also give greater efficiencies by means of decreasing the separation times.

(VI) CE also yields good separation of small molecules and resolution between two species is:

$$R = \frac{1}{4}\frac{\Delta \mu_{ep}}{\bar{u}_{ep}} \qquad 2.7$$

Where $\Delta\mu_{ep}$ is the difference in electrophoretic mobility between the two species, $\bar{u}_{ep}$ is the average electrophoretic mobility of the two species and *N* is the number of theoretical plates (Beckman Coulter 2011; Laurer and Rozing 2010; Zaidi 2011).

2.7. Factors influencing resolution

Capillary dimensions: Changing the length and diameter of the capillary does affect the separation of compounds in a sample. Increasing the length of the capillary leads to increased migration times and thus longer run times, which results in small sample throughput for the day. However, this normally increases the resolution and results in lower currents being generated. On the other hand, increasing the capillary diameter increases the current and internal temperature gradients which in turn decrease the resolution. Capillaries with larger internal diameters allow for better mass loading as well as a better signal-to-noise ratio, thus resulting in a good baseline (Zaidi 2011).

Voltage effects: Normally increasing the voltage results in a better resolution, however, using very high voltages is not encouraged as it leads to increased current flow through the buffer and additional internal heating of the buffer. The additional heating, well known as joule heating, alters the EOF and the mobilities of solutes therefore usage of very high voltages is not encouraged. Optimum resolution is obtained by increasing the voltage up to the point below the joule heating (Zaidi 2011).

pH effects: Optimization of pH is of great importance in quantification as it alters things like the EOF, resolution, selectivity, and the peak shape. The EOF is high at high pH and low at low pH; the others depend mainly on the types of compounds under investigation (Swearingen 2004; Pai and Liu 2002).

Ionic strength: Increased ionic strength results in better resolution, peak efficiency and shape, and sensitivity since better focusing is obtained. With increased ionic strength heat/current is also increased therefore it would be advantageous to limit the ionic strength in order to obtain optimum results (Blanco et al. 1998; Yi-Fen andChuen-Ying 2002).

Capillary temperature effects: By altering the capillary temperature often enough, it changes the viscosity and pH of the background electrolyte (BGE) (Fillet 1999). Increasing the temperature decreases the background electrolyte BGE viscosity and therefore, results in a slight decrease in migration times of the analytes. In cases like enantiomeric separations where CDs are used as chiral selectors, the analyte's affinity for the CD becomes altered as well, this means that there is a decrease in stability constant of the inclusion complex and thus an improvement in resolution of the enantiomers and vice versa (Blanco et al. 1998).

2.8 Different modes of electrophoresis

CE comprises of a family of techniques with different operating and separation characteristics making it a more versatile technique being able to analyse a wide range of analytes. The techniques are:

2.8.1 *Capillary Zone Electrophoresis (CZE)*

This is regarded as the easiest mode of CE also referred to as the partial filling mode, whereby the capillary is firstly filled with an electrolyte and then the sample is introduced at the anode. An electric field is then applied causing separation as the analytes will migrate at different velocities (apparent mobility) due to their charges and sizes since CZE's separation is based on mass-to-charge ratio and electrophoretic mobility being governed by the charge/size ratio. The small and highly charged molecules migrate faster than the large and less charged. Regardless of their electrophoretic mobility, the EOF is highly responsible for their movement through the capillary. The EOF always travels to the detection point and normally over powers the electrophoretic mobilities since it is normally greater than them.

Neutral molecules cannot be separated because they migrate at the velocity of the EOF. To control the separation, it is important to optimize the EOF and the mobilities since the separation principally relies on the pH controlled dissociation of acidic groups on the solute or protonation of basic groups on the solute which then affects the EOF. CZE is widely employed in the separation of proteins and peptides but however has one limitation which is electrostatic binding of cationic substances to the walls of the capillary. This disadvantage is observed greatly in the analysis of protein when the separating buffer has a pH below the *pKa* of the protein. This can be overcome by operating at least two pH units above the *pKa* of the protein. Other applications for the CZE mode include the separation of inorganic anions and cations such as those normally separated by ion chromatography, small molecules such as pharmaceuticals can also be separated provided they are charged (Beckman Coulter 2011; Główka and Karaźniewicz 2004; Tagliaro et al. 1998).

2.8.2 *Capillary Gel Electrophoresis (CGE)*

This is an adaptation of traditional gel electrophoresis into the capillary. It is mostly used for the separation of molecules such as protein and nucleic acids based on their size. In order for the separation to be feasible the molecules have to be denatured using sodium dodecyl sulfate (SDS) and passed through a suitable polymer which acts as a molecular sieve making it easier for smaller molecules to migrate through the polymer in contrast to larger ones. CGE is a very useful technique for separations of large biological molecules which have similar electrophoretic migration due to their similar charge-to-mass ratios which could not be varied and be resolved according to size without denaturing. The gels however suppresses the EOF, reduces the solute diffusion rate and also the adsorption of the solute to the walls of the capillary and therefore increasing efficiency. This mode is greatly applied to proteins, DNA analysis (Laurer and Rozing 2010).

2.8.3 *Capillary Isoelectric Focusing (CIEF)*

CIEF is however, referred to as a high resolution technique for the separation of amphoteric substances such as proteins, peptides, and amino acids based on their isoelectric points (pI) rather than their apparent mobilities. Like Capillary Gel Electrophoresis, it uses the application of gel. CIEF employs ampholytes with both basic and acidic nature being able to have pI values that last the desired pH range between the anode and the cathode for the analysis.

Its principle of separation is based on the filling of the capillary with a mixture of ampholytes and analytes forming a pH gradient where the acidic solution is at the anode and basic at the cathode. When the electric field is applied the ampholytes and solutes are migrated through the capillary to the point where they reach their isoelectric points. Simply put if the analyte has a net charge that is positive it is mostly likely to migrate towards the cathode. At their isoelectric point (pI) migration stops and solute focused into a tight zone, and the zone is moved to pass through the detection point by means of pressure or chemical means (Gübitz and Schmid 2000; Beckman Coulter 2011*).*

2.8.4 *Capillary Isotachophoresis (CITP)*

CITP is referred to as a moving boundary technique which uses two buffer systems that forms a state in which solutes can migrate as connected, but separate bands with identical velocities. This mode is capable of analyzing both anions and cations in a single run. Its principle of operation is based on the migration of solutes between the leading electrolyte and a trailing electrolyte without an EOF. This means that the capillary is filled with the leading electrolyte and the trailing on each end of the capillary, and the separation is based on differences in velocities of analyte ions within the sample zone. Taking for an example analysis of cations, the leading electrolyte should have a cation with an effective mobility higher than that of cationic analytes. When the electric field is applied the analytes will start to migrate in the direction of the cathode since they are cationic, but because the leading electrolyte has the highest mobility, it moves faster than the analyte ions followed by solutes with higher mobility. The trailing electrolyte has a lower mobility than ions of the sample (Gübitz and Schmid 2000; Laurer and Rozing 2010; Xu 1996).

2.8.5 *Electrokinetic Chromatography (EKC)*

This is a family of electrophoresis techniques including electroosmosis, electrophoresis and chromatography. This mode is best described by the cyclodextrin (CD) mediated EKC, where enantiomers interact differently with the CD and converted to diastereoisomers and allowing for their separation. This approach has made a major impact in pharmaceutical industries for analysis of chiral drugs (Xu 1996). It could be explained as a hybrid method of MEKC and CZE since it employs not only chiral micelles but also non-micellar chiral selectors (CDs) as well. EKC employs a stationary phase that is not immobilized, but distributed consistently in the solution and moves at a velocity different to that of the surrounding medium.

This method is however, the preferred method in the pharmaceutical industry as it is versatile compared to HPLC in enantioseparation since it is very difficult to separate enantiomers under normal CE and LC techniques. Additionally, it is also able to separate the neutral compound which is advantageous (Verleysen and Sandra 1998).

2.8.6 *Micellar Electrokinetic Capillary Chromatography (MEKC)*

MEKC is a form of EKC in which surfactants are added to the running buffer at concentrations that form micelles. It has attracted a number of industries including (bio) pharmaceutical, food, environmental and clinical industries. It can separate neutral solutes as well as charged ones. Its principle of operation is based on addition of a surfactant to the background electrolyte example being SDS. At a concentration above critical micelle concentration of a surfactant micelles are formed containing hydrophobic tails oriented towards the center and the charged heads oriented outside facing the buffer. The direction in which micelles travels depends on their charges, they can either migrate with or against the EOF. Those with a negative charge such as SDS travel against the EOF towards the anode. However, at neutral pH or basic pHs, the migration of micelles is slower than the EOF therefore resulting in the net migration being towards the cathode favouring the direction of the EOF. As the solutes migrate through the column, they partition between the micelles and the running buffer in a chromatographic manner through hydrophobic and electrostatic interactions. In MEKC the micelles serve as pseudo-stationary phase that resembles that of reversed phase in HPLC (Tagliaro et al. 1998; Deyl et al. 1998; Gübitz and Schmid 1997).

2.8.7 *Frontal Analysis (FA)*

This is an alternative method to zonal elution for the measurements of equilibrium constants (Hage et al. 2009). Just like the other affinity CE techniques CE-FA has been developed from chromatography. Its main area of interest has widely been in drug to protein analysis (Østergaardand Heegaard 2003). FA has several advantages over conventional methods for the analysis of drug-protein binding studies, such as its speed and information that it can provide in details and also in the high-throughput screening of drug–protein interactions (Hage et al. 2009). This method was used in this study and will be explained in detail on the methodology.

The different modes of CE benefit its versatility in analyzing different types of compounds. The modes also aid in studying different properties depending on what the researcher strives to achieve as each mode has its strongest point. This then again makes CE a preferred method, in contrast to the traditional methods.

CHAPTER 3

MECHANISM OF CHIRAL SEPARATION IN CE

This chapter briefly discusses the chiral selectors used in CE and the chiral separation mechanism involved with more emphasis being on the cyclodextrins (CD) since they were used in the present study.

3.1 Introduction

An appropriate chiral selector plays the main role in the resolution of chiral compounds. For separation to take place, the enantiomeric mixture has to interact reversibly with the chiral environment. In HPLC protein based stationary phases have been widely applied and successfully giving high selectivity. This however, has some shortcomings including low efficiency, lack of robustness and deemed expensive since the lifetime of stationary phases could be short and the reproducibility between them cannot be guaranteed. It has in turn raised a need to use mobilized chiral selectors, which is a widely used method in CE and has gained an advantage of having a great selectivity which is achieved by an addition of a suitable chiral selector as a buffer additive in either MEKC or CZE (Fraizer et al. 2000; Tickle et al. 1994; Wren 2001). The additives normally used in CE for chiral separation include metal–amino acid complexes, antibiotics, chiral crown ethers, chiral micelles, proteins and cyclodextrins (CDs) or their derivatives. Amongst these chiral selectors; CDs and their derivatives are extensively studied and practically applied for enantiomeric resolution of a large number of compounds, the main interest being on the pharmaceutical compounds. The wide application of CDs is due to their physicochemical properties and commercial availability in native and derivatized forms (Abushoffaet al. 2002; Fanali 2000;Główka and Karaźniewicz 2004).

3.2 Chiral selectors in CE

3.2.1 Crown Ethers

Separation of enantiomers with crown ethers is an enantiomeric separation method developed not so long ago using 18-crown-6-tetracarboxylic acid as an additive to the running buffer. These chiral selectors have been known to be able to separate protonated primary amine enantiomers through the formation of a co-ordination complex after interaction.

It is believed that the six oxygen atoms present in the crown ether form a planar arrangement and also form three hydrogen bonds with the three protons that are attached to the protonated primary amine (Wren 2001).

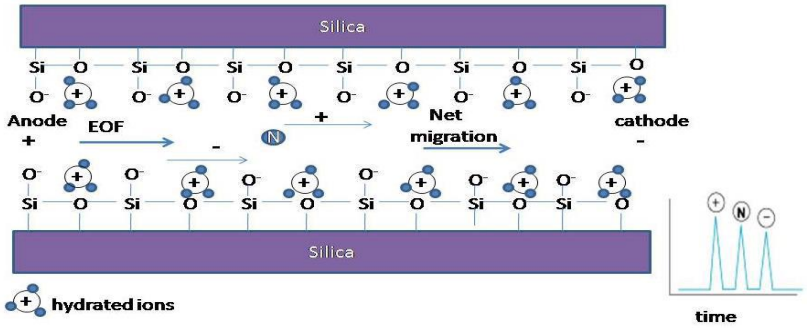

Figure 3.1: Mechanism of separation in CE

3.2.2 Macrocyclic antibiotics

Macrocyclic antibiotics in general are able to separate a number of chemically different groups of species covering a wider range of high molecular weight species. These chiral selectors have a number of stereogenic centers with different functional groups that results in various types of interactions with the analytes. Macrocyclic antibiotics however, have been widely used in CE for the separation of enantiomeric mixtures acting as chiral selectors. Vancomycin in particular, is the widely used amphoteric glycopeptide which contains about three fused silica rings. It also possesses both acidic and basic functional groups. It is widely used as an antibiotic in human medicine and acts by binding to cell wall proteins to prevent bacterial growth. This antibiotic has also been used in enantioseparation of NSAIDs with good resolution being obtained between the enantiomers (Wren 2001).

3.2.3 Proteins

Proteins have been widely applied in chiral separations due to their distinctive properties in stereoselectivity and their suitability to separate a wide range of enantiomers. These properties are due to the multiple binding sites that the proteins possess and also due to the number of interactions that happen between the protein and the solute (Haginaka 2004). Albumin and glycoprotein are chiral macromolecules which have an ability to discriminate chiral molecules. Their complex structures have made it difficult to recognize their chiral separation mechanism, but however with the development of modern techniques such as X-ray crystallography, protein NMR and docking studies the long undisclosed mechanism is now likely to unveil.

Their application as chiral selectors is expressed by immobilization or rather adsorption of them to the stationary phase in order to bring about the reversible confirmation change and thus be able to obtain different enantioselective properties of the same protein. Proteins interact with chiral compounds forming both strong and specific bonds as well as weak and non-specific interactions. α-Acid Glycoprotein (AGP) is the mostly used glycoprotein for chiral discrimination of enantiomeric mixtures. Due to its low isoelectric point (pI) it is the major plasma protein to which cationic drugs bind to as compared to HSA (Zheng and Ji 2011). On the other hand, HSA (being the drug transporting plasma) has also shown to possess a chiral recognition character for enantiomers. It has been used for separation of some pharmaceuticals such as propranolol, oxprenolol, etc., and bears an advantage of low cost per analysis. This protein has been seen to have two primary binding sites with a variety of secondary sites for drug binding depending on the specificity (Zheng and Ji 2011).

3.2.4 Micelles/Surfactants

Surfactants are amphiphilic in nature consisting of an apolar long chain hydrocarbon tail and polar head groups. Both chiral monomeric and polymeric surfactants have been used in chiral separations of enantiomeric mixtures by providing a chiral micellar environment for highly hydrophobic analytes. Polymeric surfactants are more interesting to use since they are stable and more rigid as compared to monomeric. In comparison to the other chiral selectors, polymeric surfactants are more soluble in aqueous and organic solvents. For these surfactants the polar head groups and the number of stereogenic centers can be modified and controlled (Fakayode et al. 2006). For enantioseparation to be feasible both the enantiomers of an enantiomeric mixture need to have different affinities for the micellar and also for the micellar to have a different electrophoretic mobility to each enantiomer. The separation is however assumed to take place through the partitioning of each enantiomer with the micellar formed by a surfactant (Wren 2001).

3.2.5 Cyclodextrins (CDs)

Cyclodextrins (CDs) are the most frequently used chiral selectors in CE and will be discussed in detail in this section, as the present work includes the use of a CD for chiral separation of racemic drugs. CDs are cyclic oligosaccharides consisting of six α-CD, seven β-CD, eight γ-CD or more glucopyranose units with a truncated cone providing a hydrophobic cavity and a hydrophilic exterior.

Figure 3.2 shows a glucose structure with n the number of repeat units forming a cyclic chain. Position 2 and 3 can be derivatized to provide the unique properties of CDs.

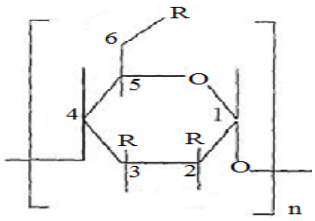

Figure 3.2: Structure of repeat unit of glucose molecules with numbered carbons.

The hydrophilicity of the exterior part of the CD is due to the presence of hydroxyl groups. The hydrophobic cavity plays an important part in separation because it includes other compounds by hydrophobic interactions (Gübitz and Schmid 2000; Del Valle 2004). To improve their poor solubility, methyl, carboxymethyl or hydroxypropyl derivatives are used with derivatization in the 2, 3 or 6 positions. Enantioselective recognition is explained by interactions between CDs, which have many chiral centers, and the guest enantiomer (Główka and Karaźniewicz 2004). "Chiral recognition is based on the inclusion of the bulky hydrophobic group of the analyte into the hydrophobic cavity of the CD and lateral interactions of the hydroxyl groups at the C-2 and C-3 at the upper rim of the CD, such as hydrogen bonds and dipole-dipole interactions with the analyte" (Gübitz and Schmid 2000). It is wise to note that both the type and concentration of CD are as important as the buffer pH (although regarded as a major factor) and also have a significant effect on enantiomeric resolution (Fillet et al. 1997). A number of CDs have been synthesized and utilized, but our main focus will be on the β-cyclodextrins since Heptakis-2, 3, 6-tri-O-methyl-β-cyclodextrin was used for this study as it was considered suitable for the separation of profens in several studies.

3.2.5.1 Properties of CDs

As mentioned above there are three types of CDs: the α-CD, β-CD, and the γ-CD with β -cyclodextrin being the most accessible, cheapest and generally the most useful of the three (Del Valle 2004). The physical properties of the three types of CDs differ according to their molecular mass, width of the cavity, solubility and so on. Solubility of a β-CD is very low about <1.8% when compared with the α-CD, and the γ-CD. Its solubility can be improved with organic solvents like methanol, ethanol, etc. (Fanali 2000).

When choosing the suitable CD for the study, one of the properties to be considered is its ability to compete with analytes in inclusion-complexation, which then results in the separation of enantiomers (Fanali 2000). Chiral recognition of a pair of enantiomers is based on one molecule having a better access to the CD resulting in hydrogen bonding or hydrophobic inclusion. Neutral CDs are used in the separation of charged analytes while charged CDs are for uncharged molecules (Laurer and Rozing 2009).

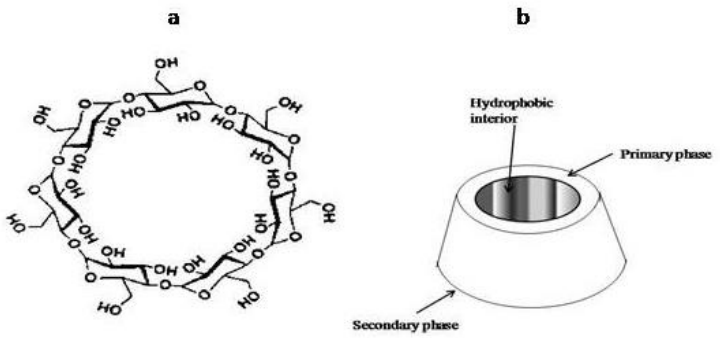

Figure 3.3: Chemical structure of cyclodextrin, (a) hept-β cyclodextrin showing R-O bonds , and (b) the different cyclodextrin phases and the hydrophobic interior.

3.2.5.2 Neutral CDs

Heptakis-(2,3,6-tri-O-methyl)-β-CD shown in Figure 3.3 falls under neutral CDs with other various CDs including Heptakis-(O-methyl)-β-CD, Heptakis-(2,6-di-O-methyl)-β-CD, and hydroxyethyl-β-CD have been synthesized and applied to various compounds. Most of the CD derivatives represent mixtures of different products showing different substitution patterns. Therefore, separations are most likely to be difficult to reproduce. Studies have shown that chiral recognition/selectivity of various chiral selectors varies with different analytes depending on their bulkiness and hydrogen bonding ability (Del Valle 2004).

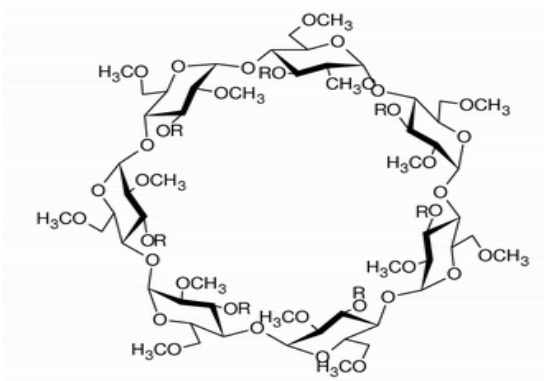

Figure 3.4: 2D structure of Heptakis-(2, 3, 6-tri-O-methyl)-β-CD

Studies have also shown that the β-CD has a cavity that covers a wide range of analytes, in particular those of pharmaceutical interest. In the inclusion-complexation process the analytes either fit in completely or their hydrophobic part interact with the CD cavity. The analyte's hydrophobic part enters the cavity through either of the two openings, i.e. primarily with the 6-hydroxyl and secondary with the 3-hydroxyl groups. To add on that, the hydroxyl group on the CDs can be easily modified via chemical reactions, in order to obtain different derivatives to suite the nature of the analyte. The compositions of the derivative will highly depend on the reaction conditions, reagents type and ratio, and other parameters (Fanali 2000).

Heptakis (2, 3, 6-tri-O-methly)-β-cyclodextrin as a chiral selector for profens

Główka and co-workers reported Heptakis (2, 3, 6-tri-O-methly)-β-cyclodextrin (TM-β-CD) to be the suitable chiral selector for profens as it gave optimum results for enantiomers of some 2-aryl propionic acid derivatives which included ibuprofen, flurbiprofen, ketoprofen, and naproxen. The main aim of their study was to develop an EKC method to study pharmacokinetic, bioavailability, and optical purity properties of these compounds in HSA. For the study, a dual background electrolyte which consisted of triethanolamine-phosphoric acid (pH 5, 0.02 M) with TM-β-CD as a chiral selector proved to be practically suitable for the feasibility of separation of these derivatives (Główka and Karaźniewicz 2004). In some cases, a single CD fails to do enantioseparation of pure compounds, and raise a necessity for the use of a mixture of CDs in dual systems. The usage of a combination of CDs results in greater resolution due to the differences in the complexation mechanisms of the two CDs with the enantiomers of the compound of interest. Abushoffa and co-workers studied a dual system of CDs for the separation of some 2-aryl propionic acid derivatives, where they employed an anionic CD [heptakis-6-sulfato-b-cyclodextrin (HS-β-CD)], and a neutral CD (TM-β-CD). In their study they highlighted the importance of using dual systems in the separation of enantiomers with regard to the principle of mobility where one of the CDs will accelerate one enantiomer, while the other CD will slow down the other enantiomer resulting in a high resolution of these enantiomers. In this study a mixture of HS-β-CD and TM-β-CD with a dual electrolyte system of 0.02 M phosphoric acid–triethanolamine (pH 2.5), the HS-β-CD alone was tested for enantioseparation of some acidic profens, and they showed poor resolution at that pH.

Mixing the sulphated CD with the methylated CD (which has been proven to possess mainly high enantioselectivity towards these compounds) improved the resolution of fenoprofen, flurbiprofen, ibuprofen and ketoprofen (Abushoffa et al. 2002). In CE, the CZE mode with a background electrolyte consisting of a CD as a chiral selector is a widely used mode for enantioseparation of optical isomers.

Blanco et al. developed a quick and simple method with high efficiency for the enantiomeric resolution of some 2-aryl propionic derivatives.In their study, they developed a method that needed minimal sample and background electrolyte (BGE) preparation with the view of routine usage; this was done by optimizing experimental parameters. They examined an influence of some various factors (namely pH and concentration of the BGE, type of CD and its concentration, and lastly cassette temperature) that have an effect on resolution. For this study as well, TM-β-CD (0.05 M) was found to be the most suitable chiral selector for these derivatives, BGE used was 0.02 M phosphoric acid–triethanolamine at pH 5 (which is generally the pH at which these derivatives are present in a dissociated form, which allows them to form complexes with CDs resulting in their selective resolution), and the temperature chosen was 35 °C. The above conditions gave optimum results with the run times of all the three compounds being less than 20min, which then makes it feasible for routine analysis (Blanco et al. 1998).

CHAPTER 4

PHARMACOKINETIC AND PHARMACODYNAMICS OF DRUGS

This chapter involves a discussion of the binding of drugs to plasma proteins and the pharmacokinetic properties involved. The different types of proteins in which drugs can bind to along with their different binding sites with emphasis on the HSA protein are discussed. Drugs under investigation in the present study are also briefly discussed.

4.1 Introduction: ADME

The pharmacokinetic and pharmacodynamic properties of drugs are mainly a function of the reversible binding process of drugs to plasma proteins. Pharmacokinetic properties can be defined as the manner in which the body deals with chemicals or as absorption, distribution, metabolism and elimination (ADME) processes with time. These processes are very broad and can also be applied to chemicals that the body produces naturally including nutrients, to which the body is exposed to through food, water or air (Barton 2007; Chaturvedi et al. 2001). Figure 4.1 below is a schematic illustration of these four processes that take place in the human body.

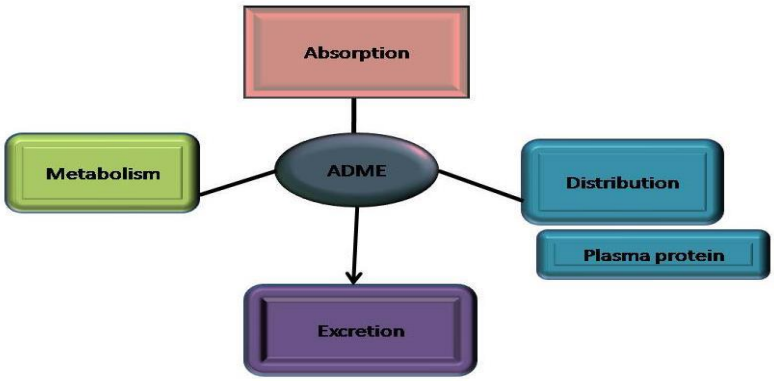

Figure 4.1: Schematic representation of the ADME processes

Pharmacodynamics is basically a study of drugs including their therapeutic and toxic effects. Orally delivered pharmacologically active compounds need to have favorable absorption properties and satisfactory metabolic stability to provide adequate systematic exposure to obtain a pharmacodynamic response (Chaturvedi et al. 2001).

Most drugs are orally administered and undergo the above mentioned processes; whereby they are absorbed, distributed to reach the targeted receptor, metabolized by the liver, and lastly excreted by the kidneys. ADME processes are said to affect the biological effects of drugs (Hage 2009). Sufficient oral bioavailability is achieved if the administered drug possesses reasonable physico-chemical properties and is reasonably absorbed into the system (Ekins et al. 2010).

4.2 Proteins

Proteins are vital nutrients and building blocks of the body tissue. In some cases, they act as transporters of substances around the human body. Proteins are polymer chains made up of amino acids joined together by peptide bonds (Genton et al. 2010). There is a variety of proteins each having different characteristics as defined below.

4.2.1 α 1-Acid Glycoprotein (AGP)

AGP has a molecular weight of 44,000 units and comprises of 0.04 to 0.1 % (which is approximately 0.5 – 0.1 g/L) of the total plasma concentration of protein. Its concentration normally varies considerably in several pathological and physiological conditions since researchers have reported its tendency to increase during contraction of diseases (Jia et al. 2002; Martínez-Pla et al. 2004; Nomura et al. 1992). AGP is produced by the liver and is a fairly heterogeneous protein. This protein contains about five carbohydrate groups and a polypeptide with about 181 amino acids. There are numerous ways in which the carbohydrates could be attached to it but their arrangement is dependent on the state of the disease in the body, which in turn affect the binding of AGP and as well as its structure (Jia 2002; Nomura et al. 1992; Zsila and Iwao 2007). Its levels increases as a response to inflammation is triggered by cytokines such as interleukin 6, as a result this means that its concentration increases with situations like pregnancy/age and pathological conditions such as lung cancer, and therefore it can be used as a disease marker (Bruno et al. 2003; Chuang and Otagiri 2006). Another study showed a decrease in AGP levels in patients responding to therapy as opposed to patients who are not. The increase of AGP concentration of patients that contracted the disease increases the binding of drugs to it (Bruno et al. 2003).

4.2.1.1 Binding Sites of α 1-Acid Glycoprotein (AGP)

AGP is known to have a single binding site, where hydrophobic interactions dominate. It is said to be the main determinant for the binding of a wide variety of basic and neutral drugs, however changes in its concentration have significance to the drugs that are bound to it (Jia 2002; Nomura et al. 1992). Genetic polymorphism of AGP has been long known. AGP has three major variants (F1, S, and A) which differ from one another in their primary structure (Zsila and Iwao 2000).

4.2.2 Lipoproteins

Plasma lipoproteins are known as the major transporter of cholesterol and triglycerides in the blood stream, but can also transport and bind to several neutral hydrophobic and/or basic drugs. Lipoproteins are categorized into subclasses based on their density, such as high density lipoproteins (HDL), low density lipoprotein (LDL), and very low density lipoproteins (VLDL). HDL and LDL are essential in transporting drugs due to their high densities meaning they are in abundance as compared to the others (Ohnishi et al. 2002). Lipoproteins are meta-stable molecular aggregates, which consist of lipophilic core (cholesterolester and triglycerides) surrounded by a surface layer, including polar lipids (phospholipids' free cholesterol) and apolar lipoproteins. Like AGP their plasma concentration varies according to the state of disease, mostly they respond to diseases like coronary artery disease. However, their varying concentration in plasma affects plasma distribution of drugs. These proteins have also displayed characteristics of enantio-selectivity due to their chiral nature but have not been investigated a lot like HSA and AGP because of their low concentration in the blood plasma and the difficulty to preserve for a long time (Mohamed et al. 2000; Ohnishi 2002).

4.2.2.1 Binding Sites of lipoproteins

Lipoproteins' binding is major when greater quantities of drugs bind to them, and also in cases whereby there are lower plasma levels of HSA and AGP. In lipoproteins the process of binding involves the suspension of drug molecules into the lipid core of the protein. Therefore, it can be concluded that the binding power is in direct relation with the lipid content of the protein.

4.2.3 Human Serum Albumin (HSA)

Human serum albumin (HSA) in Figure 4.2 is the most prominent protein in the blood plasma with a very high concentration (0.6 M, MW: 66 500 units) which accounts for about 60% of the protein in the blood plasma (Zsila and Iwao 2000). It is best known for its unique ligand binding capacity due to its multiple hydrophobic binding sites which bind various groups of drugs; particularly the negative medium sized or neutrally charged hydrophobic compounds. Smaller and less hydrophobic compounds do not bind strongly, but their binding can still be very specific (Baroni et al. 2001; Hage et al. 2009; Tajmir-Riahi 2007). Due to its high concentration in the circulatory system and its ability to store a big amount of compounds (drugs, metabolites and fatty acids), it is assigned to play a vital role in their pharmacokinetic behaviour and affects their efficiency and delivery rate (Baroni et al. 2001; Galantini et al. 2010).

Moreover, HSA acts as a carrier protein for steroids, fatty acids, and thyroid hormones so they can be available in quantities greater than the solubility in plasma. As the main carrier for fatty acids to and from the tissues, it increases their effective solubility from <1 μM to mM values (Galantini et al. 2010). HSA has been seen to be very important in regulating the colloidal osmotic pressures of blood, which enables charge balance in plasma. It also acts as the main buffering system for extravascular fluids and protects low-density lipoproteins from peroxidative effects. Additionally, owing to its abundance in the plasma HSA binds and deliver a number of substances within the body including vitamins, acidic drugs, and organic anions (Hage et al. 2009; Valko et al 2003). In some cases, HSA holds some ligands in a stressed environment, so as to allow their metabolic alteration and also reduces possible toxins by transporting them to disposal sites. HSA also acts as a nitric oxide carrier, leading to covalent alteration of macro-molecules (Baroni et al. 2001). Furthermore, it accounts for most of the antioxidant capacity of human serum, either by directly binding to radical scavengers, or by isolating transition metal ions with pro-oxidant activity. Apart from all the above mentioned functions, HSA has another function in the system, caused by drug-protein complexes which may reload the free drug concentration that is removed either by metabolic or elimination processes (Baroni et al. 2001; Tajmir-Riahi2007; Martínez-Pla et al. 2004).

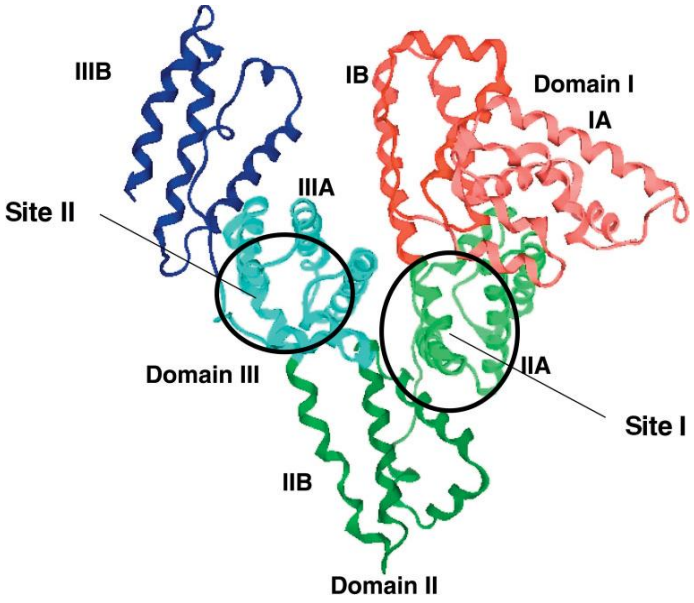

Figure 4.2: Crystallographic structure of Human Serum Albumin (HSA) showing different subdomains (Chuang and Otagiri 2006).

4.2.3.1 Binding sites and domains of HSA

The amino acid sequences of HSA showed the occurrence of three structurally similar domains (I, II and III), each containing two subdomains (A and B). These three domains are presumed from the primary structure, but do not correspond to the domains found in the three-dimensional model (Baroni et al. 2001). The regions of sequential domain contributes to the formation of the interdomain helices linking domain I to II, and II to III, respectively. Therefore, HSA can be considered as an ensemble of our globular domains, namely IA, IB + IIA, IIB + IIIA, and IIIB, freely linked by extended random coils. The three-domain design provides a variety of binding sites and the flexibility of its structure allows it to adapt readily to ligands (Tajmir-Riahi 2007). For drug like compounds, two principal binding sites (Site I&II) with high affinities were long proposed in subdomains IIA (site I) and IIIA (site II). These have highly elongated hydrophobic pockets with charged residues of lysine and arginine found near the surface that acts as an attachment point for the polar ligand features. Subdomain IIA of the albumin binds a wide variety of both endogenous and exogenous substances (Chuang et al. 1999; Galantini et al. 2010; Kratochwil et al. 2002).

The multiple binding sites are the cause of its unique ability to interact with many organic and inorganic molecules and consequently, make this protein an important regulator of intercellular instabilities. Eight binding sites are localized for fatty acids in subdomains IB, IIIA, IIIB and on the interfaces (Bertucci etal. 2003; Kratochwil et al. 2002).

4.3. Drug-Protein Binding

Drugs to protein binding interactions are important processes in the blood stream for determining the activity and outcome of drugs once they have entered into circulation. Their distribution, rate of metabolism and excretion, toxicity and therapeutic effects in the body are thus controlled by these interactions (Hage et al. 1995; Zahra et al. 2006; Tang et al. 2006; Valko et al. 2003). Moreover, a direct or indirect competition for the same binding proteins between a drug and an endogenous compound such as a fatty acid or between two drugs could be a source of drug–drug interactions or drug displacement by another therapeutic agent (drug displacement effects). A typical example of this may be seen with NSAIDs which are known to have a high binding affinity towards protein, and have a tendency of displacing drugs being bound to albumin (Zahra et al. 2006). These type of interactions gives a better understanding of how the binding of pharmaceuticals to proteins takes place in the blood and to also understand how the presence of other substances could affect the occurrence of these interactions (Hageet al. 2009). A number of plasma proteins probably participate in the plasma protein bindings of one drug concurrently, thus making the overall plasma protein binding to be the sum of each protein binding. Usually proteins like HSA and α 1-acid glycoprotein (AGP) are mostly involved in the binding; although more complex agents such as lipoproteins, red blood cells, or platelets can be involved as well. In order for one to have a clear interpretation of drug distribution in plasma, it is necessary to do *in vitro* binding studies with each component of the plasma proteins. Researchers have reported that there is a possibility for plasma binding of a racemic drug to differ between the enantiomers, which then causes a difference in their pharmacokinetic character. This therefore raises a necessity for enantioselective plasma protein binding studies for new drugs to gain information on its safety and clinical use (Ohnishi et al. 2002).

Drugs that are highly plasma protein bound tend to be limited in blood vessels since it is hard for them to pass through the blood capillary wall, therefore resulting in a low volume of distribution. On the other hand, less bound drugs have large distribution volumes, usually accessible for distribution to other organs or tissues and available for interaction with a pharmacological target e.g. receptor. Accordingly, the effectiveness of a drug is said to be related to the exposure of a target molecule to the unbound drug rather than the total concentration administered. Consequently, plasma protein binding tends to have an important effect on the pharmacokinetic and pharmacodynamic properties of a drug and its interactions (Shibukawaetal. 1999; Ohnishi et al. 2002). Researchers have also reported that highly bound drugs tend to have more elimination half-life resulting in a prolonged pharmacological activity which may encourage undesirable side effects. This again raises the importance of conducting drug-protein binding studies for the clinical use of new drugs (Singh and Mehta 2006). Albumin is in abundance in the plasma and the free effective concentration of the therapeutic drugs available for therapeutic action can be greatly decreased due to the fact that most drugs have a high binding affinity to plasma proteins. In other words, when a drug binds to the protein a drug-protein complex is formed, this complex acts as a reservoir for free drug concentrations, as the drug is removed from the body by a number of elimination processes. The physicochemical properties, targeted effective concentration and potential side effects influences how much will potentially bind to plasma protein (Kratochwil et al. 2002).

4.3.1 Determination of binding sites

This study is used to determine a location and structure of the binding regions for a drug or solute on HSA. An example of such was reported where the binding of enantiomers of ketoprofen with both the major sites (site I and site II) of HSA known to be phenylbutazon and diazepam binding sites respectively was studied (Zhivkova and Russeva 1998; Dubois et al. 1993). Another study was conducted by Wybranowski and co-workers where they studied the affinity of warfarin and flurbiprofen of site I and site II of HSA. Site I is known to bind to ligands which are bulky heterocyclic anions with a negative charge localized in the middle of the molecule whereas, site II is known to bind to ligands which are aromatic carboxylic acids with negatively charged acidic groups at the end of the molecules (Wybranowski et al. 2008).

4.3.2 Competition Studies

Zonal elution is normally a technique used for competition and displacement studies, when the drugs are competing with other solutes (drugs) or being displaced by solutes from the binding site of the proteins. Hage and co-workers used (*S*)-warfarin and a racemic verapamil, where these two compounds were competing on HSA and showed a shift in warfarin retention as the concentration of verapamil was varied. There are various equations that could be used to determine the kind of interaction happening between the competing compounds, with the extent of the shift being measured as a function of competing agent's concentration. These equations can also be used to measure the equilibrium constants corresponding to each agent or their coupling constants for the interaction (Hage et al. 1995).

4.3.3 Strength and degree of binding to HSA

Dicarboxylic acids and/or bulky heterocyclic molecules with a negative charge localized in the middle of the molecule prefer to bind at site I, which is located in subdomain IIA. This site is assumed to be large since ligands as big as bilirubin can be bound on this site. Site II which is in subdomain IIIA is preferred by aromatic carboxylic acids possessing a negatively charged acidic group at one end of the molecule away from a hydrophobic centre e.g. ibuprofen. This site comprises of all six helices of subdomain IIIA and is topologically similar to site I, but gives the impression of being smaller and more narrower, as it can't bind to large ligands (such as bilirubin, haemin etc.). It is also said to be less flexible, because of its stronger binding properties that are affected by stereoselectivity. Ibuprofen for example presents a binding affinity that is totally different for its enantiomers (Galantini et al. 2010). Binding affinity of the (*R*)-ibuprofen is approximately 2.3 times larger than that for (*S*)-ibuprofen (Galantini et al. 2010). The two subdomains IIA and subdomain IIIA are said to be highly elongated hydrophobic pockets with charged lysine and arginine residues near the surface that acts as attachment points for polar ligand features. Binding to HSA controls the free and active concentration of a drug, and provides a reservoir for a long duration of action. HSA also affects drug absorption, metabolism, distribution and excretion. Drug metabolism and activity are brought about by different types of interactions with specific biological targets and high regard of these interactions may explain the mechanism of the interactions (Bertucci et al. 2003).

4.4 Drugs: Nonsteroidal anti-inflammatory drugs (NSAIDs)

4.4.1 General properties

Salicylic acid and salicylates, obtained from natural sources, have long been used as therapies. They were used as antiseptics, antipyretics, and antirheumatics, almost 40 years after their discovery; aspirin was synthesized and marketed as a more edible form of salicylate. Soon after, compounds with similar actions to aspirin were discovered; these were then collectively termed "nonsteroidal anti-inflammatory drugs" (NSAIDs) (Vane and Botting 1998; Zhaet al 2004). The term "non-steroidal" is to differentiate them from the anti-inflammatory activity of steroids i.e. NSAIDs do not act via the same path as steroids to prevent the immune system from producing fever, pain and inflammation (Nirogi et al. 2006). NSAIDs are within the widely used class of drugs especially in elderly patients, and are said to be absorbed well. These drugs have shown a high degree of binding to HSA with many being approximately 99% bound to the serum albumin thus resulting in a very low distribution of about 10% of the body weight (Brater 1988; Dubois et al. 1993). The majority of NSAIDs are eliminated through the liver with the remainder being eliminated through hepatic metabolism which explains the need for being cautious of changes in drug disposition when dealing with patients with hepatic disease (Brater1988). The main concern with NSAIDs is their severe gastrointestinal side effects. Their cause has not been exactly understood but could quite frankly be associated with the other enantiomer of the racemate which is not therapeutically involved (Somasundaram et al. 1997).

4.4.2 Clinical considerations

NSAIDs have the following main clinical effects:

(i) Anti-inflammatory

Anti-inflammatory effects are due to the inhibition of the enzyme cyclo-oxygenase (COX), which converts arachidonic acid to prostaglandins. COX has at least two different forms, the constitutive isoform, COX-1, and the inducible isoform COX-2. COX-2 produces prostaglandins which respond to stimulation at the spot of inflammation, whereas COX-1 is responsible for baseline levels of prostaglandins. It is therefore more attractive to say that the anti-inflammatory actions of NSAIDs are due to inhibition of COX-2, since COX-2 is encouraged by inflammatory stimuli (Vaile and Davis 1998; Mitchell 1994; Lü et al. 2004).

(ii) Analgesic

NSAIDs are inhibitors of prostaglandin production in humans, and therefore indicated for use in the treatment of rheumatoid arthritis be it for long-term or short term treatment (Patel and Mashru 2011). This action however has a side effect of causing ulcers in the stomach since the prostaglandins that protect the stomach, support platelets and blood clotting.

(iii) Antipyretic effects

This is said to be related to the inhibition of the interleukin-1β and interleukin-6 which encourages the production of prostaglandins in the hypothalamus. The synthesis of prostaglandins in circumventricular organ triggers the hypothalamus to raise the body temperature and result in lipo polysaccharide encouraged fever (Crofford 2013). Its inhibitions by NSAIDs result in management of fever.

NSAIDs are also believed to be responsible for the inhibition of platelet aggregation. Oral treatment of these drugs is very effective, but their clinical use is often limited because of their ability to cause side effects such as irritation and ulceration of the intestinal lining. It is believed that the gastric irritation caused by NSAIDs is influenced by their administration, thus using a different route such as the dermal route (injection) can overcome the oral route disadvantages and maintain consistent plasma levels (Attia 2009). All NSAIDs are highly lipophilic substances; their absorption after oral administration is generally rapid and complete. Their most significant aspect of distribution is plasma protein binding, which will be part of this study. NSAIDs are known as competitive inhibitors for arachidonic acid binding to COX, this known mechanism of action makes it easier to predict whether they are metabolites or not. As mentioned above their metabolism and elimination is via hepatic conjugation with glucoronic acid (*http://www.wedgewoodpharmacy.com/monographs/dipyrone.asp*). These drugs are said to be excreted unchanged in small percentages in urine. If the drug is excreted unchanged, its rate of excretion is expected to increase if it was co-administered with agents that increases the urine pH.

NSAIDs are divided into many sub-categories, including the salicylates, aryl alkanoic acids, 2-arylpropionic acids (profens), N-arylanthranilic acids (fenamic acids), pyrazolidine derivatives, oxicams, COX-2 inhibitors, and sulphonanilides. All these are non-steroidal.

The ‘salicylates’ are derived from a Latin name for a willow tree from which salicylic acid was isolated, these are well known to be effective pain killers and also blood thinners. The most famous one in this category is the aspirin (Vane and Botting 1998). Aryl alkanoic acids have a charged atom (aryl) on a ring of carbon atoms, profens have propionic acid attached to a carbon ring in their structure. Fenamic acids are based on the molecule fenamic acid, which is formed by two carbon rings attached in the middle with one nitrogen atom, and with one carboxyl group (COOH) on one of the rings. Pyrazolidine derivatives contain pyrazolidine (a ring with carbons and nitrogens), oxicams derived from enolic acid, a carbon- and hydroxyl-containing molecule (C=C–OH) made from carboxylic acid, COX-2 inhibitors act specifically to block COX-2, and lastly the sulphonanilides which contain nimesulide, but has been suspended in other countries due to their side effects leading to liver failure possible liver failure (Deschamps-Labat 1997).

The main focus of this study is based on the 2-arylpropionic acid derivatives, well known as the profens. These derivatives form an important class of NSAIDs since they represent the main group of available NSAIDs. The 2-arylpropionic acid side chain possesses an asymmetric α-carbon therefore it occurs as either (*S*)- or (*R*)- enantiomers (Blanco et al. 1998). Separation and detection of a mixture of such a complex family is very important. The fact that they are chiral compounds, their enantiomers very often show differential pharmacological and toxicological properties. This has raised a need for enantiomeric purity controls of pharmaceuticals based on selective, sensitive and rapid techniques. Primarily these controls are done by high-performance liquid chromatography (HPLC) that requires chiral columns; these are expensive and are not efficient since, they are lose columns (Blanco et al. 1998; Patel and Mashru 2011). Even though their pharmacological activity resides mainly in the (+)-*S* enantiomer, these drugs are marketed as 50/50 racemic mixtures (except for naproxen), generally with their plasma protein binding being above 99% (Deschamps-Labat et al 1997; Główka and Karaźniewicz 2004).

The commercially available drugs that were used for this study include fenoprofen, flurbiprofen, ketorolac, ketoprofen, naproxen, ibuprofen, indoprofen, and fenbufen. The table below gives a brief description each drug.

Table 4.1: 2D structures and pharmacological actions for each NSAID

IUPAC and commercial name	**2D Structure and pharmacological action**
2-(3-phenoxyphenyl)propionic acid and Fenoprofen	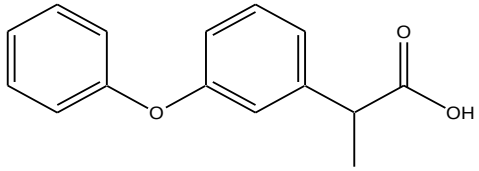 Inhibits prostaglandin synthesis by decreasing the enzyme needed for biosynthesis.
2-(3-fluoro-4-phenylphenyl)propanoic acid and Flurbiprofen	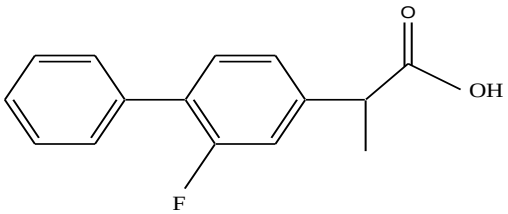 Inhibitor of cyclooxygenase (COX) both COX-1 and COX-2, this then decreases the prostaglandins which cause inflammation, pain, swelling and fever
2-(3-benzoylphenyl)propanoic acid and Ketoprofen	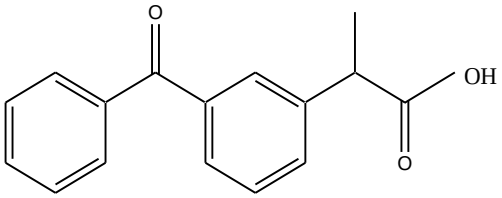 Inhibit synthesis of prostaglandin.
2-(6-methoxynaphthalene-2-yl)propanoic acid and Naproxen	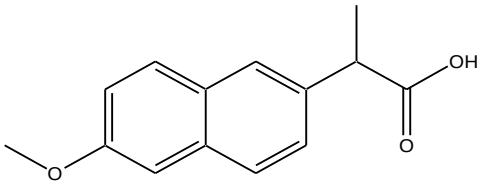 Inhibitor of cyclooxygenase both COX-1 and COX 2

IUPAC and commercial name	2D Structure and pharmacological action
2-[4-(2-methylpropyl)phenyl]propanoic acid and Ibuprofen	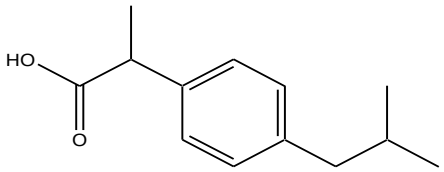 Inhibit synthesis of prostaglandin.
2-4-(1-oxo-1,3dihydro-2H-isondol-2-yl phenyl) and Indoprofen	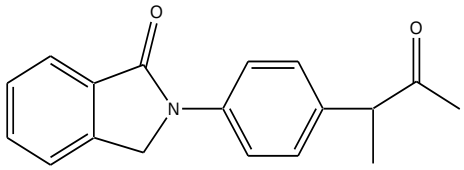 Cyclooxygenase Inhibitor
4-oxo-4(4-phenylphenyl) butanoic acid and Fenbufen	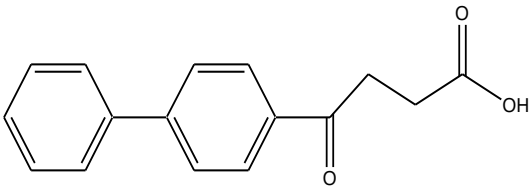 Block the synthesis of prostaglandin by inhibiting the cyclooxygenase.
5-benzoyl-2-3-1H-pyrrilizine-1-carboxylic acid and Ketorolac	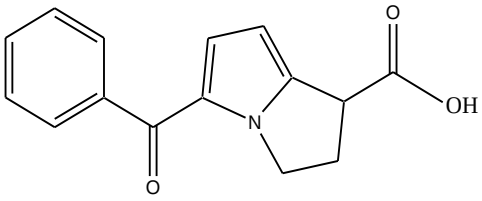 Cyclooxygenase (COX) inhibitor which that is only selective to COX-1

CHAPTER 5

METHODOLOGY

This chapter deals with the experimental section, which involves a brief description of each method used for the analysis and the methodology are explained stepwise. Specifications for all instruments along with details of the chemicals and reagents used in this work are provided.

5.1 Introduction

NSAIDs differ in their effectiveness, duration of action and the way in which they are eliminated from the body. Another important difference is their ability to cause ulcers and promote bleeding. The more an NSAID blocks COX-1, the greater is its tendency to cause ulcers and promote bleeding (McConathy and Owens 2003).

Almost 50% of chiral drugs are marketed as racemic mixtures, whereas it is often the case that only one of the two enantiomers shows pharmaceutical activity (Shimazawa 2008; Verleysen and Sandra 1998). In pharmaceutical and chemical reactions, chirality of each enantiomer does play an important role in defining the properties of the product, especially in the pharmaceutical industry when safety is of greatest importance (Fazlena et al. 2006). In some cases, a single enantiomer will provide superior medication while the racemic mixture will result in undesirable effects like decreasing the drug interaction with the target molecule (Shimazawa 2008). Ibuprofen for example, is commonly marketed as a racemic mixture with 50/50 amounts of (*S*) and (*R*) enantiomers as they are easier to obtain through chemical synthesis. In this form, it is widely used for the treatment of rheumatoid arthritis, headache, and muscular strain. In this instant the physiological activity is mainly from the (*S*)-enantiomer which showed about 100 times more potential in therapeutics effects, whereby the presence of (*R*)-ibuprofen causes gastrointestinal pain (a serious side effect) to humans. It can then be concluded that the two ibuprofen enantiomers can be regarded as two different drugs based on their pharmacological properties (Fazlena et al. 2006). A study of stereoselective protein binding is therefore essential for the development of new racemic drugs and for safety in their clinical use (Shibukawa 1999). Racemates are also known to be stereoselective in both action and disposition thus raising a greater need for stereoselective protein binding studies (Nirogi et al. 2006).

5.2 Experimental Analysis

5.2.1 Instrumentation

A capillary electrophoresis 7100 system (Agilent technologies, South Africa) equipped with a diode array detector, HPCE standard capillary with an internal diameter of 50 µm and a total length of 56 cm and an effective length of 47.5 cm (Agilent Technologies, South Africa). Agilent chemstation software was used for instrument control and data handling throughout the study. A Crison Micro-pH 2000 pH meter (Crison instruments, South Africa) was used to adjust the pH of solutions, then the prepared solutions were filtered through a Teflon disc filter (0.45 µm pore size and 9 mm diameter), and incubated in a thermostatized memmert water bath. HeidolphReax 2000 (Heidolph instruments, South Africa) vortex was used to homogenize the drug-HSA mixtures. For CZE 10 K omega centrifugal filters together with a Hermle Z233M-2 centrifuge (Lasec, South Africa) were used for centrifugation throughout this study.

5.2.2 Data processing

Experimental data were analyzed with EXCEL 2013 and MATLAB 4. The script used for MATLAB calculations was edited from the original file created by Prof Salvador Sagrado. Some of the data were treated with GraphPad Prism 5.

5.2.3 Reagents

All reagents were of analytical grade. HSA lyophilized powder (≥ 96 %), (±)-ketorolac (≥ 99 %) and (±)-flurbiprofen, indoprofen, fenbufen, (±) fenoprofen calcium salt hydrate (≥ 97 %), (+)-ketoprofen (99 %) and (+)-ibuprofen (99 %), (+)–naproxen, ethanol (99.8 %) and methanol (≥ 99.9 %) were purchased from Sigma-Aldrich (JHB, South Africa). Heptakis (2, 3, 6-tri-O-methly)-β-cyclodextrin (≥ 98 %) used for enantioseparations was purchased from Fluka (JHB, South Africa). Sodium hydroxide pellets were purchased from Associated Chemical Enterprises (JHB, South Africa), and sodium dihydrogen orthophosphate dihydrate purchased from SARCHEM (JHB, South Africa).

5.2.4 Preparation of stock solutions

A phosphate buffer solution of 67 mM (pH 7.4) was used, and the choice of buffer conditions were based on their closeness to physiological conditions. The buffer was prepared by dissolving an appropriate amount of sodium dihydrogen orthophosphate dihydrate in deionized water and pH adjusted by addition of 1 M NaOH.

The buffer was then filtered through a 0.45 μm Teflon filter. The stock solution of 2 mM for each drug was prepared at 1:9 ratio of methanol:phosphate buffer and a stock solution of 2 mM HSA prepared in phosphate buffer. All further dilutions of standards and mixture preparations were done with the running buffer (phosphate) in order to prevent disequilibrium changes in the reaction mixture during the electrophoretic analysis and to avoid system peak appearance. Heptakis (2, 3, 6-tri-O-methly)-β-cyclodextrin was prepared separately and also dissolved in a running buffer.

5.2.5 Capillary conditioning

New capillaries were conditioned at 60 °C by flushing for 15 min with 1 M NaOH, rinsed for 5 min with deionized water and 15 min with phosphate buffer. Prior to every injection the capillary was cleaned and conditioned at a temperature of 36.5 °C in four steps as follows: Firstly with a 2-minute rinse with deionized water, followed by a 2-minute rinse with 0.1 M NaOH, thereafter with a 2-minute rinse with deionized water and lastly 5 minutes with phosphate buffer at 1000 mbar in each case.

5.2.6 CE-FA methodology

In Frontal Analysis (FA) the known concentrations of the drugs and the proteins were mixed in the same sample vial and made up to volume with a running buffer. The mixture was homogenized by means of a vortex and allowed to equilibrate. Thereafter, the equilibrated sample was introduced into the buffer filled capillary as a large plug which takes about 10 % of the capillary's effective volume. During analysis the free drug and the drug-protein complex zones were separated due to the differences in mobility. The bound drug remains within the complex zone. Injection of large sample plugs gave rise to the appearance of plateau peaks. The height of the free drug plateau peak was proportional to the free drug concentration in the original sample, and the degree of binding was determined with the aid of a calibration curve.

5.2.6.1 Procedure for NSAIDs and HSA interaction using CE-FA

A sequence of mixtures was prepared, where the concentration of the drug in each case was varied from 50 to 300 μM and HSA concentration kept constant at 525 μM as illustrated in Table 5.1.

Table 5.1: Outline of experimental design used for sample preparation for all the compounds studied with CE-FA and CE-CZE.

ID	Drug/µM	HSA/µM
1	50	525
2	100	525
3	150	525
4	200	525
5	250	525
6	300	525
7 Cal 1	50	0.00
8 Cal 2	120	0.00
9 Cal 3	250	0.00

Data in Table 5.1 illustrates the experimental design that was used for the preparation of standards and sample mixtures. The samples were thoroughly mixed by vortex and incubated for 35 min at a temperature of 37 ºC. After incubation, the samples were mixed again by vortex, and then injected by means of hydrodynamic injection at 50 mbar for 60 s at the anodic end of the capillary. A high voltage of 20 kV was applied for separation, with a capillary temperature of 36.5 ºC and UV detection in a region of 220 to 317 nm. Moreover, experimental design was done using MATLAB. The samples were prepared as outlined above in Table 5.1, and were randomly run to avoid system biasness. Runs were done in duplicate for each sample to assess reproducibility and repeatability.

5.2.7 CZE Methodology

CZE is one of the widely used methods in CE, and it was used in this study to investigate the interaction of NSAIDs with HSA protein. The mixtures prepared in a vial as per Table 5.1 were vortexed to ensure that the drug and the protein were thouroughly mixed. The mixture was then incubated to reach equilibrium in a thermostatized water bath at 37 ºC for 35 minutes. Thereafter, ultra-filtration was applied to separate the free drug from the drug-protein complex. This was achieved by centrifugation of the samples at 9000 rpm through 10 K cellulose filters. The filtrate was then quantified using the CZE approach, where the capillary was first conditioned with the separation buffer.

Sample injections were done for 5s with the aid of hydrodynamic injection at 50 mbar in each case at the anodic end of the fused silica capillary by a potential of 20 kV at a 36.5 ºC thermostated capillary. UV detection regions were varied as per maximum absorbance of each drug (ranging from 220 to 317 nm).

A sequence was created by MATLAB shuffle command and was run for all the analysis performed including CE-FA analysis to account for biasness.

5.2.8 EKC Methodology

Traditional methods such as ultra-filtration were used as one of the approaches for the investigation of enantioselectivity, whereby a free drug fraction would be separated from the bound drug once the drug-protein equilibrium had been reached. This method involves the ultra-filtration of pre-equilibrated samples containing HSA and a drug, thus resolution and analysis of unbound fraction of enantiomers performed with EKC.

Different concentrations of CD were prepared to try and make the separation feasible; four different concentrations were prepared 25, 50, 75, and 100 μM. For this study the instrument was programmed in such a way that the CD be injected before and after the sample into the capillary. Injections were done for 5s with the aid of hydrodynamic injection at 50 mbar in each case at the anodic end of the fused silica capillary by a potential of 20 kV at a 36.5 ºC thermostated capillary. UV detection wavelengths were set to suit each compound.

5.3 Computational: Docking Methodology

The complexes of HSA protein for site I (pdb id: 2BXD) and site II (pdb id: 2BXG) were obtained from RCSB protein data bank (http://www.rcsb.org). For protein preparation, the whole enzyme was selected and hydrogen atoms were added to it. Docking studies were performed using the CDOCKER module of DS. CDOCKER is a grid-based molecular docking method where the receptor is held rigid while the ligands are allowed to flex during the refinement. The CHARMm force field was used as an energy grid force field for docking and scoring function calculations. Random ligand conformations were generated from the initial structure through high temperature molecular dynamics, followed by random rotations which were further refined by grid-based (GRID 1) simulated annealing and a final grid-based minimization. Of the 10 best poses, one (conformation) having highest docking score (-CDOCKER energy) was used for the binding energy calculations and further analysis. The higher negative value of binding energy represents more favorable binding of the complex.

CHAPTER 6

RESULTS AND DISCUSSION

This chapter discusses results obtained experimentally for the interaction of NSAIDs with HSA and supported by computational work. This study was divided into three sections for experimental work: (i) Interaction studies of NSAIDs with HSA protein using CE-FA, (ii) Interaction studies of NSAIDs with HSA protein using CE-CZE and (iii) Enantioseparation of the racemic NSAIDs with the aid of a chiral selector using CE-EKC. A comparison between the results obtained by CE-FA and CE-CZE are presented. On the other hand, molecular simulations of drug-protein interactions were perfomed by docking and the results are compared to experimental findings.

6.1 Interaction studies of NSAIDs with HSA protein using CE-FA.

Trial runs were performed on the NSAIDs using the wavelengths obtained from literature and the wavelength with the best signal was chosen as represented on the last column in Table 6.1.

Table 6.1: Tabulation of literature wavelengths and the best wavelengths obtained for each drug for the trial runs by CE (references sited in Appendix 1a).

Compound	Literature Wavelength/nm	Best Wavelength/nm
Fenoprofen	214	220
Fenbufen	279	285
Naproxen	235, 210	220
Flurbiprofen	246, 254	246
Ketoprofen	262, 256	220
Indoprofen	220, 254, 280	220
Ibuprofen	220, 226,253	220
Ketorolac	230, 243, 317	317

This section examines the interaction of eight NSAIDs with HSA protein employing CE-FA. An external calibration curve for each drug was plotted to examine the linearity between the standards and signals obtained, with the concentrations of the standards ranging from 50 to 250 μM.

The electropherogram in Figure 6.1 shows a reproducibility that is not so good for fenoprofen in terms of migration times for the five calibration standards. It can be observed that the peaks (saturations) are not well superimposed due to a slight shift in peak migration times. However, that was accounted for by peak normalization performed during the preparation of the calibration curve. Good correlation coefficients were obtained (0.9933 and 0.9896) on the calibration graphs for replicates one and two of fenoprofen. Concentrations of 50, 75, 120, 180 and 250 µM were chosen since they bracketed the concentration prepared for interaction with the HSA protein. From the electropherogram in Figure 6.1, it is noted that the peaks/saturations are plateau at the apex, due to large volumes being injected into the capillary (Knjazeva and Kaljurand 2010). In all the experiments the peak heights for calibration standards of the drugs increased consistently with an increase in concentration. Figure 6.1 shows an electropherogram with fenoprofen standards and Figure 6.2 with flurbiprofen standards at a wavelength of 220 nm and 246 nm respectively. The migration time for fenoprofen was 10.598 ± 0.42, with a limit of detection (LOD) 5.1 µM.

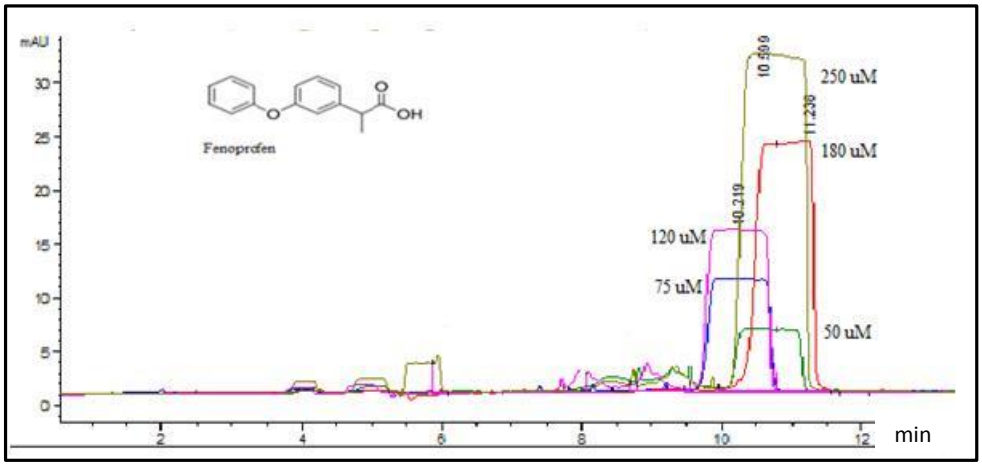

Figure 6.1: CE-FA electropherogram showing calibration standards 50, 75, 120, 180 and 250 µM of fenoprofen injected by applying 50 mbar for 60s. The capillary was thermostated at 36.5 °C, with a normal polarity of 20 kV with 67 mM sodium dihydrogen phosphate buffer used as BGE. UV-detection was done at 220 nm.

Figure 6.2 also shows a not so good reproducibility for flurbiprofen, with a good increase in peak height observed with each increase in the concentration. The shift in migration times was accountated for by means of peak normalization during preparation of a calibration curve. The migration time for flurbiprofen was 11.874 ± 0.49, with an LOD of 4.2 µM.

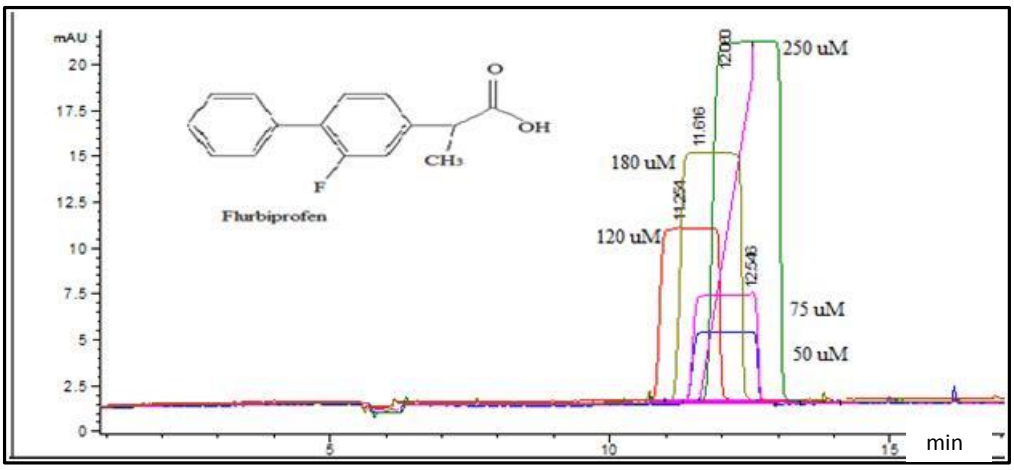

Figure 6.2: CE-FA electropherogram showing 50, 75, 120, 180and 250µM of flurbiprofen standards obtained using 67 mM sodium dihydrogen phosphate buffer as a BGE, 20 kV voltage applied and 60 s injection time.

The calibration graph in Figure 6.3 shows the linearity between the calibration standards of fenoprofen for the first replicate while the rest are shown in Appendix1a. The correlation coefficients for the eight drugs ranged from 0.9933 to 0.9921. In the graph below peak normalization was performed to account for the peak shifts.

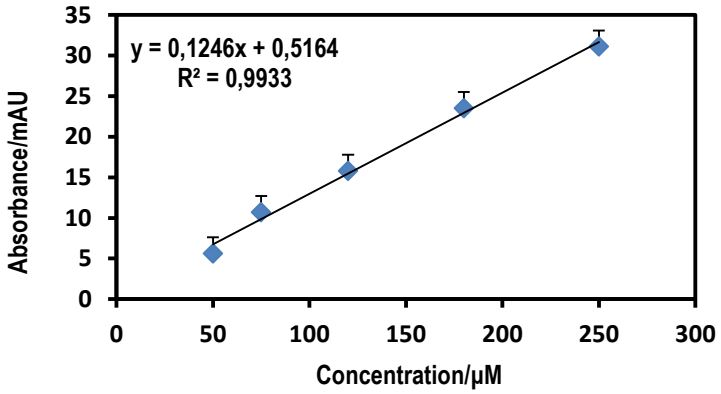

Figure 6.3: External calibration graph for five fenoprofen standards, showing linearity between the standards as well as error bars.

In CE-FA, the separation is based on the differences in the electrophoretic mobilities of the free and bound ligand (Jia et al 2002). In principle the sample mixture is introduced to the buffer filled system as a large plug and based on the separation of a ligand from the protein and ligand-protein complex (Østergaard and Heegaard 2003).

The electropherogram in Figure 6.4 is for a mixture of 200 µM fenbufen and 525 µM HSA showing the free drug zone and the protein zone where the drug is bound. In principle, when the steady state conditions and equilibrium are maintained the bound drug remains in the protein zone (where the protein and bound drug zones overlap). The unbound drug leaves the protein zone due to differences in electrophoretic mobilities (Østergaard and Heegaard 2003). An arrow is used in Figures 6.4 and 6.5 to show maximized free drug zone which is used for the determination of the free drug concentrations with the aid of an external calibration graph. All the experimental analysis for the interactions were conducted near physiological conditions i.e. 36.5 °C capillary temperature, buffer pH of 7.4, 525 µM of HSA and the NSAIDs drugs varied from 50 - 300 µM (Knjazeva and Kaljurand 2010; Guillaume et al. 2002).

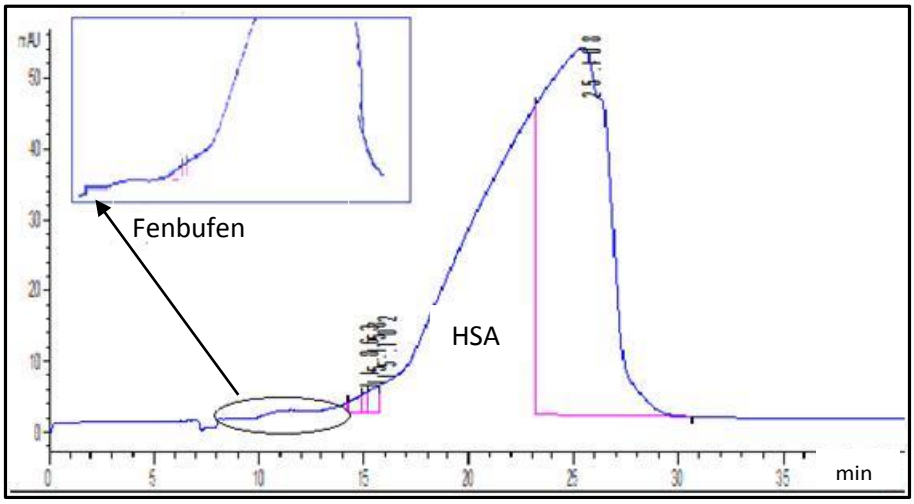

Figure 6.4: CE-FA electropherogram showing a mixture of 200 µM fenbufen and 525 µM HSA obtained using 67 mM sodium dihydrogen phosphate buffer, 20 kV and 60 s injection time.

In both Figures 6.4 and 6.5; it is noted that the differences between the electrophoretic mobilities of the free drug and the protein are sufficient to differentiate between the protein and the free drug peaks. Due to a high injection time, the injection volume becomes larger giving rise to plateu peaks which are proportional to the concentration of the free drug initially present in the sample. The calibration graphs plotted are used to determine the degree of binding of each drug to HSA protein with the help of the free drug obtained from the analysis of the mixture.

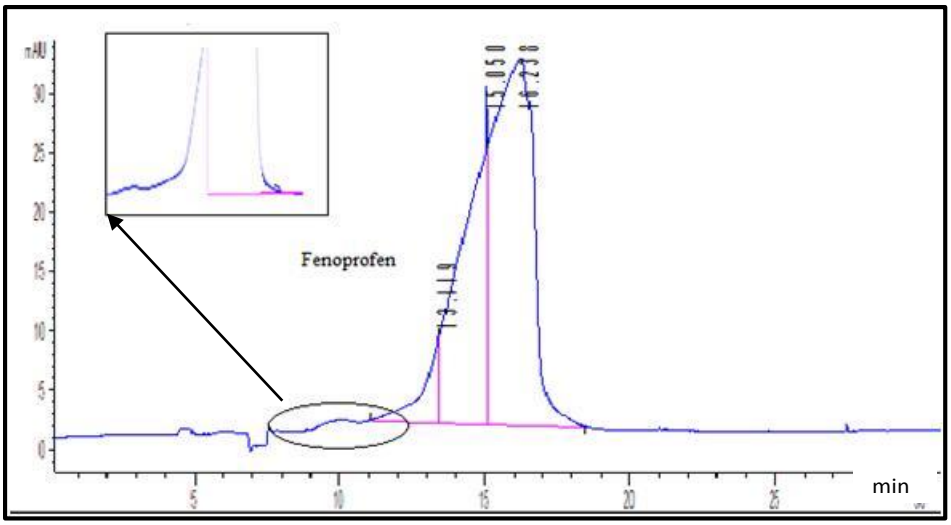

Figure 6.5: CE-FA electropherogram showing a mixture of 200 µM fenoprofen and 525 µM HSA obtained using 67 mM sodium dihydrogen phosphate buffer, 20 kV and 60 s injection time.

6.1.1 D and P constant experiments

It is important to obtain experimental conditions that will maintain equilibrium between all the contents. The main benefits of using CE-FA are the near-physiological conditions, ease of automation, robustness and accuracy of results. The method is said to be robust due to the plateau peaks which are not affected by the shift in migration times, changes in EOF, or in voltages (Knjazeva and Kaljurand 2010; Martínez-Pla et al. 2004; Østergaard and Heegaard 2003). In many cases, CE-FA is employed in the estimation of binding constants (K) in binding studies. However it can be applied for the estimation of K in the range of 10^3– 10^8 M^{-1}. For very strong interactions where K >10^8 M^{-1}, the free drug height on the frontal peaks become too small to be measured experimentally. On the contrary with lower interactions bearing K <10^3 M^{-1} becomes difficult to measure the free drug peak height, as it is hard to differentiate between it and the drug-protein complex peak (Tanaka and Terabe 2002).

The exact concentrations prepared for fenoprofen are represented by D_{exp} and d represent the calculated shown in Table 6.2. It is important to use exact concentrations in interaction studies because the mass used is crucial for understanding the nature of the interactions. From the table below, the data presented shows that experimental design was structured in such a way that the 'P' parameter was held constant while D was varied.

For all the drugs experimental design was the same. Experimetal designs for the other drugs are shown in Appendix 1b. Regarding the experimental design, it was observed that with a variation of D_{exp}, the concentration of d increased, as D_{exp} increased while keeping Pconstant. Table 6.2 shows the experimentally obtained results of the pharmacokinetic data for each drug.

Table 6.2: Experimental design for fenoprofen and pharmacokinetic parameters obtained using Excel, where P was kept constant throughout.

ID	D, µM	P, µM	D_{exp}, µM	P_{exp},µM	d,µM	d/P	K, x10^3	Log K1	D/P
	50		51		8.03	0.0152	9.27	3.97	0.0962
	100		101		9.54	0.0175	15.6	4.19	0.192
	150		152		11.4	0.0197	18.9	4.28	0.289
	200	525	203	527	13.8	0.0252	17.3	4.24	0.385
	250		253		16.5	0.0288	16.3	4.21	0.481
	300		304		18.1	0.0313	15.0	4.18	0.577

D: Total drug concentration, P: total protein concentration, D_{exp}: Total prepared drug concentration used during the experiment. P: Total concentration of protein, P_{exp}: Total prepared protein concentration used during the experiment. d: free drug concentration

6.1.2 Statistical Analysis

As previously mentioned, saturation binding studies of NSAIDs to HSA-protein were done by CE-FA and CE-CZE using GraphPad prismas shown in Table 6.3 for CE-FA. In studies such as saturation binding of ligands, the concentration of the ligand has to be varied and then the binding measurements are investigated. In this case, data analysis were done using a non-linear regression method to establish best-fit value parameters. Unlike linear regression, the non-linear regression doesn't fit the data in a straight-line, but has an advantage of finding a curve/line that best fits the data (Motulsky and Brown 2006). It does this by making a hypothesis about the scatter of data around the curve. Non-linear regression assumes that the scatter of data around an ideal curve follows a Gaussian curve or a normal distribution. With this particular regression, the aim is to adjust the values of the concentration that triggers a reaction halfway between the minimum and maximum responses and the slope of the curve. This is achieved by minimizing the sum of the squares of the Y-value distances between the points (Motulsky and Brown 2006).

Included in Table 6.3 are the best fit values for each drug such as the maximum number of binding sites (Bmax) and the ligand concentration that binds to half the receptor sites (HSA in this case) at equilibrium (Kd), then the sum of square and more.

Table 6.3: FA results for the NSAIDs under investigation obtained by GraphPad Prism for the estimation of best fit values like Bmax, Kd and NS using the non-linear regression. Included in the table are the absolute sum of squares, R square, and Sy.x (graphic representation is in Appendix 1c).

	No. of data points	**Best-fit values**					
		Bmax	Kd	NS	**R square**	**Absolute Sum of Squares**	**Sy.x**
Naproxen	6	~ 2.500	~ 7911	~ 0.09289	0.9363	0.009676	0.06956
Ketoprofen	6	16.76	2.453	-0.01094	interrupted	interrupted	interrupted
Indoprofen	6	~ 1722	~ -1.318e+010	~ 0.01204	0.8544	0.01853	0.09626
Flurbiprofen	6	~ 118.0	~ 0.02178	~ 0.03111	0.9839	0.002368	0.03441
Fenoprofen	6	~ 119.3	~ 0.02178	~ 0.03146	0.9839	0.002418	0.03477
Fenbufen	6	97.61	0.04940	0.01366	interrupted	interrupted	interrupted
Ketorolac	6	~ 10244	~ -3.342e+008	~ 0.08659	0.9676	0.004870	0.04934
Ibuprofen	6	4.947e+016	~ -6.135e+023	0.03519	0.9550	0.006673	0.05776

*Bmax: the maximum specific binding in the same units as Y, *Kd: the equilibrium binding constant, in the same units as X, *Sy.x: the standard deviation of the residuals

In the case of ketoprofen, all the data obtained were low as compared to the other drugs of the same class and the absolute sum of squares, but Sy.x and the R square values could not be obtained, the latter was true for fenbufen as well. Even though, the non-linear regression tries to minimize the sum-of-squares of the data, one experimental error leads to outliers, which causes errors in the calculations of the sum-of squares thus leading to errors in end results. For this purpose it is of great importance to conduct analysis for the determination of outliers in a set of data (Motulsky and Brown 2006).

In Figure 6.6 it is observed that with linear regression, the goal was to obtain a slope and an intercept that is close to the data giving a straight line, in other words it takes an average and obtains a line which will be a model used to assess the points which are most likely to be correct or accepted. However, with the non-linear regression it is noted that the line of a model takes the shape of a curve in order to find the best fit values that will accommodate the whole experimental data.

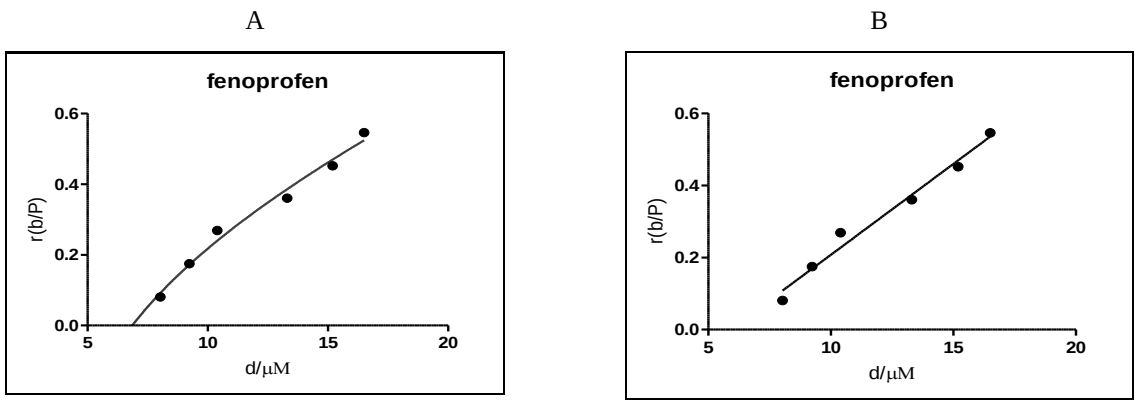

Figure 6.6: Graphical representation of A: nonlinear and B: linear regressions of fenoprofen obtained by GraphPad Prism with r on y-axis and d on the x-axis (d is the concentration of free drug).

The statistical evaluation data obtained with MATLAB calculations for the determination of outliers are presented in Table 6.4 using the z-score and the Grubbs' test. The evaluations were done based on logK instead of K, because K gives relatively higher values which makes it difficult to interpret the extent of binding. The z-score is considered as a method for the identification of outliers, showing how much the data point deviates from a mean or a specific point. The approach used in this study is such that the value in question is analyzed on how much it deviates from the median.

Table 6.4: Statistical analysis done by MATLAB calculations on the FA data of the drugs under investigation for the estimation of outliers using the Z-score and the Grubbs' test.

Compound	No. of data points	**Z- Score on Log K**			**Grubb's Test on Log K**			Eliminated Points
		Z-Critic	Median	Eliminable Points	DCV (%)	DTV(%)	Eliminable Points alpha = 2.5 %	
Naproxen	6	2	4.146	none	40.40	90.3	1 and 6	none
Ketoprofen	6	2	4.274	none	48.03	64.0	1 and 6	none
Indoprofen	6	2	3.850	none	44.72	81.3	1 and 6	none
Flurbiprofen	6	2	4.580	none	46.37	81.3	1	none
Fenoprofen	6	2	4.567	none	39.00	81.3	1 and 6	none
Fenbufen	6	2	4.897	none	43.66	81.3	1 and 6	none
Ketorolac	6	2	4.691	none	33.55	81.3	1 and 6	none
Ibuprofen	6	2	4.191	none	30.02	81.3	1 and 6	none

*DCV: decrease in the calculated variance, *DTV: decrease in the tabulated variance

From Table 6.4 the median value computed for fenoprofen is 4.567, which is demonstrated by the dotted lines in Figure 6.7A. Based on the analysis performed, no values were discarded or regarded as deviating too much from the median. With all the compounds the tests were performed with the z-score = 2. All data points were retained at z-score = 2 for all the compounds, therefore no need of expanding the range to 2.5. For indoprofen at z-score = 2 for K results point 6 was regarded as eliminable, but retained at z-score 2.5. However, for logK results at z-score = 2 point 6 was retained. In Table 6.4 no points were discarded for indoprofen, since the data presented is only for logK. More graphical representation of all the above tabulated results are presented in Appendix 1d.

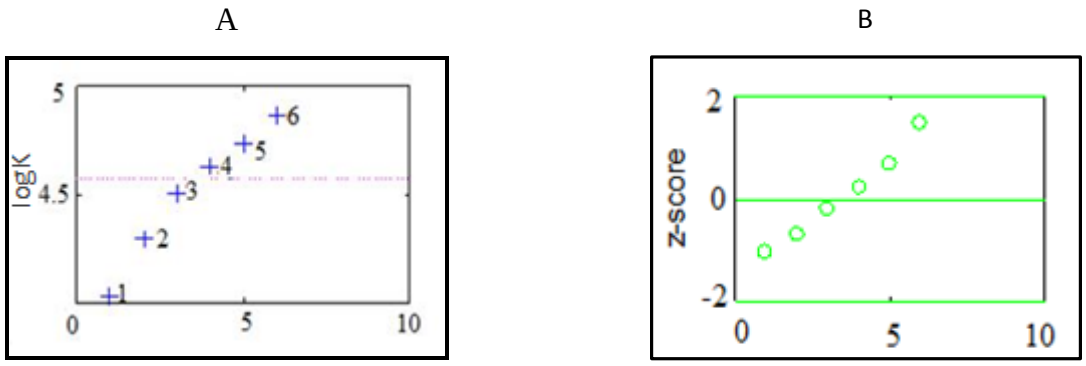

Figure 6.7: Z-score test diagrams for fenoprofen generated from MATLAB based on the data obtained via CE-FA. A: Dotted lines represent the median of the data set, B: represents the z-critic at which the analysis was conducted.

Table 6.4 also consists of data computed using the Grubbs' test approach in MATLAB. The Grubbs' test is also considered as a statistical test for the treatment of outliers; however unlike the z-score the Grubbs' test compares outlying data points to the average and a standard deviation of a set of data. The test is done by calculating Grubbs' statistic value G defined as:

$$G_{calc} = \frac{|Y_{outlier} - \bar{Y}|}{S} \qquad 6.1$$

Where S is the standard deviation of the set of data, $Y_{outlier}$ is the data point in question, and $\bar{Y}$ is the mean of the set of data. The calculated G is then compared to the tabulated G and point is either retained or discarded. If the calculated G is smaller than the G from tabulated then the point should be retained, but if the calculated value is greater than the tabulated the outlying point should be discarded.

Once the point has been discarded a new mean and standard deviation for the remaining data points has to be calculated. In the case of fenoprofen, the calculated G value is 39.00 while the tabulated is 81.3, from these values it is observed that the tabulated G is greater than the calculated value 39.00 meaning that data point number 1 and 6 which were in question are retained and no longer regarded as outliers. In Figure 6.8 the small circle outside the line demonstrates where the DCV value for fenoprofen lies in a graphical format. The value of 40.4 % is less than the DTV and points number 1 and 6 in questions are retained. Other graphical representations for the other seven compounds are available in Appendix 1e.

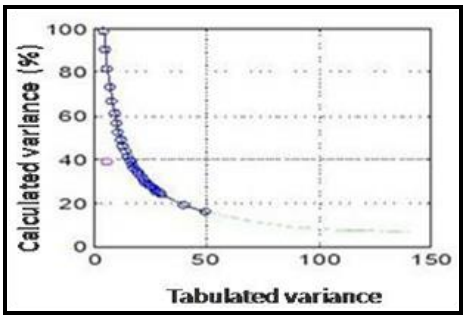

Figure 6.8: Grubbs' test graphical demonstration of fenoprofen generated from MATLAB based on the data obtained via CE-FA. The small circle represents the decrease in calculated variance.

Frontal analysis has demonstrated the qualities of being an effective alternative to chromatographic methods suitable for the analysis of strong binding properties of proteins such as NSAIDs (Jin et al 2005). This is because with FA unbound drug concentrations are measured at the plateau peak heights. Table 6.5 show results for the drug to protein binding parameters obtained by the Klotz's plot, Scatchard's plot and linear regression using MATLAB calculations. In each case the number of binding sites (n) on the protein molecule, logarithmic of the binding constant (logK) and the logarithmic of the number of binding sites by binding constant [log(nK)] were estimated using the three methods. Current studies were done with the P variable kept constant throughout the experiments, and only the drug concentrations varied from 50 – 300 μM. When looking at the table similarities as well as some diversities are observed; logK results are observed to be higher than the others for ketorolac and fenbufen experiments (around 5, when it is around 4 for the rest of the drugs). Although there are some discrepancies in the values of logK but they suggests that this class of drugs has a stronger binding affinity towards HSA.

Table 6.5: Pharmacokinetic parameters of all the NSAIDs under investigation obtained using MATLAB calculations with the data obtained by Frontal Analysis.

	No. of data points	**Klotz**			**Scatchard**			**Y-regression**		
		n1	logK1	log(n1K1)	n1	logK1	log(n1K1)	n1	logK1	log(n1K1)
Naproxen 1	6	-0.015	4.466	2.635	-0.017	4.462	2.694	-0.0150	4.466	2.639
Ketoprofen 1	6	-0.038	4.570	3.145	-0.065	4.536	3.350	-0.044	4.558	3.199
Indoprofen 1	6	-0.101	4.198	3.202	-0.119	4.176	3.252	-0.114	4.178	3.235
Flurbiprofen 1	6	-0.130	4.735	3.849	-0.210	4.661	3.984	-0.167	4.692	3.916
Fenoprofen 1	6	-0.104	4.752	3.767	-0.157	4.695	3.892	-0.126	4.723	3.825
Fenbufen 1	6	-0.095	5.060	4.040	-0.139	5.019	4.163	-0.112	5.039	4.088
Ketorolac 1	6	0.064	5.829	4.635	0.064	5.812	4.616	0.0628	5.786	4.584
Ibuprofen 1	6	-0.052	4.492	3.207	-0.077	4.457	3.345	-0.0587	4.480	3.248

Figure 6.9 below shows a graphical representation of the naproxen results reported in Table 6.5; in addition an experimental design structure and non-linear plots are also shown. Graphs for the other drugs can be found in Appendix 1f. When looking at the plots for simplex models in the figure below when P is kept constant, A: shows experimental design structures with protein constant design when the concentration of free drugs and the prepared drugs increases. It is observed that for the Klotz's plot in B, the points are very close to each other, whereas with the Scatchard's plot in C the points are constantly increasing and lie within the regression curve. E: shows the non-linear plot obtained using the SIMPLEX algorithm in MATLAB calculations.

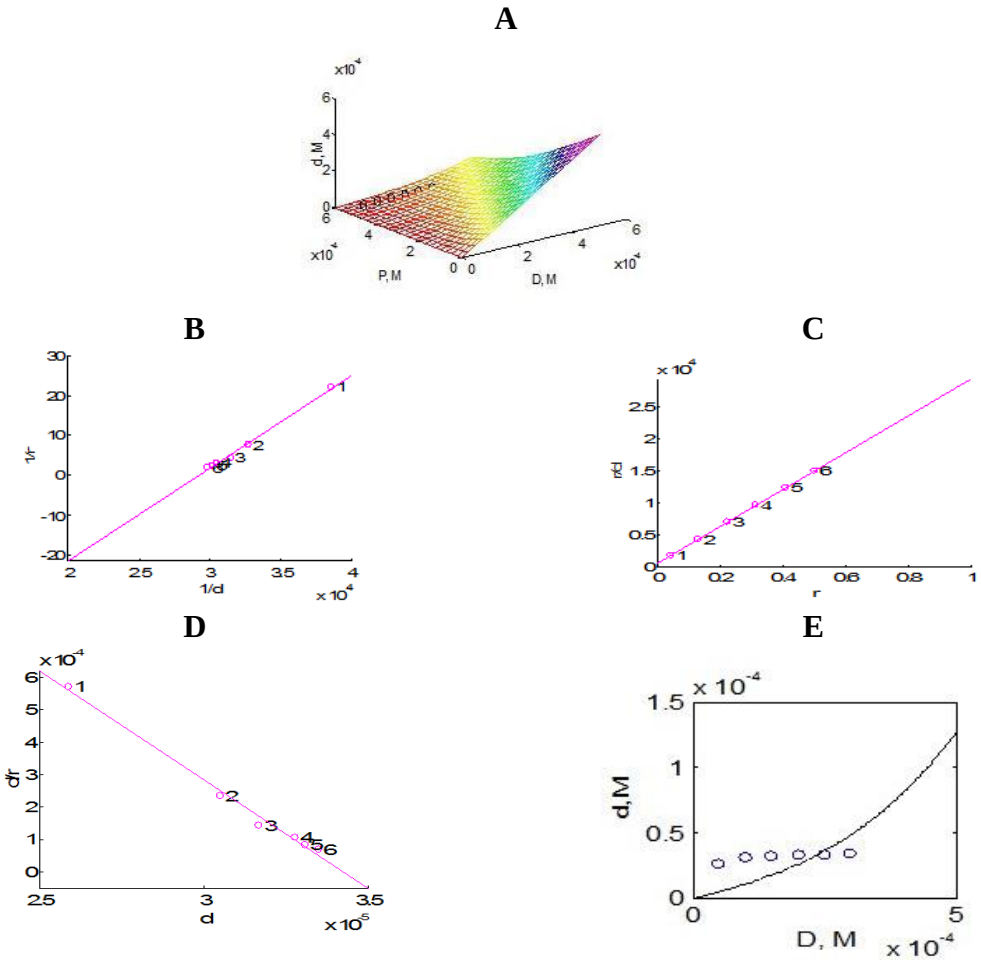

Figure 6.9: Frontal Analysis results for naproxen shown in five plots, A: Protein constant design, B: Klotz plot for estimation of log*K*, C; scatchard plot, D; Y-regression plot and E; non-linear plot obtained using the SIMPLEX algorithm.

6.2 Interaction Studies of NSAIDs with HSA protein using CE-CZE method

This section involves a study of the interactions between HSA and NSAIDs using the CE-CZE method with the view to obtaining pharmacokinetic properties/behaviour of NSAIDs towards HSA in comparison to the findings of CE-FA. The shape of peaks obtained in CZE have higher peak efficiencie as opposed to the ones obtained by FA due to the electroosmotic flow (Gübitz and Schmid 2008). For all eight drugs under investigation, an external calibration was prepared with the concentrations of the standards ranging from 50 to 250 µM. This range of concentrations was based on the idea of bracketing the experimental drug concentrations used for the drug-protein interactions and to extrapolate the unknowns from the calibration curve. The prepared standard concentrations were 50, 75, 120, 180 and 250 µM, while the protein concentrations were kept constant at 525 µM throughout the experiment.

Figure 6.10 shows the electropherogram for ibuprofen calibration standards with a consistent increase in peak heights with every increase in concentration. Poor reproducibility is observed between the five peaks in terms of migration times and therefore peaks are not superimposed when overlayed due to a slight shift in retention times. The migration time of ibuprofen was 12.12 ± 0.18 with an LOD of 3.9 µM.

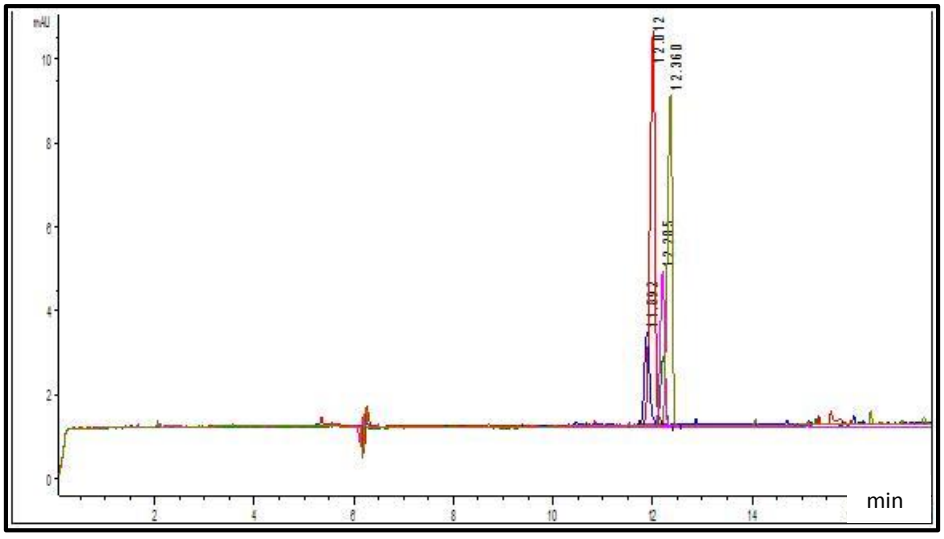

Figure 6.10: Electropherogram showing calibration standards 50, 75, 120, 180 and 250 µM of ibupofen injected by applying 50 mbar for 5 s at a capillary temperature of 36.5 °C, with a normal polarity of 20 kV. 67 mM concentration of sodium dihydrogen phosphate buffer was used as BGE with UV-detection done at 220 nm.

To account for the peak shifts in Figure 6.10, peak normalization was performed during the preparation of the calibration curve. Good correlation coefficients of 0.9896 and 0.9905 were obtained for replicate one and two of ibuprofen respectively. Calibration curves showing linearity between calibration standards of the other seven drugs are presented in Appendix 2a.

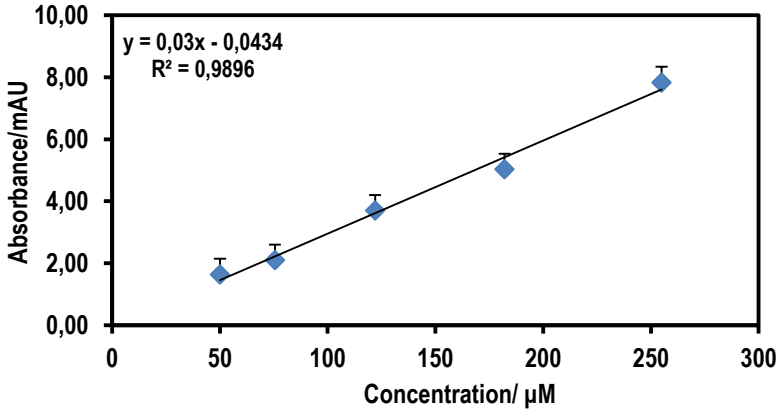

Figure 6.11. External calibration graph for five ibuprofen standards, showing linearity between the standards and error bars included.

The next section 6.2.1 deals with the actual drug-protein interactions for the determination of pharmacokinetic properties. These properties are ruled by the strength of the drug-protein complex formation. Free drug is responsible for the pharmacological responses (Amranet al.2008). The type of buffer and concentration and pH are important in such experiments since, the type and nature of the binding merely dependent on the physicochemical properties of the drugs. Hence, in order to estimate the pharmacological properties one had to mimic the conditions of the body plasma for this study.

6.2.1 D and P constant experiments

The data in Table 6.6 below was extracted from GraphPad Prism using the non-linear regression method for the estimation of the best fit values in the binding interaction studies. The experimental data obtained using CE-CZE was employed to compute the data reported in Table 6.6 by fitting total and non-specific binding creating a graphical representation of a saturation isotherm. Looking at fenoprofen results there was an error when the GraphPad was attempting to generate results for the sum of squares, r-square and sy.x. It is such errors that stress the need for statistical evaluations of experimental data since this could have risen from an outlier.

Table 6.6: CZE results for the eight drugs under investigation obtained by GraphPad Prism for the estimation of best fit values like Bmax, Kd and NS using the non-linear regression.

	No. of data points	Best-fit values			R square	Absolute Sum of Squares	Sy.x
		Bmax	Kd	NS			
Naproxen	6	~ 1.794	~ 24301	~ 0.060	0.831	0.025	0.112
Ketoprofen	6	~ 30347	~-1.234e+010	~ 0.005	0.922	0.007	0.059
Indoprofen	6	6.721e+010	~ -.735e+019	~ 0.011	0.852	0.017	0.095
Flurbiprofen	6	~ 1.008	~ 8313	~ 0.086	0.996	0.001	0.017
Fenoprofen	6	72.86	0.08252	0.032	interrupted	interrupted	interrupted
Fenbufen	6	~ 1.339	~ 1272	~ 0.13	0.974	0.004	0.046
Ketorolac	6	~ 1.082	~ 4389	~ 0.095	0.970	0.005	0.049
Ibuprofen	6	~ 7.175	~ 0.5375	~ 0.017	0.996	0.0006	.0169

*Bmax: the maximum specific binding in the same units as Y, *Kd: the equilibrium binding constant, in the same units as X, *Sy.x: the standard deviation of the residuals

The graphs were plotted using 'r' vs. 'd' values, where 'r' is the fraction of bound drug per molecule of protein and 'd' is the free drug. 'r' was computed using the following equation:

$$r = \frac{b}{P} = \frac{D-d}{P} = \sum_{i=1}^{m} n_i = \frac{K_i d}{1+K_i d} \quad 6.1$$

'P' is the total protein concentration and 'b' is the bound drug concentration after equilibrium, calculated by subtracting the free drug (d) from the total drug concentration (D). The number of classes of independent active sites in the protein is represented by 'm', each class '1' accounting for 'n_1' binding sites, and 'K_1' the affinity constant of the binding interaction. Generally, the protein HSA has one binding site with high-affinity when it binds to small molecules therefore, m =1 is normally accepted. Where m =1 the complex Equation 6.1 above can be reduced into two simplified models shown below giving 'n_1' and 'K_1'parameters.

$$K_1 = \frac{1}{d}\frac{r}{n_1 - r} \quad 6.2$$

$$n_1 = r\frac{1+K_1\,d}{K_1 d} \quad 6.3$$

Sabela and co-workers proposed Equation 6.4 that combines Equation 6.2 and 6.3 collectively. This equation however, requires the previous algorithms for assumption of 'n_1' and estimation of 'K_1' in Equation 6.2 for 'n_1' a default value can be used (Sabela et al. 2012).

This study was based on a simulation that m =1, it is however required to consider a situation where m >1 since that might have an impact on the estimations based on the m =1 simulation. Experimental designs were done such that the multiple bindings with m >1 were look at by calculation of $\log K_1$. Equation 6.4 is a model connected to the experimental design, and is actually based on the assumption that there is one major protein binding site that NSAIDs bind to under physiological conditions (Diniz et al. 2008; Sabela et al. 2012). Equation 6.4 relates to the concentration of free drug 'd' with the prepared concentrations of protein and drug indicated by 'P' and 'D' respectively. 'K_1' correspond to the primary affinity constant with 'n_1' being the primary binding site (Martínez-Gómezet al. 2007). Both 'K_1' and 'n_1' parameters were obtained by fitting the free drug concentration measure experimentally into Equation 6.4.

$$d = \frac{(1-K_1 D+ n_1 K_1 P)+\sqrt{(1-K_1 D+ n_1 K_1)^2+4K_1 D}}{2 K_1} \qquad 6.4$$

Table 6.7 shows the experimental design used for the estimations of logK in connection with the ratio of D/P for flurbiprofen. It can be observed that during the course of the experiment 'P' was kept constant throughout at a concentration of 525 μM whilst the 'D' concentration was varied from 50-300 μM. As the concentration of the free drug increases the K increases. The methodology used for establishing the pharmacokinetic properties of these drugs at physiological conditions was clearly explained in section 5.1.7.

Table 6.7: Experimental design for flurbiprofen and pharmacokinetic parameters obtained using MATLAB calculations.

ID	D, μM	P, μM	D_{exp}, μM	P_{exp}, μM	d,μM	d/P	K	$LogK_1$	D/P
	50		50.2		10.7	0.020	6479.8	3.81	0.10
	100		100.4		11.9	0.023	11742.1	4.07	0.19
	150	525	150.6	527	12.8	0.024	15086.6	4.18	0.29
	200		200.8		14.1	0.027	16224.3	4.21	0.39
	250		251.0		15.2	0.029	16265.6	4.21	0.47
	300		301.2		16.0	0.030	15519.0	4.19	0.57

D: Total drug concentration, P: total protein concentration, D_{exp}: Total prepared drug concentration used during the experiment. P: Total concentration of protein, P_{exp}: Total prepared protein concentration used during the experiment. d: free drug concentration.

In Figure 6.12 it is observed that with linear regression, the goal was to obtain a slope and intercept that is close to the data giving a straight line. In other words it takes an average and obtains a line which will be a model used to assess the points which are most likely to be correct or accepted. With the non-linear regression, it is noted that the line of a model takes a shape of a curve in order to try to find best fit values that will accommodate the whole experimental data.

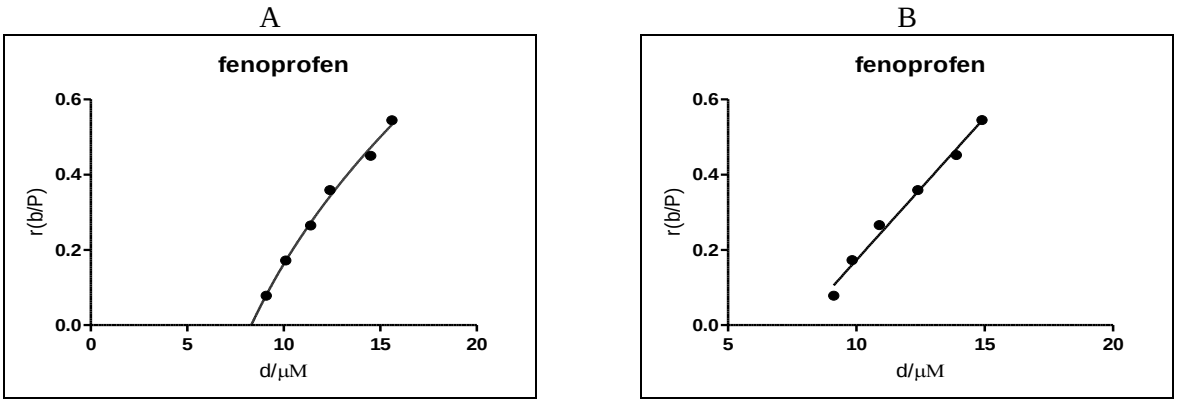

Figure 6.12: Graphical representation of non-linear (A) and linear regressions (B) of fenoprofen obtained using GraphPad Prism. r on the y-axis and d on the x-axis (concentration of free drug).

6.2.2 Statistical Evaluation

Introducing statistical evaluation for experiments is helpful in elimination of outliers. It helps in verifying that the method can be used for investigation of interaction to protein with other drugs apart from NSAIDs. The data reported in Table 6.8 were generated using MATLAB calculations for calculated logK. From the experimental data obtained by CE-CZE, 'K' was determined and hence logK to avoid big numbers yielded by K. The reported data in the Table 6.8 for the NSAIDs were obtained using z-critical = 2.0 with the exception of ibuprofen where z-critical had to be extended to 2.5. At z-critical = 2.0 there was one eliminable point but was retained at z-critical = 2.5, resulting in all the points being retained throughout the calculations. For z-critical = 2, and z-critical = 2.5 it was however, noted that the median was the same.

Table 6.8: Statistical analysis done by MATLAB calculations on the CE-CZE data of the drugs under investigation for the estimation of outliers using the Z-score and the Grubbs' test.

	No. of data points	Z- Score on Log K			Grubb's Test on Log K			
		Z-Critic	Median	Eliminable Points	DCV(%)	DTV(%)	EliminablePoints alpha = 2.5 %	Eliminated Points
Naproxen	6	2	4.174	none	39.63	81.3	1 and 6	None
Ketoprofen	6	2	3.761	none	29	81.3	1 and 6	None
Indoprofen	6	2	3.833	none	44.98	81.3	1 and 6	None
Flurbiprofen	6	2	3.347	none	26.32	64	1 and 6	None
Fenoprofen	6	2	4.589	none	26.76	64	1 and 6	None
Fenbufen	6	2	4.515	none	34.51	64	4	None
Ketorolac	6	2	4.572	none	38.45	81.3	1 and 6	None
Ibuprofen	6	2.5	3.958	none	47.17	81.3	1 and 6	None

Figure 6.12 represents the z-score test diagrams for flurbiprofen generated by MATLAB based on the experimental data obtained from CE-CZE method. In the Figure 6.13A a dotted line below 5 represents the median of the set of data which has an exact value of 3.347 reported from Table 6.8, Figure 6.13B shows that all flurbiprofen points lie below z-critical = 2. Based on the data reported no values were discarded. All the values were in line, or not too far from the median allowing for them to be retained throughout the test. Graphical representations for the other seven drugs are attached in Appendix 2d**.**

A B

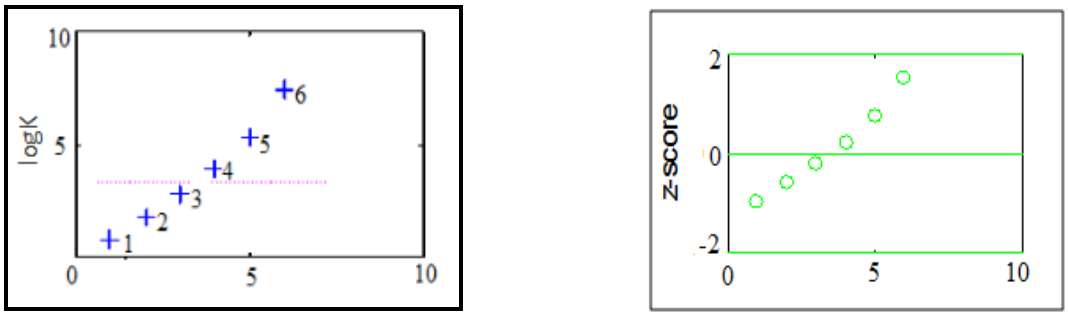

Figure 6.13: Z-score test diagram for flurbiprofen generated from MATLAB based on the data obtained via CE-CZE. Dotted line on A: represent the median of the data set. B: represents the z-critic at which the analyses were conducted.

Figure 6.14 below shows a graphical representation of flurbiprofen results obtained using Grubbs' test on MATLAB. The data used to generate the plot were extracted from CE-CZE experimental data. This test identifies the outliers by comparing the experimental data to the average and the corresponding standard deviation. It was emphasized in Section 6.1.2 that in Grubbs' test, a G value is calculated and then compared to the tabulated value. In Table 6.8 the G value is expressed as (DCV), and the tabulated value as DTV. In Figure 6.14 a circle representing the DCV above 20 which corresponds to the exact value of 26.32. Since DCV is greater than DTV it means that data points 1 and 6 were retained. This plot provides insight on where the calculated value lies exactly in a graphical representation, such plots for other seven drugs are represented in Appendix 2e.

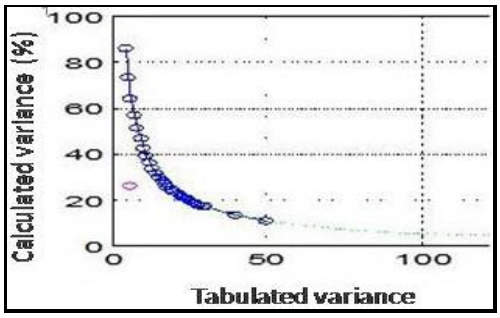

Figure 6.14: Grubbs' test graphical demonstration of flurbiprofen generated from MATLAB based on the data obtained via CE-FA. The small circle represents the decrease in calculated variance.

The results shown Table 6.9 were obtained using MATLAB calculations for the determinations of pharmacokinetic properties by Klotz's plot, Scatchard's plot and a linear regression. The values for the number of binding sites on the protein molecule, the logarithmic of the binding constants and the logarithmic of the binding constants for the number of binding site were obtained using the three methods. For the current study the 'P' was kept constant throughout the analysis with only the prepared drug (D) concentrations being varied from 50-300 μM. Concentration of free drug then used for the estimations of the pharmacokinetic parameters. Looking at the data presented in the table some similarities as well as some discrepancies were observed.

Table 6.9: Pharmacokinetic parameters of all the NSAIDs under investigation obtained using MATLAB calculations with the data obtained by CE-CZE method.

	No. of data points	Klotz			Scatchard			Y-regression		
		n_1	$logK_1$	$log(n_1K_1)$	n_1	$logK_1$	$log(n_1K_1)$	n_1	$logK_1$	$log(n_1K_1)$
Naproxen	6	-0.041	4.506	3.124	-0.064	4.474	3.282	-0.046	4.497	3.164
Ketoprofen	6	-0.972	3.564	3.552	-0.899	3.593	3.547	-1.270	3.466	3.569
Indoprofen	6	-0.096	4.200	3.185	-0.114	4.177	3.237	-0.109	4.180	3.218
Flurbiprofen	6	-0.048	4.785	3.471	-0.074	4.753	3.627	-0.055	4.773	3.514
Fenoprofen	6	-0.073	4.808	3.672	-0.114	4.763	3.822	-0.086	4.789	3.725
Fenbufen	6	0.436	4.894	4.533	0.010	4.973	2.958	0.203	6.264	5.573
Ketorolac	6	-0.053	4.839	3.561	-0.073	4.813	3.678	-0.059	4.832	3.592
Ibuprofen	6	0.001	4.499	1.415	0.003	4.540	2.019	0.001	4.479	1.293

For fenbufen, it can be observed that the data outputs for logK were quite high for the y-regression (around 6.3 as opposed to 4.5 for the other two), and the $\log(n_1K_1)$ and n_1 values were observed to be very low for the Scatchard's plot, as opposed to the other two. However average the obtained data have high logK values, in aggrement with those having that these drugs have high binding affinity for HSA. Graphical representations in the Figure 6.14 are only for flurbiprofen. Included there in are the experimental design, data plots and simplex algorithms all obtained using MATLAB. Other graphs can be found in Appendix 2f. On closer inspection of the plots for the simplex models in Figure 6.15, it can be observed that on C (Scatchard's plot) the points are constantly increasing and lie within the regression line giving a good correlation, with D (y-regression) points not giving a good correlation.

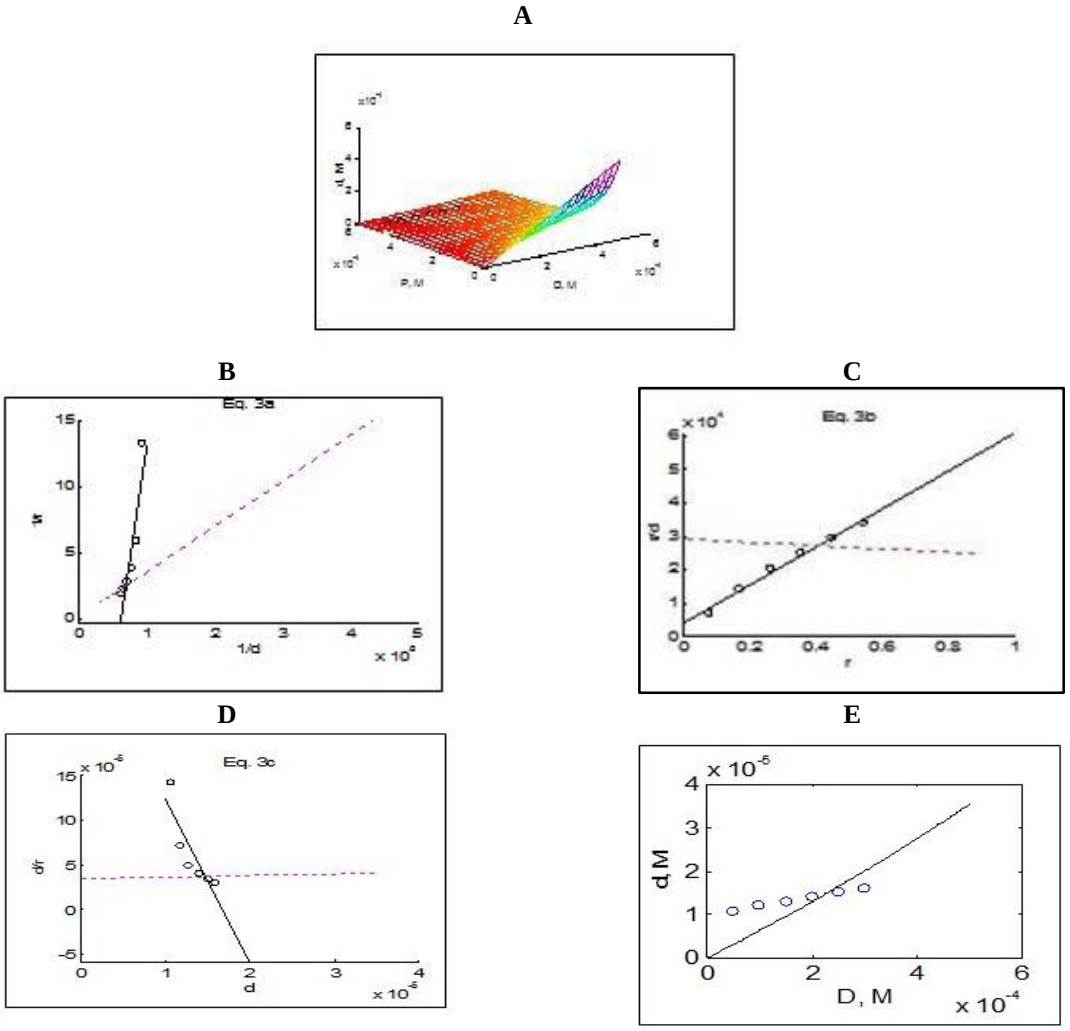

Figure 6.15: CE-CZE results for flurbiprofen, A: Protein constant design, B Klotz plot, C: scatchard plot, D: the Y-regression plot and E: the non-linear plot obtained using the SIMPLEX algorithm in MATLAB calculations.

6.3 Molecular docking of NSAIDs-HSA interactions

This section involves the investigation of the binding affinities of NSAIDs with HSA to support the experimental data obtained from both methods. The section is divided into two parts, the protein preparation, which includes all the stages that were followed before docking and the molecular docking results which suggested more than one binding sites for NSAIDs.

In molecular docking, there is a protocol followed prior to docking which includes the protein and ligand preparation outlined in Figure 6.16. A function called "Prepare Protein" was used to clean up the common problems in the input protein structure of human serum albumin (2BXD) in preparation for further processing using other protocols. Table 6.10 below shows the basic information about the protein molecule of interest 2BXD.

6.3.1 Protein preparation

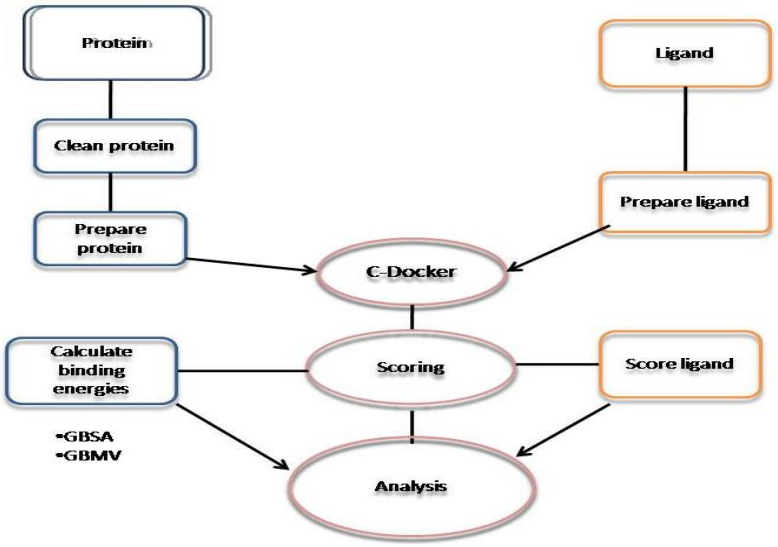

Figure 6.16: shows procedure/stages followed in ligand and protein preparation

Table 6.10: Basic information for molecule 2BXD

PDB code	2BXD
Crystallographic Resolution	3.05 angstroms
Molecular Weight of Protein	65681.5
Amino Acid Chain Names	A
Experimental pH	7.4

6.3.1.1 Cleaning and Preparation stages

The following steps were performed during the preparation of the prorein:

- Firstly, atom names were standardized
- Side-chain conformation was optimized for residues with inserted atoms
- Missing loops modelled based on SEQRES information were inserted
- The remaining loop regions were minimized
- Lastly, the calculation of pKa and protonation of the structure

Following the Cleaning and Preparation stages, a protein report was generated and is illustrated in Appendix 3a, showing the amino acid sequences in comparison with the actual sequence versus PDB SEQRES. The reports revealed that there were no missing segments with no alternate conformations hence no incomplete residues were found in the structure. Additional details of the protein report are listed in Table 6.11 below.

Table 6.11: Illustration of a prepared protein report

Protonate	True
Protein Dielectric Constant	10
pH for Protonation	7.4
Ionic Strength	0.145
Energy Cutoff	0.9
Forcefield	CHARMm
Keep Ligands	True
Keep Water	None

A full protein clean report for 2BXD is shown in Appendix 3b. Protonation was performed at the predicted pH of 7.4, side chains were unmodified and the loops were set to false. There were no alternate conformations found in this structure and an incomplete side-chain handled for the 72 residues are listed in Appendix 3b.

Thereafter, a prepared protein protocol was used to insert missing atoms for the incomplete residues. Calculation of the protein ionization and the pKa of the residues along with the results obtained are shown in (Appendix 3c).

The ionization stage is very critical, since it suggests that the pKa of each residue enables us to extract more information specifically on the residues participating in the ligand-protein interactions (Spassov et al 2008; Spassov and Yan 2008).

The plot of the total charge against the pH shown in Figure 6.17 suggests that the pH is stable between 6 and 8. During the protonation stage, a pH of 7.4 was used. The pH was chosen because it matches the physiological conditions shown in Figure 6.15, suggesting that a suitable pH for protein was not affected by ionization.

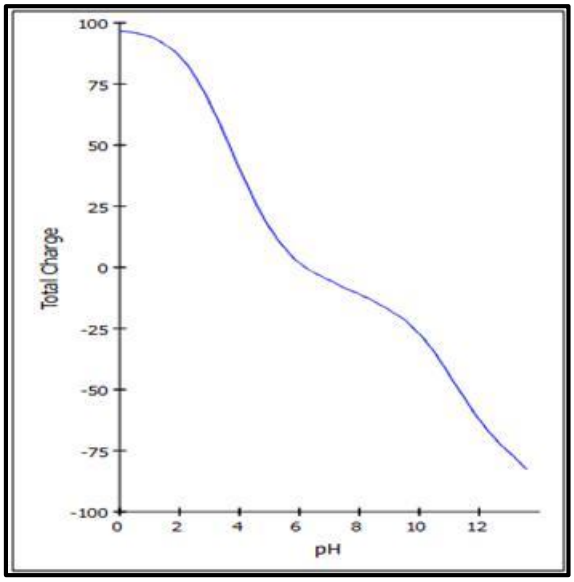

Figure 6.17: Titration curve showing the ionization profile of human serum albumin (2BXD).

After the protein preparation, Ramachandran and hydrophibicity plots were generated for 2BXD shown in Figure 6.18. Ramachandran plots are mainly used for protein structure research, as they provide useful information and understanding of the fundamental protein conformations. The information extracted from this plot includes bond angles, different protein regions and nomenclature of the protein conformations to name a few (Hollingworth and Karplus 2010).

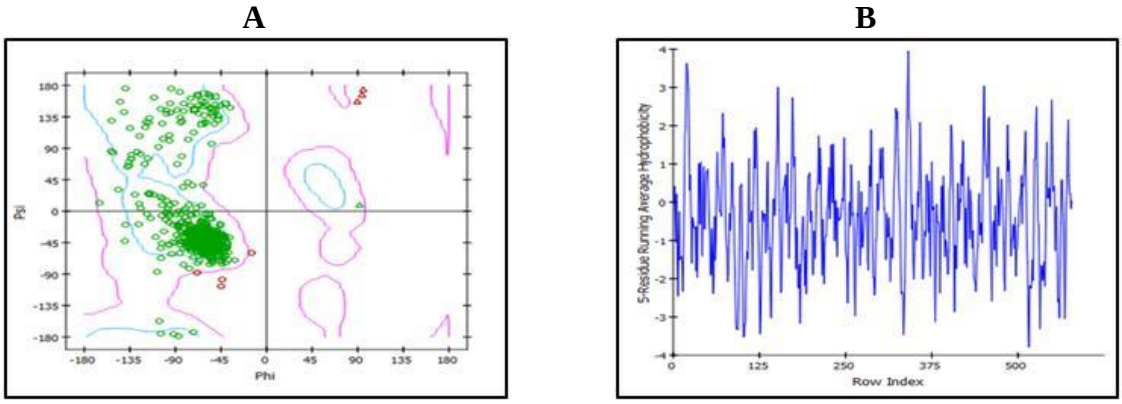

Figure 6.18: A: The Ramachandran plot and B: hydrophobicity plot generated for prepared 2BXD prior to docking.

Figure 6.19 below shows different types of plots for HSA. This is due to the monomeric subunits of protein (amino acids) with different properties. All amino acids have a –COOH group (with the exception of proline), the $–NH_2$ group and the R- group. Some amino acids bear the hydrophilic R-groups, and some bear the hydrophobic R-groups (represented by Figure 6.17C and 6.17D respectively), the acidic due to the –COOH group and basic due to the NH_2.

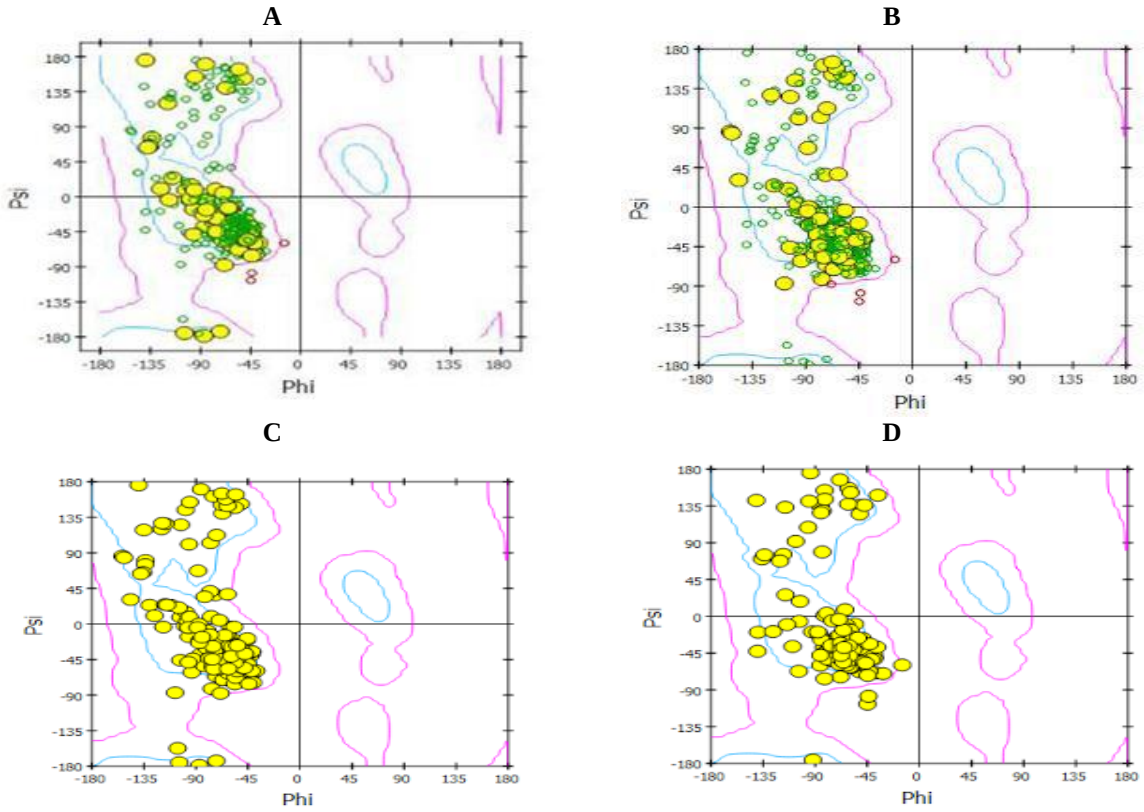

Figure 6.19: The 2BXD Ramachandran plots for A: Basic protein, B: Acidic protein, C: Hydrophilic and D: Hydrophobic.

6.3.1.2 Selection of binding site

A CHARMm force field was applied to the entire protein prior to selection of the binding sites. The binding sites on the protein were identified from the PDB site records by selecting a bound ligand "warfarin" for site I (see Figure 6.20A). Thereafter, all the amino acids outside the binding sites were removed (see Figure 6.20B) as they have no influence on the docking.

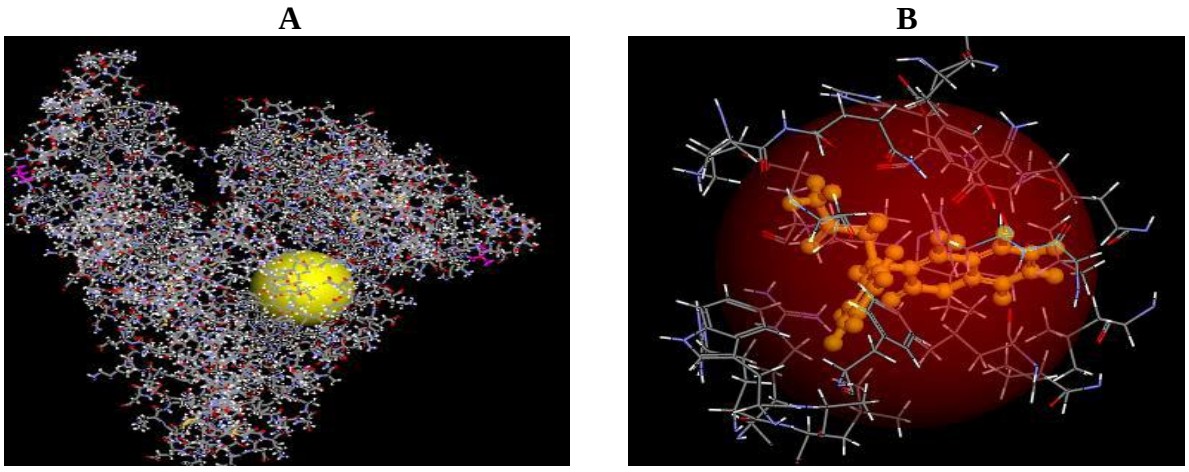

Figure 6.20: A) Binding site 1 marked with a yellow sphere created on the bases of the docked ligand. B) Binding site 1 in the absence of the molecules outside the binding sphere.

6.3.1.3 Ligand Preparation

It is well understood that different ligand protonation states, isomers and tautomers typically have different 3D geometries and binding characteristics. Therefore, a consistent and uniform approach is pivotal to enumerate a number of likely configurations. Herein, a prepare ligand protocol was automatically used to add hydrogens, calculate 3D coordinates, enumerate ionization states, ionize functional groups, generate tautomers and isomers and standardize charges for the common groups and most importantly retain the largest fragment. Table 6.12 gives a clear illustration of NSAIDs properties obtained after they were prepared prior to docking. Clearly, each ligand is represented by a code and all other extracted information are reported on the table.

Table 6.12: Molecular properties of the ligands calculated after ligand preparation.

Index	Code	ALogP	Molecular Weight	H-Acceptors	Rotatable Bonds	Rings	Aromatic Rings	MFPSA
1	3335	1.459	253.273	3	5	2	2	0.216
2	3342	2.043	241.262	3	4	2	2	0.195
3	3394	2.206	243.253	2	3	2	2	0.158
4	3826	1.358	254.261	3	3	3	2	0.246
5	181817	1.358	254.261	3	3	3	2	0.246
6	3825	1.887	253.273	3	4	2	2	0.214
7	667550	1.887	253.273	3	4	2	2	0.214
8	156391	1.375	229.251	3	3	2	2	0.2
9	114864	2.133	205.273	2	4	1	1	0.164
10	39912	2.133	205.273	2	4	1	1	0.164
11	3718	1.227	280.298	3	3	3	2	0.212
12	68700	1.227	280.298	3	3	3	2	0.212

*MFPSA: Molecular Fraction Polar Surface Area

Table 6.13: The properties of the NSAIDs ligands used for molecular docking.

Index	Code	Name	HAC	ADSC	MMFF94 energy	Shape-OS	Shape_ Volume
1	3335	fenbufen	19	0	52.29	801.52	205.80
2	3342	fenoprofen	18	0	56.42	757.16	194.00
3	3394	flurbiprofen	18	0	50.02	759.57	193.40
4	3826	(+/-)-ketorolac	19	0	56.35	816.46	199.40
5	3825	ketoprofen	19	0	58.87	805.42	204.00
6	156391	naproxen	17	1	54.48	715.96	183.50
7	114864	(-)-ibuprofen	15	1	33.43	605.09	172.20
8	181818	(+)-Ketorolac	19	1	55.81	816.33	199.50
9	180540	(-)-ketoprofen	19	1	58.86	805.33	204.00
10	3672	ibuprofen	15	0	33.43	605.09	172.20
11	3718	indoprofen	21	0	67.02	901.28	220.10
12	39912	(+)-ibuprofen	15	1	32.43	603.78	172.70
13	68700	(+)-indoprofen	21	1	66.87	901.21	220.10
14	181817	(-)-ketorolac	19	1	55.80	816.26	199.50
15	667550	(+)-ketoprofen	19	1	58.93	805.91	204.10

*HAC: Heavy Atom Count, ADSC: Atom Different Stereo Count, OS: Self Overlap

The ionization was set true based on the allowance of 6.5 to 8.5 to simulate our experimental conditions, which were performed at pH 7.4. Furthermore, all tautomers were generated for a maximum number of 10 and the aromaticity was never preserved. The MMFF94 energy does not change after ligand preparation C-DOCKER initially positions the ligand in the center of the site sphere. Docking poses are ordered by C-DOCKER ENERGY where a higher

value indicates a more favorable binding this score includes internal ligand strain energy and receptor-ligand interaction energy.

6.3.2 Molecular Docking Results

The docking studies were conducted to assess the binding propensities of NSAIDs in both binding sites (site I&II) of the HSA protein. The C-DOCKER module [1] of Discovery Studio (DS, version 2.5, Accelrys Software Inc.) were used for the docking simulations where the position of the proteins were kept fixed, while the ligands were allowed to flex during the refinement process. Docking results for both HSA binding sites (site I&II) were evaluated in terms of the binding energies (Energy of complex-Energy of ligand-Energy of protein) of the complexes and are depicted in Table 6.14.

Table 6.14: Showing binding energies for both site I and II and binding constants for each NSAIDs.

NSAIDs	Abbr.	Binding Constant (M^{-1})	Binding Energy (Site I) ($kcalmol^{-1}$)	Binding Energy (Site II) ($kcalmol^{-1}$)
Fenbufen	Fnb	30000	-90.7	-61.8
Indoprofen	Ipf	3890	-55.1	Failed
Flurbiprofen	Fpf	15300	-69.6	-50.9
Naproxen	Npx	5390	-60.3	-42.5
Ketorolac	Ktl	19900	-71.1	-41.2
Fenoprofen	Fnp	15400	-64.8	-69.5
Ibuprofen	Ibf	6770	-43.8	-37.3
ketoprofen	Kpf	7860	-56.0	Failed

A closer inspection of Table 6.14 reveals that the binding energies (BEs) of the inclusion complexes vary significantly, suggesting different binding affinities of these drugs for site I and site II of the HSA. The calculated binding energies (BEs) were further plotted against the binding constant (K) for both binding sites (I&II) to monitor the relationship between the experimental and computational data, and are shown in Figures 6.21A-B. For site I, with the exception of two drugs (fenoprofen and ibuprofen), the remaining six drugs exhibited a good correlation between BEs and K values. For instance, fenbufen showed a strongest interaction with the HSA (K=30000) exhibited the lowest binding energy (-90.7) at site I, whereas the indoprofen exhibiting the weakest interaction (K = 3890) showed the highest binding energy (-55.1) with site I as depicted in Figure 6.21. No such relationships between the computed BEs and K values were established on the basis of the docking results for site II (Figure B), and supports the earlier

observations that site II is not the preferred binding site for the NSAIDs. Ketoprofen and indoprofen drugs failed to dock with the binding site II of the HSA.

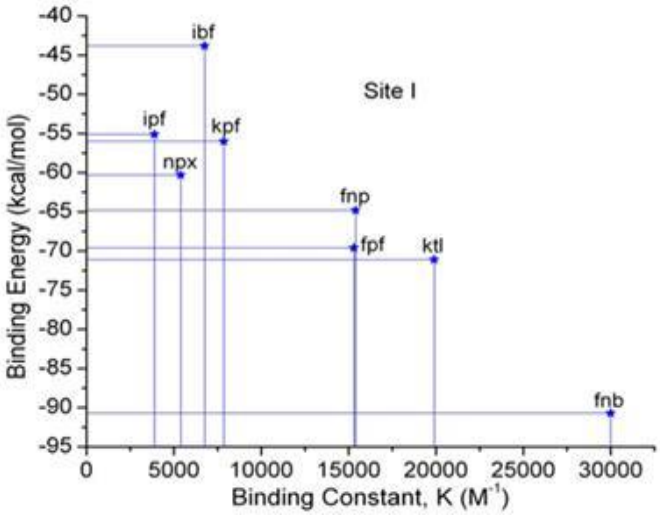

Figure 6.21A: Relationship between binding constant (experimental) and binding energies for site I (docking) of HSA. Horizontal and vertical lines are used to monitor the relationship between docking (BE) and experimental (K) data for a specific drug. Drugs are abbreviated according to Table 6.14.

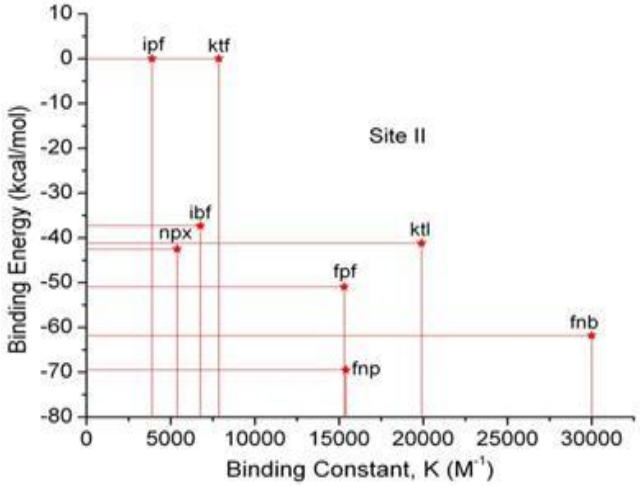

Figure 6.21B: Relationship between binding constant (experimental) and binding energies for site II (docking) of HSA. Horizontal and vertical lines are used to monitor relationship between docking and experimental data for a specific drug. Drugs are abbreviated according to Table 6.14.

The inclusion complexes of the four drugs (fenbufen, ketorolac, fenoprofen and Flurbiprofen) showed the strongest interactions with HSA at site I and are diagrammatically represented in Figures 6.22A-D. Fenbufen formed single hydrogen bonds between its carbonyl

oxygen (proton acceptor) and Arg257 (proton donor) along with three cation-π interactions between its aromatic rings and Lys199 and Arg222 residues of HSA (Figure 6.22A).

Ketorolac, on the other hand established predominant hydrogen bonds through its oxygen rings with Tyr158, Lys199 and Arg222 in addition to a cation-π interaction with Arg257 (Figure 6.22B).

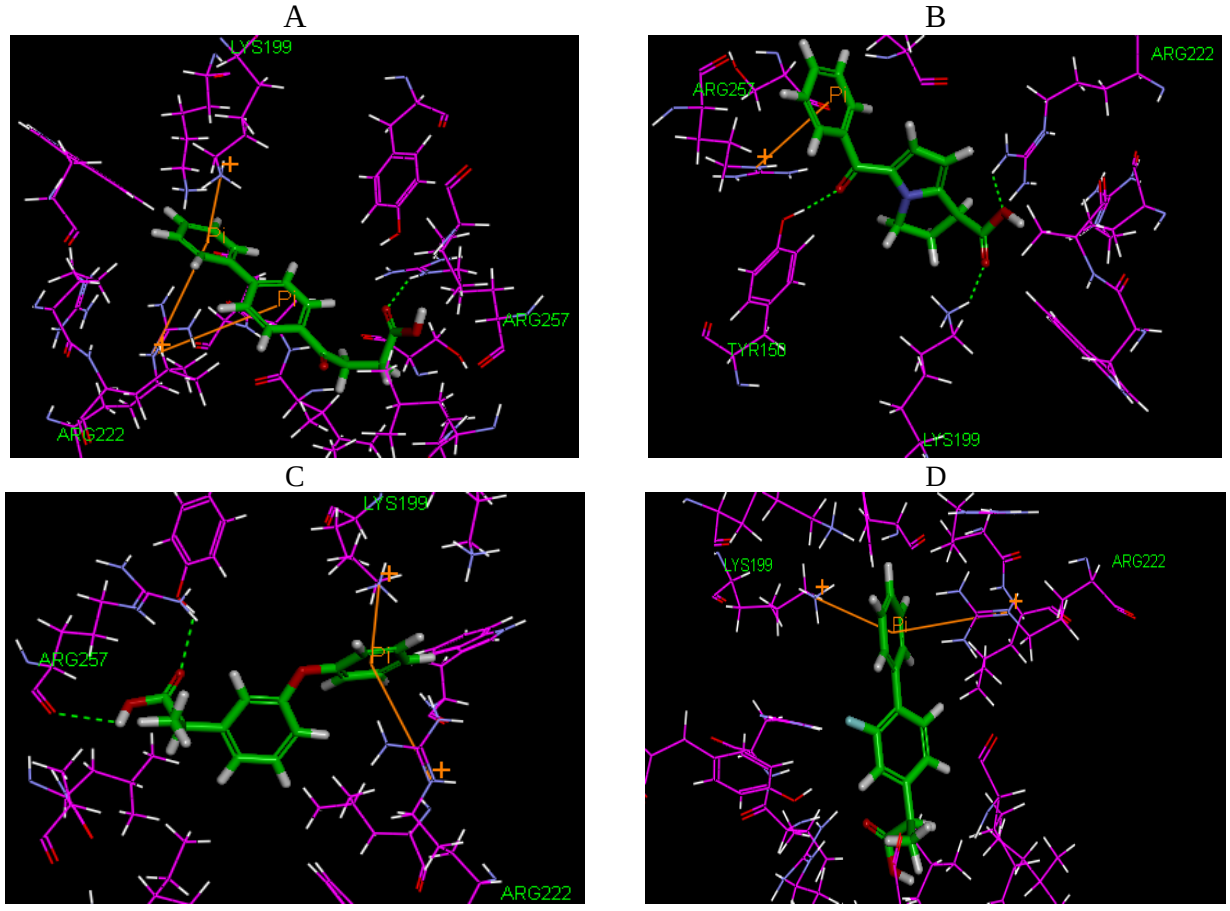

Figure 6.22: Docked conformation of fenbufen (A), ketorolac (B) fenoprofen (C) and flurbiprofen (D) with the HSA. Drug molecules are shown in stick (in green) form, while protein amino acid residues are depicted in line format (in pink). Hydrogen bonds are shown as green dotted lines, whereas cation-π interactions are represented as brown lines.

Both fenoprofen (Figure 6.22C) and flurbiprofen (Figure 6.22D) interacted with similar amino acids of HSA (Lys199 and Arg222) *via* cation-π interactions, although two additional hydrogen bonds between fenoprofen and Arg257 were also observed. Finally, the root mean square deviation (RMSD) between the docked poses of ibuprofen obtained from the current

docking experiments and its X-ray structures were less than 1Å (data not shown) and clearly supported the proposed binding conformations of NSAIDs in the present study.

The second part involved the molecular docking studies conducted with Discovery Studio 4.0 for site I. In this case a more detailed presentation of the results were shown for both proteins and NSAIDs. Table 6.15 included the binding energies describing the binding affinities of the ligands (NSAIDs) to the protein (HSA).

The evaluation of the BEs for the ligands, proteins and complexes is presented as well as the thermodynamics of the ligand-protein complex, ligand and protein entropy contributions.

Table 6.15: Showing a more detailed presentation of results molecular docking studies for different binding properties obtained for HSA-NSAIDs extracted from Discovery Studio 4.0.

Code	Binding Energy (kcal/mol)	Ligand Energy (kcal/mol)	Protein Energy (kcal/mol)	Complex Energy (kcal/mol)	Complex Entropy	Protein Entropy	Ligand Entropy	Entropic Energy
3335	4,102.72	6,196.02	2.29E+08	2.29E+08	-32.64	-32.64	-19.40	19.40
3342	2,319.55	3,036.12	2.29E+08	2.29E+08	-32.64	-32.64	-19.11	19.10
3394	3,070.87	3,868.63	2.29E+08	2.29E+08	-32.64	-32.64	-19.08	19.08
3826	6,159.77	9,532.61	2.29E+08	2.29E+08	-32.64	-32.64	-19.33	19.32
3825	4,290.99	7,323.38	2.29E+08	2.29E+08	-32.64	-32.64	-19.29	19.29
156391	140.231	466.91	2.29E+08	2.29E+08	-32.64	-32.64	-18.84	18.84
114864	725.65	949.94	2.29E+08	2.29E+08	-32.64	-32.64	-18.61	18.61
3718	158.06	447.59	2.29E+08	2.29E+08	-32.64	-32.64	-19.40	19.39
39912	1,674.20	2,194.50	2.29E+08	2.29E+08	-32.64	-32.64	-18.35	18.35
68700	58.30	450.55	2.29E+08	2.29E+08	-32.64	-32.64	-19.41	19.41
181817	2,229.86	3,108.01	2.29E+08	2.29E+08	-32.64	-32.64	-19.09	19.09
667550	1,280.72	813.71	2.29E+08	2.29E+08	-32.64	-32.64	-19.22	19.22

An interaction process of the protein with a ligand involved a formation and a breakage of the hydrogen bonds. However, for drug design a detailed molecular description and a thermodynamic evaluation of such measurements are crucial. The binding energies consist of both the enthalpic and entropic contributions, that in many reactions of biological systems compensate each other. This means that when binding between ligand and a protein is strong, the entropy tends to decrease and the enthalpy concurrently becomes more negative, even if the bonds are weak the entropy increases and the enthalpy becomes less negative (Cozzini et al. 2004).

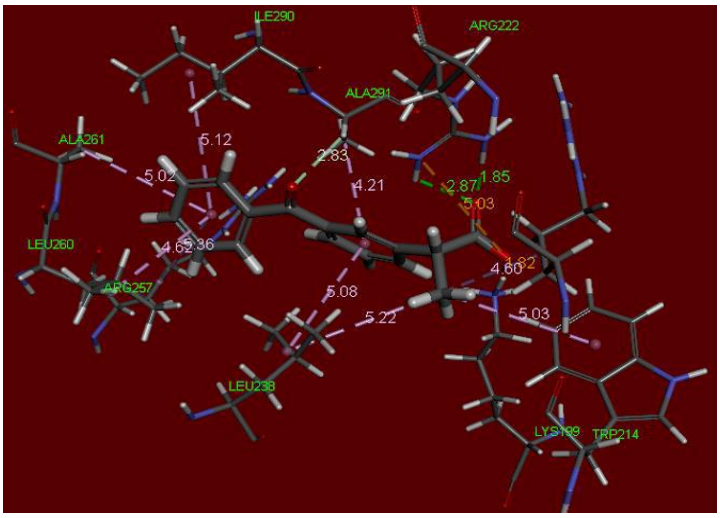

Figure 6.23: Showing docked information of ketoprofen (3825) where π- interactions represented by purple and hydrogen bonds by dark grey (where ligand it bonded once) and green where it bonded twice with the residue. The bold molecule in the middle is the drug and others surrounding it are protein residues.

A closer inspection of Figure 6.23 suggests that ketoprofen forms weak numerous π-alkyl interactions between its aromatic ring and the residues. Clearly shown are the bonds between these six residues (ALA261 at a distance of 5.02, LEU260 at a distance of 5.36, ARG257 at a distance of 4.62, ILE290 at a distance of 5.12, LEU238 at a distance of 5.08 and ALA291 at a distance of 4.21). Additionally, the π-interactions between the ligands and the aromatic rings for TRP214 and LEU238 were at a distance of 5.03 and 5.22 respectively. Hydrogen bonds between the carbonyl oxygen of ketoprofen (proton acceptor) and ALA291 (proton donor) were at a distance of 2.83 and with ARG222 two hydrogen bonds observed at a distance of 2.87 and 1.85. Attached in Appendix 3h is a statistical analysis of the residues which are important in giving information on the residues favored for the interaction. Listed there are residues with favorable interactions, residues with unfavorable interactions, residues with hydrogen bond interactions, residues with charge interactions, residues with hydrophobic interactions, residues with halogen interactions and residues with other interactions.

6.4 Enantioseparation of the racemic NSAIDs

The experimental work involved a method development of enantioseparation of ketorolac, flurbiprofen and fenoprofen racemic mixtures using 2, 3, 6-tri-O-methyl-β-cyclodextrin (TM- β-CD) as a chiral selector. A number of parameters such as the CD concentration, concentration and the pH of the background electrolytes, and the voltage were varied in order for the separation to be feasible. It is important to consider that the resolution of the enantiomers depend mainly on the complex formation of the cyclodextrin with the analytes as well as the electro-osmotic flow in the capillary. Two methods of injection were used; in the first method, the analytes were injected first followed by the cyclodextrin, and in the second method the cyclodextrin was injected first. In the first method, no separation were observed for all the analytes due to analytes having higher mobilities than the cyclodextrin resulting in them being eluted before interacting with cyclodextrin. In the second, method separation was observed for ketorolac, with no separation for the other two compounds. After varying some parameters only 40 % resolution was obtained. The electropherogram shown in Figure 6.24 depicts the two ketorolac peaks not completely resolved.

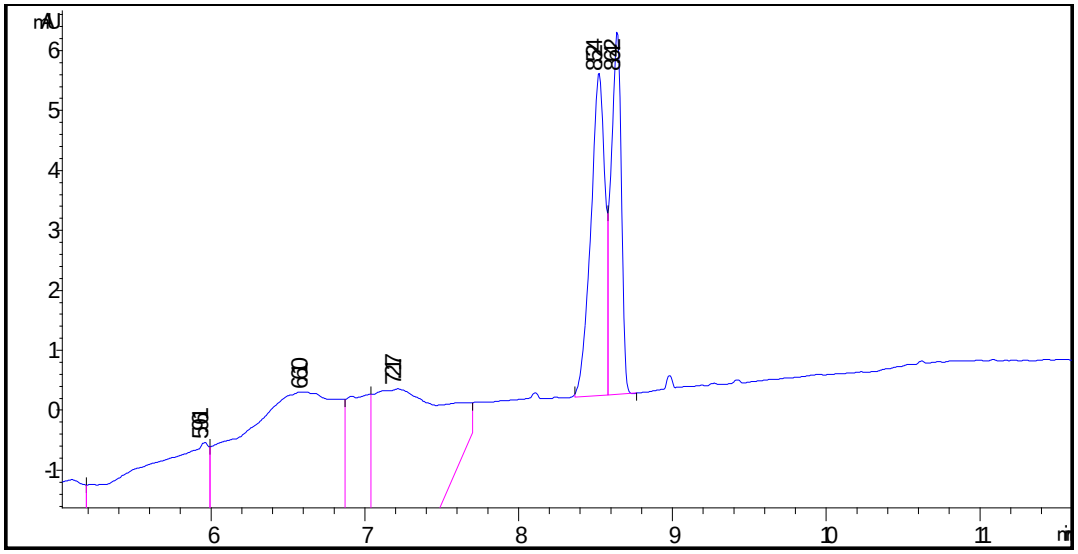

Figure 6.24: electropherogram showing two partially resolved peaks of 200 µM ketorolac obtained using 50 mM phosphoric acid:triethanolamine buffer, 20 kV, and 5 s injection time.

In Table 6.16 a comparison between experimental and docking findings for this work and literature values is reported.

Table 6.16: A comparison between the data obtained from the current work via experimental and computational methods and the data from literature.

ID	Ref (year)	Details	Estimation method	Compound	$LogK_1$
1[a]	Deschamps-Labat et al. 1997	HPLC-UV, incubation at 37 ºC, pH 7.4 (0.06 M acetonitrile-phosphate buffer).	Scatchard	Fenoprofen Flurbiprofen Indoprofen Ketoprofen ibuprofen Fenbufen	6.005 5.936 5.238 5.692 5.638 6.067
2[a]	Kosa et al. 1997	HPLC-fluorescence, incubation at 25 ºC, pH 4.5 of 0.1 M acetate buffer-acetonitrile (40:60v/v)	Scatchard	Ibuprofen	6.552
3[a]	Pîrnău and Bogdan 2008	UV-Vis spectroscopy measurement at 25 ºC, deionized water use as solvent.	dissociation constant Beer -Lambert	naproxen	3.319
4[a]	Wybranowski et al. 2008	Spectroflouremeter, dilutions done by phosphate buffered saline at pH 7.4.	Burke and Tritton formula (Linear plots)	flurbiprofen	7.114
5[a]	Hage et al. 1995	HPAC-zonal elution, 0.05 M sodium phosphate buffer (pH 6.9) containing 15 % (v/v) acetonitrile.	Y-regression	ibuprofen	5.041

ID	Ref (year)	Details	Estimation method	Compound	$LogK_1$
6[a]	Hailin et al 1997	HPLC-UV, drug and HSA dissolved in 0.067 M potassium phosphate buffer, temperature 37 ºC, mobile phase methanol/water/acetic acid (72.5/27.5/1.0).	Scatchard Klotz	ketoprofen	6.502
7[a]	Kober and Sjöholm 1980	Equilibrium dialysis, 0.1M KCl,0.005M sodium phosphate pH 7.5	Scatchard	Flurbiprofen Ibuprofen naproxen	6.699 6.114 6.255
8[b]	This work	CE-FA at pH 7.4 (0.067 M phosphate buffer), with temperature of 37 ºC, injection done for 60 s	Scatchard Klotz Y-regression	fenoprofen flurbiprofen indoprofen ketoprofen ibuprofen fenbufen ketorolac naproxen	4.723 4.696 4.184 4.555 4.476 5.039 5.809 4.465
9[b]	This work	CE-CZE, temperature at 37 ºC, with buffer pH 7.4 (0.067 M phosphate buffer), injection done for 5 s.	Scatchard Klotz Y-regression	fenoprofen flurbiprofen indoprofen ketoprofen ibuprofen fenbufen ketorolac naproxen	4.787 4.779 4.186 3.541 4.506 5.377 4.828 4.492
10[b]	This work	C-DOCKER module of Discovery Studio, pH 7.4 used to mimick experimental work.	CHARMm force field used for docking and scoring calculations	fenoprofen flurbiprofen indoprofen ketoprofen ibuprofen fenbufen ketorolac naproxen	4.188 4.185 3.590 3895 3.831 4.477 4.299 3.732

a: data from literature, all necessary information reported, b: current work, experimental data reported

CHAPTER 7

CONCLUSIONS

NSAIDs are arylpropionic acid derivatives comprising of an identical chemical group bearing a common chiral acid centre as can be observed in their structures in Table 4.1. Having said that in most cases, these drugs are marketed as 50/50 racemic mixtures with their plasma protein binding resulting to about 99 %, studying their protein binding is therefore essential (Deschamps-Labat et al. 1997, Brater 1988). In this work, CE was chosen for the binding estimation studies, due to their advantages over the other chromatographic techniques. Overall, the approaches (CE-FA and CE-CZE) dedicated for NSAIDs–HSA interactions were able to provide the required pharmacokinetic properties of all eight commercially available NSAIDs used in this study. However, with the racemic drugs such as ketorolac, fenoprofen and flurbiprofen it was impossible to obtain such parameters for the interaction of each enantiomer with HSA, since the study was conducted with racemic mixtures. To obtain such information the enantiomers have to be separated prior to analysis. The *in vitro* incubation of the NSAID-HSA mixtures mimicking the physiological conditions followed by ultracentrifugation for CE-CZE helped to provide results that resembles those done under *in vivo* experiments making these approaches preferred alternatives.

However, in the case of CZE, it was easier to extract and analyze the experimental data in the absence of protein complexes in the electropherogram. The results obtained in this study for the estimation of the binding affinities of NSAIDs to HSA were comparable to those obtained in literature (Table 6.16). Literature suggests that NSAIDs have higher binding affinities to HSA (Brater 1988), in agreement with the data presented in this study. Additionally, molecular docking studies gave a better insight into the interaction studies and provided useful information such as binding energies and entropies. Binding properties obtained by docking studies were in agreement with the experimental data and with those reported in the literature. However, differences could be caused by many factors involved in the experimental work of each method.

Future work

It was unfortunate that for this work enantioseparation was not feasible with heptakis-(2,3,6-tri-O-methyl)-β-CD (TM-β-CD) and thus EKC studies could not be perfomed. According to literature TM-β-CD was able to separate some of the NSAIDs, which in our case failed after exhausting numerous approaches. Generally in EKC, the free drug is separated from the bound drug-protein complex via ultracentrifugation, and is then injected into the capillary where it is allowed to interact with a chiral selector resulting in the resolution of its enantiomers. Understanding the influence of the factors that affect resolution, it was noted that the cyclodextrin chosen for this study did not have strong interactions with the compounds. A choice of cyclodextrin would have to be reconsidered and its interactions with the analytes validated by computational methods, which was beyond the scope of this study. An experimental design for multivariate optimization of all the factors influencing resolution will have to be perfomed in order to obtain complete resolution of the enantiomers with the view to obtaining pharmacokinetic properties of each enantiomer after the drug-protein interactions. Another study that could be looked at, is the determination of binding sites of HSA in which these NSAIDs bind to, with the aid of site markers since literature suggests that these drugs have higher binding affinities to towards site II as opposed to site I of the HSA.

REFERENCES:

AbouI-Enein H.Y. and Ali I. (2000). Macrocyclic Antibiotics as Effective Chiral Selectors for Enantiomeric Resolution by Liquid Chromatography and Capillary Electrophoresis. *Chromatographia 52: 679-691*

Abushoffa A.M., Fillet M., Hubert P., Crommen J. (2002). Prediction of selectivity or enantiomeric separations of uncharged compounds by capillary electrophoresis involving dual cyclodextrin systems. *J. Chromatogr. A 948:321–329*

Albrecht C., Reichen J., Visser J., Meijer D.K.F. and Thormann W. (1997). Differentiation between naproxen,naproxen–protein conjugates, and naproxen–lysine in plasma via micellar electrokinetic capillary chromatography—a new approach in the bioanalysis of drug targeting preparations. *Clin. Chem. 43:2083–2090*

Amran S., Morshed S.N., Khandakar J.A., Rahman M., Rahman M. and HossainA. (2008). The *In vitro* Effects of Atenolol andZinc Chloride on the Protein Binding of Amlodipine in Aqueous Medium. *J. Pharm. Sci. 7:15-21*

Attia D.A. (2009). In vitro and in vivo evaluation of transdermal absorption of naproxen sodium. *Aust. J. Basic Appl. Sci. 3:2154-2165.*

Aturki Z., Desiderio C., Mannina L., and Fanali S. (1998). Chiral separations by capillary zone electrophoresis with the use of cyanoethylated-β-cyclodextrin as chiral selector. *J Chromatogr. A 817:91–104*

Baroni S., Mattu M., Vannini A., Cipollone R., Aime S., Ascenzi P.and Fasano M. (2001). Effect of ibuprofen and warfarin on the allosteric properties of haem–human serum albumin. *Eur J. Biochem. 268:6214–6220*

Barton H. (2007). Roles of Quantitative In Vitro ADME in Toxicology and Risk or Safety Assessment. *US Environ Protection Agency* http://www.alttox.org/ttrc/toxicity-tests/pharmacokinetics-metabolism/way-forward/barton/ (accessed 11 September 2013)

Bertucci C., Bartolini M., Gotti R., Andrisano V. (2003). Drug affinity to immobilized target bio-polymers by high-performance liquid chromatography and capillary electrophoresis. *J. Chromatogr. B 797:111–129.*

Blanco M., Coello J., Iturriaga H., Maspoch S. and Peŕez-Maseda C. (1998). Separation of profen enantiomers by capillary electrophoresis using cyclodextrins as chiral selectors. *J. Chromatogr. A 793: 165–175*

Brater D.C. (1988). Clinical pharmacology of NSAIDs. *J. Clin.Pharmacol. 28:518-523*

Bruno R., Olivares R., Berille J., Chaikin P., Vivier N., Hammershaimb L., Rhodes G.R. and Rigas J.R. (2003). α-1-Acid Glycoprotein As an Independent Predictor for Treatment Effects and a Prognostic Factor of Survival in Patients with Non-small Cell Lung Cancer Treated with Docetaxel. *Clin. Cancer Res. 9: 1077–1082*

Chankvetadze B. (1997). Separation selectivity in chiral capillary electrophoresis with charged selectors. *J Chromatogr. A 792:269–295*

Chaturvedi P.R., Decker C.J. and Odinecs A. (2001). Predictions of Pharmacokinetic properties using experimental approaches during early drug discovery. *Curr. Opin. Chem. Biol. 5:452-463*

Chuang V.T.G. and Otagiri M. (2006). Stereoselective Binding of Human Serum Albumin. *Chirality 18:159–166*

Chuang V.T.G., Kuniyasu A., Nakayama H., Matsushita Y., Hirono S., Otagiri M. (1999). Helix 6 of subdomain III A of human serum albumin is the region primarily photolabeled by ketoprofen, an arylpropionic acid NSAID containing a benzophenone moiety. *Biochim. Biophys. Acta 1434:18-30*

Cozzini P., Fornabaio M., Marabotti A., Abraham D.J., Kellogg G.E. and Mozzarelli A. (2004). Free Energy of Ligand Binding to Protein: Evaluation of the Contribution of Water Molecules by Computational Methods. *Curr. Med. Chem. 11:1345-1359*

Crofford L.J. (2013). Use of NSAIDs in treating patients with arthritis. *Arthritis Res. Ther.15:1-10*

Del Valle E.M.M. (2004). Cyclodextrins and their uses: a review. *Process Biochem. 39:1033–1046*

Deschamps-Labat L., Péhourcq F., Jagou M.and Bannwarth B. (1997). Relationship between lipophilicity and binding to human serum albumin of arylpropionic acid non-steroidal anti-inflammatory drugs. *J. Pharm. and Biomed. Anal. 16:223–229.*

Deyl Z., Mikšík I., Tagliaro F. (1998). Advances in capillary electrophoresis. *Forensic Sci. Int. 92:89–124*

Diniz A., Escuder-Gilabert L., Lopes N.P., Villanueva-Camañas R. M., Sagrado S., and Medina-Hernández M. J. (2008). Characterization of interactions between polyphenolic compounds and human serum proteins by capillary electrophoresis. *Anal. Bioanal. Chem. 391:625–632*

Dubois N., Lapicque F., Abiteboul M., and Netter P. (1993). Stereoselective protein binding of ketoprofen: effect of Albumin concentration and of the biological system. *Chirality 5:126-134*

Ekins S., Honeycutt J.D. and Metz J.T. (2010). Evolving molecules using multi-objective optimization: applying to ADME/Tox. *Drug Discov. Today 15:451-460*

Fakayode S.O., Williams A.A., Busch M.A., Busch K.W. and Warner I.M. (2006). The Use of Poly(Sodium *N*-Undecanoyl-l-Leucylvalinate), Poly(Sodium *N*-Undecanoyl-l-Leucinate) and Poly(Sodium *N*-Undecanoyl-l-Valinate) Surfactants as Chiral Selectors for Determination of Enantiomeric Composition of Samples by Multivariate Regression Modeling of Fluorescence Spectral Data. *J. Fluoresc. 16:659–670*

Fanali S. (2000). Enantioselective determination by capillary electrophoresis with cyclodextrins as chiral selectors. *J. Chromatogr. A 875:89–12*

Fazlena H., Kamaruddin A. H., and Zulkali M.M. (2006). Dynamic kinetic resolution: alternative approach in optimizing S-ibuprofen production. *Bioprocess Biosyst. Eng. 28:227-233*

Fillet M., Bechet I., Piette V. and Crommen J. (1999). Separation of nonsteroidal anti-inflammatory drugs by capillary electrophoresis using non-aqueouselectrolytes. *Electrophoresis 20: 1907-1915*

Fillet M., Hubert P., Crommen J. (1997). Enantioseparation of nonsteroidal anti-inflammatory drugs by capillary electrophoresis using mixtures ofanionic and uncharged P-cyclodextrins as chiral additives. *Electrophoresis 18:1013-1018*

Fraizer R.A., Ames J.M. and Nursten H.E. (2000). Capillary Electrophoresis for food Analysis Method development. ISBN 0-85404-492-2

Galantini L., Leggio C., Konarev P.V. and Pavel N.V. (2010). Human serum albumin binding ibuprofen: A 3D description of the unfolding pathway in urea. *Biophys. Chem. 147 111–122*

Genton L., Melzer K. and Pirchard C. (2010). Energy and macronutrient requirements for physical fitness in exercising subjects. *Clin. Nutr. 29:413-423*

Główka F. K. and Karaźniewicz M. (2004). High performance capillary electrophoresis for determination of the enantiomers of 2-arylpropionic acid derivatives in human serum:Pharmacokinetic studies of ketoprofen enantiomers following administration of standard and sustained release tablets. *J. Pharm. Biomed. A35:807-816*

Gübitz G. and Schmid M.G. (2000). Recent progress in chiral separation principles in capillary Electrophoresis. *Eletrophoresis 21:4112-4135*

Gübitz G. and Schmid M.G. (2008). Chiral separation by capillary electromigration techniques. *J. Chromatogr. A 1204:140–156*

Gübitz G., Schmid M.G. (1997). Chiral separation principles in capillary electrophoresis. *J. Chromatogr. A 792:179–225*

Guillaume Y.C., Millet J., Nicod L., Truong-Thanh T., Guinchard C., Xicluna A. and Thomassin M. (2002). *J. Chromatogr. B 768:121–127*

Hage D.S., Jackson A., Sobansky M.R., Schiel J.E., Yoo M.J., Joseph K. S. (2009). Characterization of drug–protein interactions in blood using high-performance affinity chromatography. *J. Sep. Sci. 32:835 – 853*

Hage D.S., Noctor T.A.G. and Wainer I.W. (1995). Characterization of theprotein binding of chiral drugs by high-performance affinity chromatography Interactions of R- and S-ibuprofen with human serum albumin. *J. Chromatogr. A 693:23-32*

Haginaka J.(2004). Chiral Separations by Capillary Electrophoresis Using Proteins as Chiral Selectors. *Methods Mol. Biol. 243:291-305*

Hailin W., Hanfa Z. and Yukui Z. (1997). Microdialysis-liquid chromatographic study on competitive binding of drugs to protein. *Sci. China B 40:643-649*

Hailin W., Hanfa Z. and Yukui Z.(1997). Microdialysis-liquid chromatographic study on competitive binding of drugs to protein. *Sci. China B 40:643-649*

Hollingworth S.A. and Karplus P.A. (2010). A fresh look at the Ramachandran plot and the occurance of standard structures in proteins. *Biomol. Concepts 1:271-283*

http://www.beckmancoulter.com/literature/Bioresearch/360643-CE Primer1.pdf (*accessed 11/2011)*

http://www.wedgewoodpharmacy.com/monographs/dipyrone.asp (*accessed 09/2013*)

Huang H., Jin J.Y., Hong J.H, Kang J.S. and Lee W. (2009). Liquid Chromatographic Enantiomer Separation of Non-steroidal Anti-inflammatory Drugs on Immobilized Polysaccharide Derived Chiral Stationary Phase under Reversed and Normal Phase Mode. Bull. *Korean Chem. Soc. 30:2827-2829*

Huanga C.Z., Santa T., Okabe K. and Imai K. (2003). Capillary electrophoresis with laser induced-fluorescence detection of profens derivatized with the water-soluble fluorogenic reagent 4-N-(4-N9-aminoethyl)piperazino-7-nitro-2,1,3-benzoxadiazole. *J. Chromatogr. A 1011:193–201*

Jia Z., Ramstad T. and Zhong M. (2002). Determination of protein–drug binding constants by pressure-assisted capillary electrophoresis (PACE)/frontal analysis (FA). *J. Pharm. Biomed. Anal. 30:405–413*

Jin L., Choi D.Y., Liu H., and Row K.H. (2005). Protein Binding Study of S-Ibuprofen Using High-Performance Frontal Analysis. *Bull Korean Chem. Soc. 26:126-128*

Knjazeva T. and Kaljurand M. (2010). Capillary electrophoresis frontal analysis for the study of flavonoid interactions with human serum albumin. *Anal. Bioanal. Chem. 397:2211–2219*

Kober A. and Sjöholm I. (1980). The Binding Sites on Human Serum Albumin for Some Nonsteroidal Anti-inflammatory Drugs. *Mol. Pharmacol. 18:421-426*

Kosa T., Maruyama T. and Otagiri M. (1997). Species differences of Serum Albumins: I. Drugs Binding Sites. *Pharm. Res. 14:1607-1609*

Koppenhoefer B., Epperlein U., Christian B. Christian, Yibing J., Yuying C. and Bingcheng L. (1995). Separation of drugs by capillary electrophoresis I. γ-Cyclodextrin as chiral solvating agent. *J. Chromatogr. A 717:181-190*

Kratochwil N.A., Haber W., Müller F., Kansy M., Gerber P.R. (2002). Predicting plasma binding of drugs: a new approach. *Biochem. Pharmacol. 64:1355-1374*

Laurer H.H. and Rozing G.P. (2009). High Performance Capillary Electrophoresis, A primer Agilent Technologies 5990-3777EN

Lin B., Zhu X., Wuerthner S., Epperlein U. and Koppenhoefer B. (1998). Separation of enantiomers of drugs by capillary electrophoresis Part 8. b- Cyclodextrin as chiral solvating agent. *Talanta 46:743–749*

Lü J.X., Shen Q., Jiang J.H, Shen G.L., and Yu R.-Q.(2004). QSAR analysis of cyclooxygenase inhibitor using particle swarm optimization and multiple linear regression. *J. Pharm. Biomed. Anal. 35:679–687*

Mannschreck A. and Kiesswetter R. (2005). Differentiations of Enantiomers via Their Diastereomeric Association Complexes—There Are Two Ways of Shaking Hands. *J. Chem. Ed. 82:1034-1039*

Martínez-Gómez M.A., Sagrado S., Villanueva-Camañas R., Sunfornsuk L.M., Medina-Hernández M.J. (2007). Enantioseparation of phenotiazines by affinity electrokinetic chromatography using human serum albumin as chiral selector Application to enantiomeric quality control in pharmaceutical formulations. *Anal. Chim. Acta 582:223–228*

Martínez-Pla J.J., Martínez-Gómez M.A., Martín-Biosca Y., Sagrado S., Villanueva-Camañas R.M., Medina-Hernández M.J. (2004). High-throughput capillary electrophoresis frontal analysis method for the study of drug interactions with human serum albumin at near-physiological conditions. *Electrophoresis 25: 3176–3185*

Martínez-Gómez M.A., Carril-Avilés M.M., Sagrado S., Villanueva-Camañas R.M., Medina-Hernàndez M.J. (2007). Characterization of antihistamine–human serum protein interactions by capillary electrophoresis. *J. Chromatogr. A 1147:261–269*

Marín A., Barbas C. (2004). CE versus HPLC for the dissolution test in a pharmaceutical formulation containing acetaminophen, phenylephrine and chlorpheniramine. *J. Pharm. Biomed. Anal. 35:769–777*

McConathy J., and Owens M.J. (2003). Stereochemistry in Drug Action. *J. Clin. Psychiatry 5:70-73 (2003)*

Millot M.C. (2003). Separation of drug enantiomers by liquid chromatography and capillary electrophoresis, using immobilized proteins as chiral selectors. *J. Chromatogr. B 797:131–159*

Mitchell J.A., Akarasereenont P., Thiemermann C., Flower R.J.and Vane J.R. (1994). Selectivity of nonsteroidal antiinflammatory drugs as inhibitors ofconstitutive and inducible cyclooxygenase. *Proc. Natl. Acad. Sci. 90:11693-11697*

Mohamed N.A.L., Kuroda Y., Shibukawa A., Nakagawa T., Gizawy S.E., Askal H.F., Kommos M.E.E. (2000). Enantioselective binding analysis of verapamil to plasma lipoproteins by capillary electrophoresis–frontal analysis. *J. Chromatogr A 875 (2000) 447–453*

Motulsky H.J. and Brown R.E. (2006). Detecting outliers when fitting data with non-linear regression – a new method based on robust nonlinear regression and the false discovery rate. *BMC Bioinformatics 123:1-20*

Nagori B.P., Deora M.S. and Saraswat P. (2011). Chiral Drug Analysis and Their Application. *Int. Pharm. Sci. Rev. and Res. 6:106-113*

Nirogi R.V.S., Kota S., Peruri B.G., Kandikere V.N., and Mudigonda K. (2006). Chiral high-performance liquid chromatographic method for enantioselective analysis of zaltoprofen. *Acta Chromatogr. 17:202-209*

Nomura A., Yasuda H., Kobayashi T., Kishino S., Kohri N., Iseki K., and Miyazak K. (2002). Serum alpha-l-acid glycoprotein and protein binding of disopyramide in patients with congestive heart failure. *Eur. J. Clin. Pharmacol. 42:115-116*

Ohnishi T., Mohamed N. A.L., Shibukawa A., Kuroda Y., Nakagawa T., Gizawy S. E., Askal H.F., and Kommos M. E. E. (2002). Frontal analysis of drug–plasma lipoprotein binding using capillary electrophoresis. *J. Pharm. Biomed. Anal. 27: 607–614*

Østergaard J. and Heegaard N. H. H. (2003). Capillary electrophoresis frontal analysis: Principles and applications for the study of drug-plasma protein binding. *Electrophoresis 24:2903–2913*

Patel D., Mashru R. (2011). Enantiomeric Resolution of (±)Flurbiprofen Using L(–)-Serine Impregnated Silica as Stationary Phase by Thin Layer Chromatography. *Int. J. Pharm. Pharm. Sci. 3:131-133*

Pîrnău A. and Bogdan M. (2008). Investigation of the interaction between naproxen and Human Serum Albumin. *Romanian J. Biophys. 18:49–55*

Qi Z., Zhou B., Xiao Q., Shi C., Liu Y., Dai J. (2008). Interaction of rofecoxib with human serum albumin: Determination of binding constants and the binding site by pectroscopic methods. *J. Photochem. Photobio. A 193:81–88*

Sabela M.I., Gumede N.J., Escuder-Gilabert L., Martín-Biosca Y., Bisetty K., Medina-Hernández M.J., and Sagrado S. (2012). Connecting simulated, bioanalytical, and molecular docking data on the stereoselective binding of (±)-catechin to human serum albumin. *Anal. Bioanal. Chem. 402:1899–1909*

Sanchez-Vega B. (2005). Introduction to Capillary Electrophoresis of DNA:Biomedical Applications. Medical Biomethods Handbook10.1385/1-59259-870-6:095 95-116

Schmitt U., Bojarsk J.and Holzgrabe U. (2009). Enantioseparation of chiral thiobarbiturates using cyclodextrin modified Capillary Electrophoresis. *Electrophoresis 22:3237-3242*

Shibukawa A., Kuroda Y., and Nakagawa T.(1999). High-performance frontal analysis for drug–protein binding study. *J. Pharm. Biomed. Anal. 18:1047–1055*

Shimazawa R., Nagai N., Toyoshima S., and Okuda H. (2008). Present State of New Chiral Drug Development and Review in Japan. *J. Health Sci. 54:23-29*

Singh S.S., and Mehta J.(2006). Measurement of drug–protein binding by immobilized human serum albumin-HPLC and comparison with ultrafiltration. *J. Chromatogr. B 834:108–116*

Somasundaram S., Rafi S., Hayllar J., Sigthorsson G., Jacob M., Price A.B., Macpherson A., Mahmod T., Scott D., Wrigglesworth J.M., Bjarnason I. (1997). Mitochondrial damage:a possible mechanism of the "topical" phase of NSAID induced injury to the rat intestine. *Gut. 41:344–353*

Spassov V.Z., Flook, P.K., Yan L. (2008). A molecular mechanics-based algorithm for protein loop prediction. *Protein Eng. Des. Sel. 21:91-100.*

SpassovV.Z. and Yan L.A (2008). Fast and accurate computational approach to protein ionization. *Protein Sci. 17:1955-1970.*

Sunfornsuk L. (2007). Capillary Electrophoresis in Pharmaceutical Analysis:A Survey on Recent Applications. *J. chromatogr. Sci. 45:559-577*

Sunfornsuk L. (2010). Recent Advances of Capillary Electrophoresis in pharmaceutical analysis. *Anal. Bioanal. Chem. 398:29-52*

Swearingen R.A. ., Zhorov E., Cohen A., Sybertz T. and Barry E.F. (2004). Determination of the binding parameter constants of Renagel® capsules and tablets at pH 7 by high performance capillary electrophoresis. *J. Pharm. Biomed. Anal. 35:753–760*

Tagliaro F., Manetto G., Crivellente F., Smith F.P. (1998). A brief introduction to capillary electrophoresis. *Forensic Sci. Int. 92:75–88*

Tajmir-Riahi H.A. (2007). An overview of drug binding to Human Serum Albumin: Protein folding and unfolding. *Sci. Iran* 14:87-95

Tanaka Y.and Terabe S. (2002). Estimation of binding constants by capillary electrophoresis. *J. Chromatogr. B 768:81–92*

Tanaka Y. (2002). Method development of enantiomer separations by Affinity capillary Electrophoresis, Cyclodextrin Electrokinetic Chromatography and Capillary Electrophoretic-Mass spectroscopy. *Chromatography 23:13-23*

Tang Y., Zhu H., Zhang Y., and Huang C. (2006). Determination of human plasma protein binding of baicalin by ultrafiltration and high-performance liquid Chromatography. *Biomed. Chromatogr. 20:1116–1119*

Tickle D.C., Okafo G.N., Camilleri P., Jones R.F.D. and Kirby A.J. (1994). Glucopyranoside-Based Surfactants as Pseudostationary Phases forchiral separation in Capillary Electrophoresis. *Anal. Chem. 66:4121-4126*

Vaile J.H., and Davis P.(1998). Topical NSAIDs for Musculoskeletal Conditions. *Drugs 56:783-799*

Valko K., Nunhuck S., Bevan C., Abraham M.H., Reynolds D.P. (2003). Fast Gradient HPLC Method to Determine Compounds Binding to Human Serum Albumin. *J. Pharm. Sci. 92:2236–2248*

Vane J.R., and Botting R.M. (1998). Mechanism of Action of Nonsteroidal Anti-inflammatory Drugs. *Am. J. Med. 104:2S-8S*

Verleysen K. and Sandra P (1998). Separation of chiral compounds by capillary electrophoresis. *Electrophoresis 19: 2798-2833*

Wren S. (2001). Other Chiral selectors. *Chromatographia Supplement 54:78-92*

Wu G., Robertson D.H., Brooks III C.L., Vieth M (2003). Detailed analysis of grid-based molecular docking: A case study of CDOCKER-a CHARMM-based MD docking algorithm. *J. Comp. Chem. 24:1549-1562*.

Wybranowski T., Cyrankiewicz M., Ziomkowska B., and Kruszewski S. (2008). The HSA affinity of warfarin and flurbiprofen determined by fluorescence anisotropy measurements of camptothecin. *BioSyst. 94:258–262*

Yan Xu (1996). Chem. Edu. 1 ISSN 1430-4171

Ye J., Yu W., Chen G., Shen Z., and Zeng S.(2009). Enantiomeric separation of 2-non-steroidal anti-inflammatory drugs by HPLC with hydroxypropyl-β- cyclodextrin as a chiral mobile phase additive. *Biomed. Chromatogr. 24:799-807*

Yi-Fen P., Chuen-Ying L. (2002). Capillary electrochromatographic separation of non-steroidal anti-inflammatory drugs with a histidine bonded phase. *J. Chromatogr. A 982:293–301*

Zahra R., Ahmadb R., Ali-Asghar M.S., Ali A., Soghra K. (2006). A study of the interaction between ropranolol and nsaids in protein binding by gel filtration method. *Ind. J. Clin. Biochem. 21:121-125*

Zaidi K, Capillary electrophoresis general chapters 05 727:2696, USP29-NF24 (accessed July 2011)

Zhab S., Yegnasubramanian V., Nelson W.G., Isaacs W.B., De Marzo A.M. (2004). Cyclooxygenases in cancer:progress and perspective. *Cancer Lett. 215:1-20*

Zheng Y., JiY. (2011). Monoliths with Proteins as Chiral Selectors for Enantiomer Separation. *World Congress Eng. Comp. Sci. 2:1-6*

Zhivkova Z.D. and Russeva V. N. (1998). Stereoselective binding of ketoprofen enantiomers to human serum albumin studied by high-performance liquid affinity chromatography. *J. Chromatogr. B 714: 277–283*

Zsila F., IwaoY. (2007). The drug binding site of human α-1-acid glycoprotein: Insight from induced circular dichroism and electronic absorption spectra. *Biochim. Biophys. Acta 1770:797–809*

Appendix 1

CE-FA drug-protein interactions (NSAIDs-HSA)

Appendix 1a

References of literature wavelengths for each drug

Compound	Literature Wavelength/nm	reference
Fenoprofen	214	Abushoffa et al. 2002
Fenbufen	279	Deschamps-Labat et al. 1997
Naproxen	235, 210	Aturki et al. 1998
Flurbiprofen	246, 254	Ye J et al. 2009
Ketoprofen	262, 256	Ye J et al. 2009, Salvatore Fanali (2000)
Indoprofen	220, 254, 280	Fillet 1997, Yi-Fen and Chuen-Ying 2002
Ibuprofen	220, 226,253	Blanco et al. 1998, Fazlena 2006, Martínez-Pla et al. 2004

Calibration Experimental output: Graphical representation

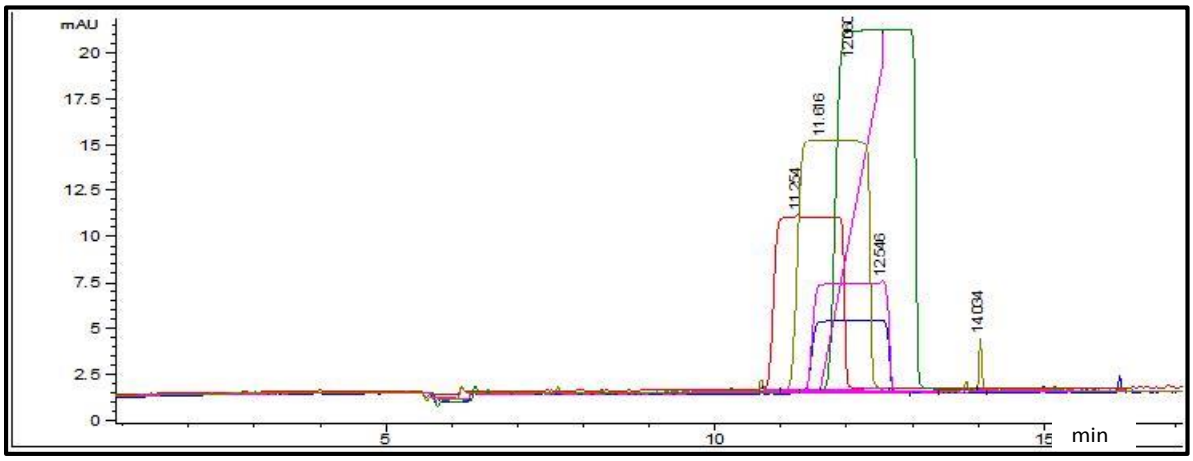

CE-FA electropherogram showing calibration standards 50, 75, 120, 180 and 250µM of Ketorolac injected by applying 50 mbar for 60s, with the capillary temperature being 36.5 °C at 317 nm.

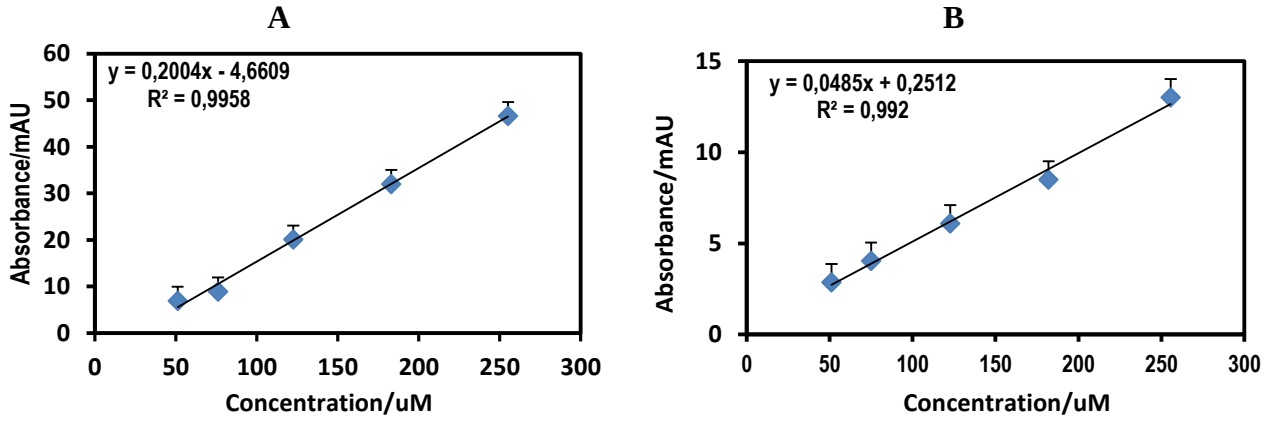

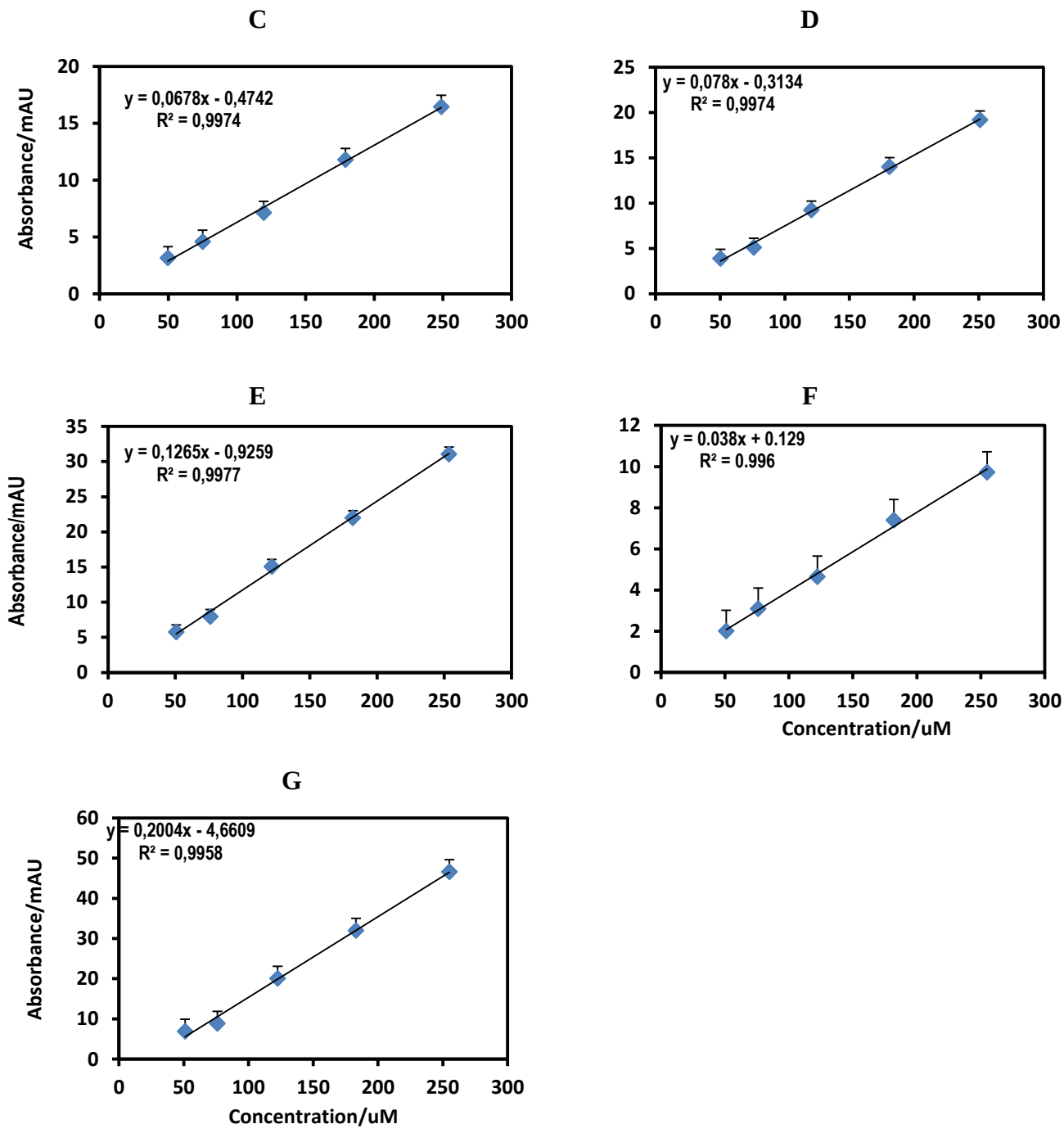

A: ketorolac, B: ketoprofen, C: indoprofen, D: flurbiprofen, E: fenbufen, F: ibuprofen, G: naproxen

Appendix 1b : Experimental designs

CE-FA Experimental design for fenbufen and pharmacokinetic parameters obtained using MATLAB calculations when prepared standards were varied from 50-300 µM, and P kept constant throughout as can be seen from table.

ID	D, µM	P, µM	D_{exp}, µM	P_{exp}, µM	d,µM	d/P	K	$LogK_1$	D/P
1	50	525	51.12	527	4.87	0.009	16439.21	4.22	0.10
2	100		102.20		5.09	0.010	29531.28	4.47	0.19
3	150		153.40		5.76	0.011	35011.59	4.54	0.29
4	200		204.50		6.53	0.012	35917.03	4.56	0.39
5	250		255.60		7.72	0.015	32272.94	4.51	0.49
6	300		306.70		7.94	0.015	30926.21	4.49	0.58

CE-FA Experimental design for naproxen and pharmacokinetic parameters obtained using MATLAB calculations.

ID	D, µM	P, µM	D_{exp}, µM	P_{exp}, µM	d,µM	d/P	K	$LogK_1$	D/P
1	50	525	49.94	526	21.00	0.040	2476.09	3.39	0.09
2	100		99.89		22.80	0.043	5485.77	3.74	0.19
3	150		149.83		23.20	0.044	7878.69	3.90	0.28
4	200		199.77		23.60	0.045	9438.67	3.97	0.38
5	250		249.72		25.60	0.049	9552.18	3.98	0.47
6	300		299.66		25.80	0.049	9673.40	3.99	0.57

CE-FA Experimental design for ibuprofen and pharmacokinetic parameters obtained using MATLAB calculations

ID	D, µM	P, µM	D_{exp}, µM	P_{exp}, µM	d,µM	d/P	K	$LogK_1$	D/P
1	50	525	50.97	527	18.10	0.034	3236.84	3.51	0.10
2	100		101.94		23.40	0.044	5428.32	3.73	0.19
3	150		152.91		25.00	0.048	7361.74	3.87	0.29
4	200		203.88		26.90	0.051	8299.56	3.92	0.39
5	250		254.85		28.80	0.055	8509.25	3.93	0.48
6	300		305.83		32.00	0.061	7799.26	3.89	0.58

CE-FA Experimental design for flurbiprofen and pharmacokinetic parameters obtained using MATLAB calculations.

ID	D, µM	P, µM	D_{exp}, µM	P_{exp}, µM	d,µM	d/P	K	$LogK_1$	D/P
1	50	525	50.20	527	8.03	0.015	9167.61	3.96	0.10
2	100		100.40		9.24	0.018	15482.40	4.19	0.19
3	150		150.60		10.40	0.020	18775.00	4.27	0.29
4	200		200.80		13.30	0.025	17233.29	4.24	0.38
5	250		251.00		15.20	0.029	16265.61	4.21	0.48
6	300		301.20		16.50	0.031	15053.44	4.18	0.57

CE-FA Experimental design for indoprofen and pharmacokinetic parameters obtained using MATLAB calculations.

ID	D, µM	P, µM	D_{exp}, µM	P_{exp},µM	d,µM	d/P	K	$LogK_1$	D/P
1	50	525	51.12	527	23.40	0.044	2129.61	3.33	0.10
2	100		102.20		30.00	0.057	3941.08	3.60	0.19
3	150		153.40		45.00	0.085	3630.74	3.56	0.29
4	200		204.50		48.40	0.092	4307.18	3.63	0.39
5	250		255.60		51.50	0.098	4607.68	3.66	0.49
6	300		306.70		53.00	0.101	4710.46	3.67	0.58

CE-FA Experimental design for ketoprofen and pharmacokinetic parameters obtained using MATLAB calculations.

ID	D, µM	P, µM	D_{exp}, µM	P_{exp}, µM	d,µM	d/P	K	$LogK_1$	D/P
1	50	525	51.12	527	18.80	0.036	3062.08	3.49	0.10
2	100		102.20		19.80	0.038	6662.09	3.82	0.19
3	150		153.40		21.60	0.041	8682.75	3.94	0.29
4	200		204.50		23.00	0.044	9816.93	3.99	0.39
5	250		255.60		25.00	0.047	9844.11	3.99	0.49
6	300		306.70		27.40	0.052	9091.28	3.96	0.58

Appendix 1c

Statistical evaluation

Graphical representation of nonlinear and linear regressions obtained by GraphPad Prism for estimations of best fit values using the CE-FA experimentally obtained data.

Non-linear fit	Linear fit
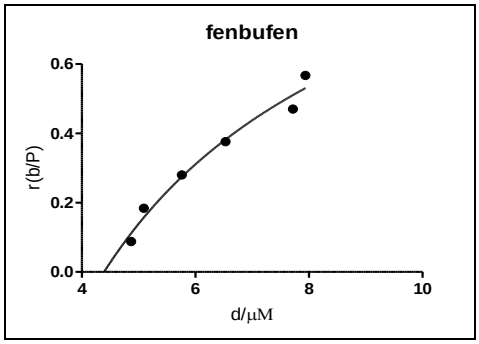	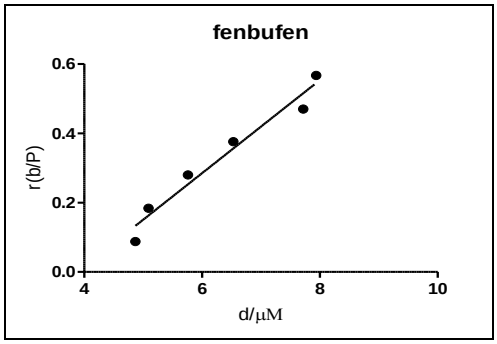
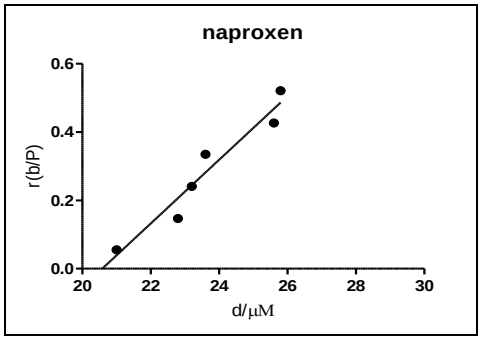	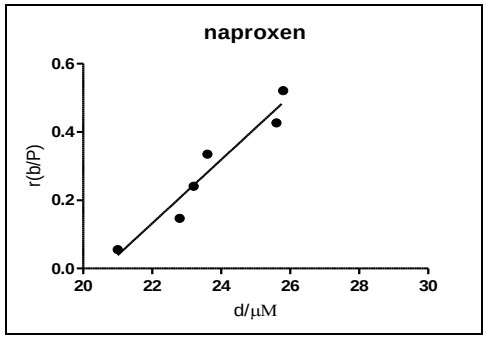
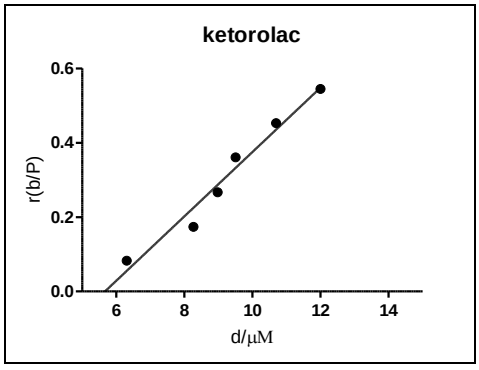	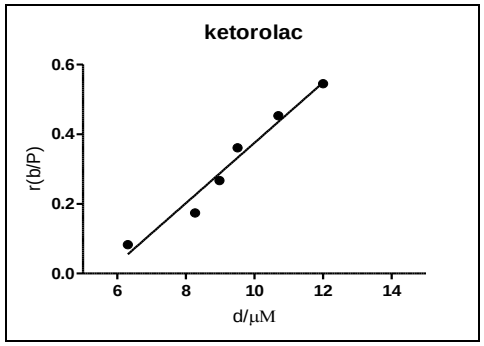
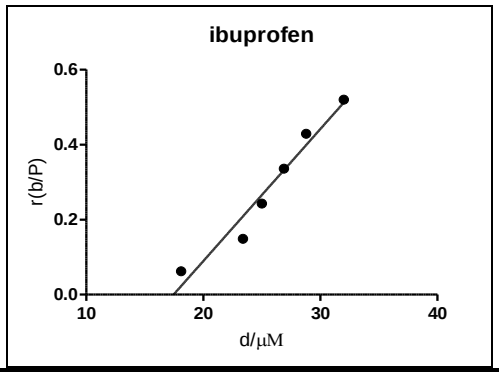	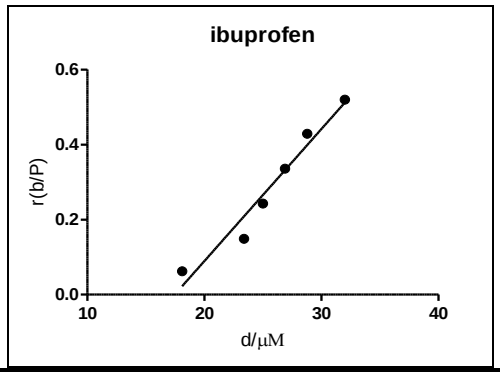

Non-linear fit	Linear fit
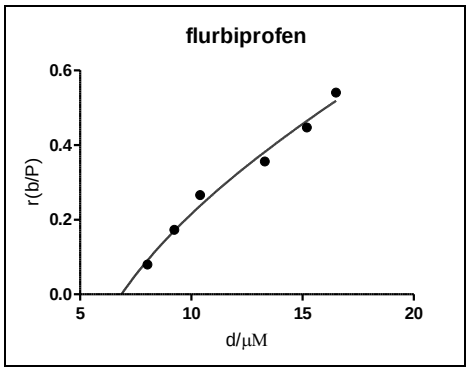	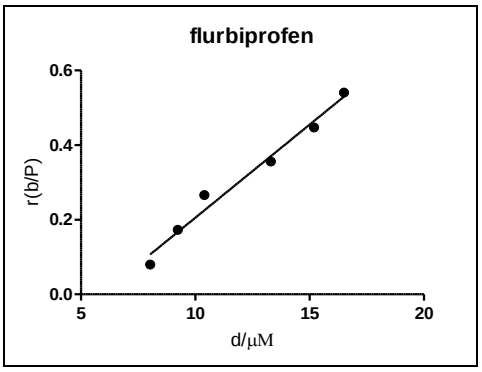
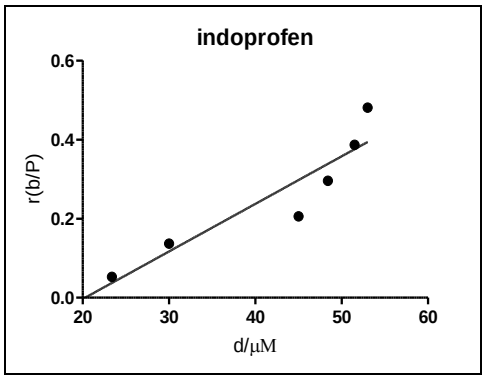	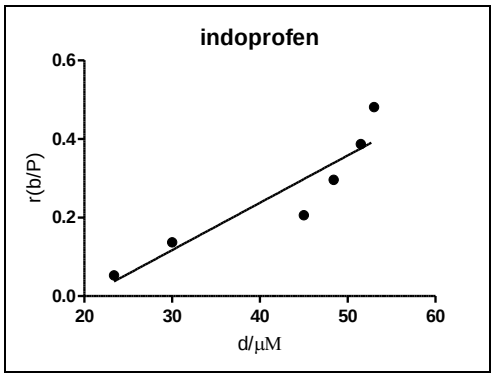
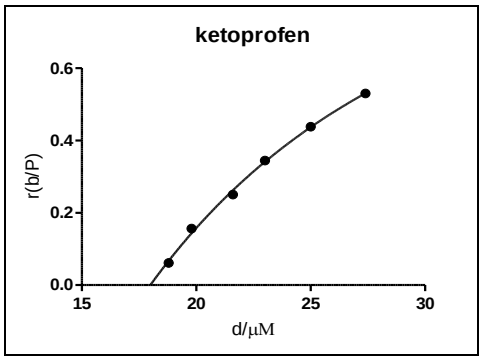	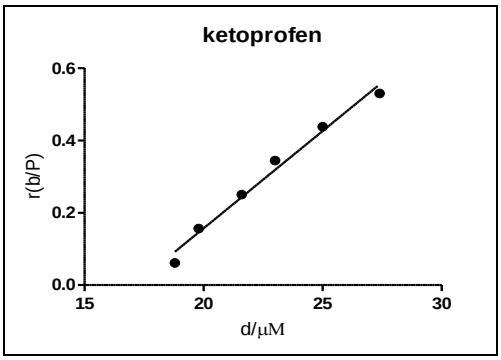

Appendix 1d

Z-score test diagrams for NSAIDs generated by METLAB based on the data obtained via CE-FA. A: Pink doted lines represent the median of the data set calculated based on logK at Z-score = 2 , B: shows where the data lies in a graph of Z-score=2.

	Z-score	
ID	**A**	**B**
I	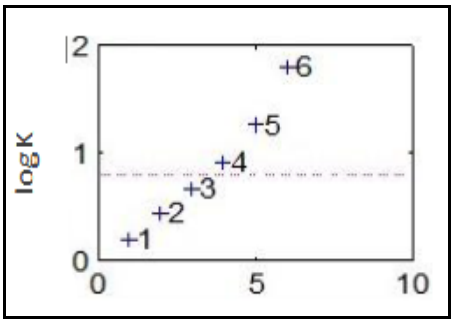	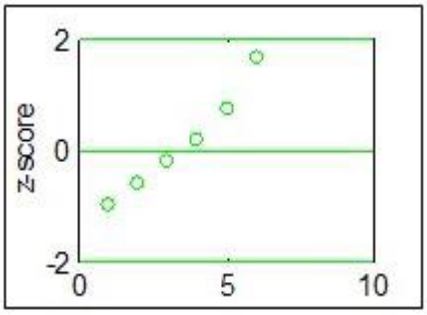
II	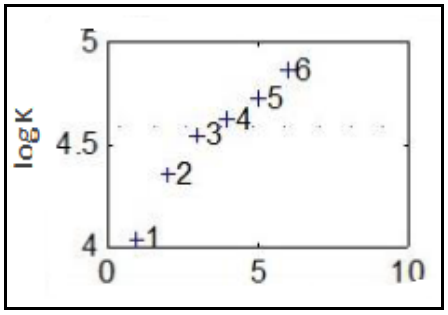	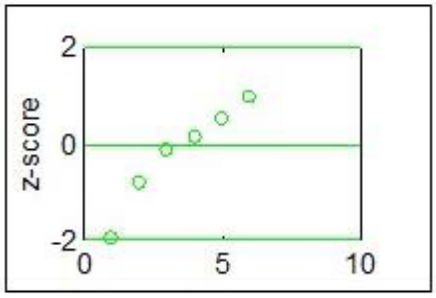
III	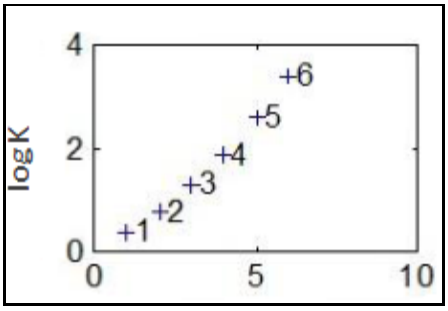	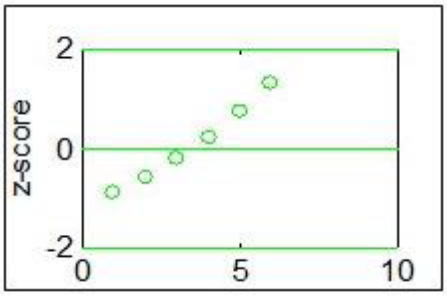
IV	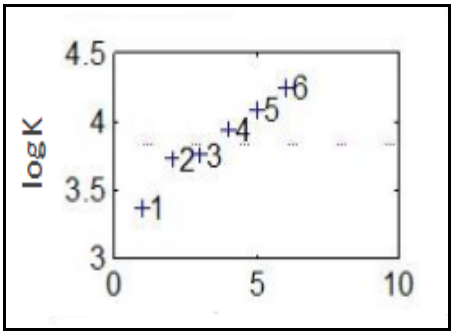	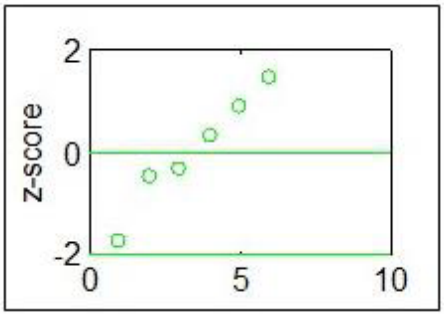

I:fenbufen, II:flurbiprofen, III: ibuprofen, IV:indoprofen, V: ketorolac, VI: naproxen, VII: ketoprofen

ID	Z-score	
	A	**B**
V	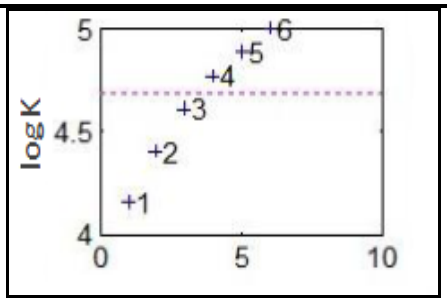	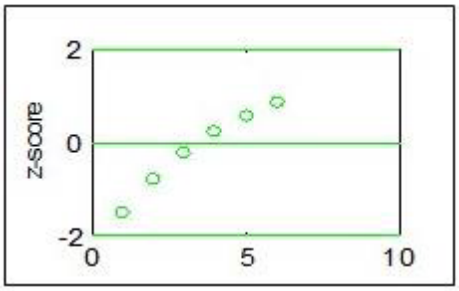
VI	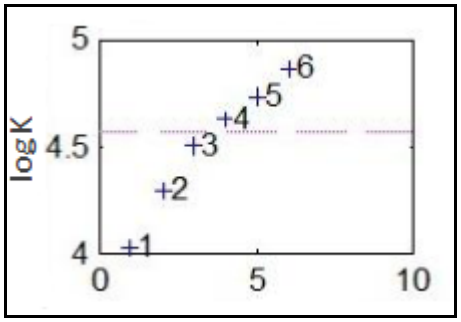	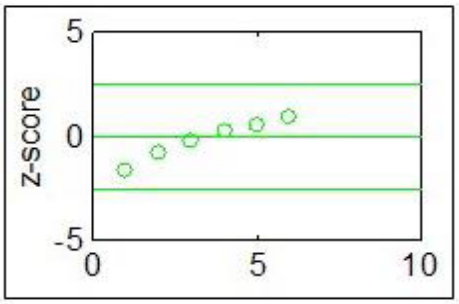
VII	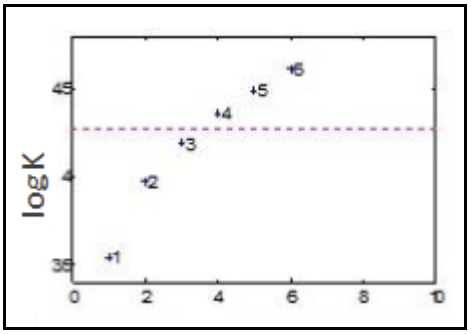	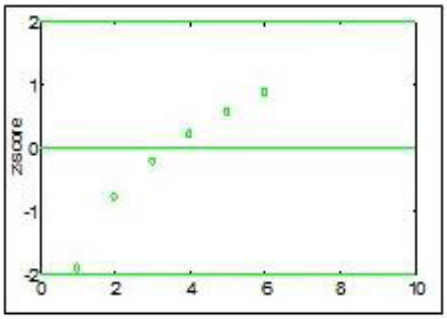

Appendix 1e

Grubbs' test graphical demonstration for the NSAIDs generated by METLAB based on the data obtained via CE-FA. The small pink circle in B represents the decrease in calculated variance in percentage.

ID	Grubb's Test	
	A	B
I	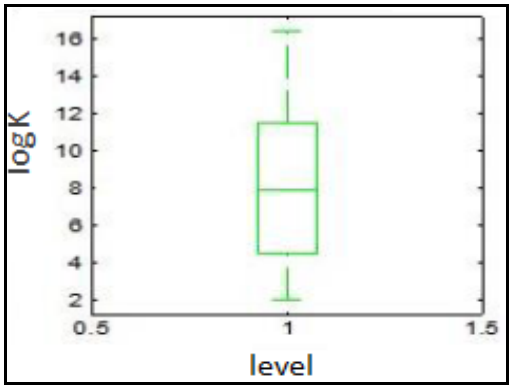	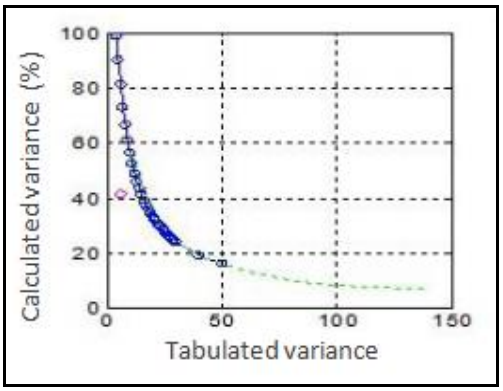
II	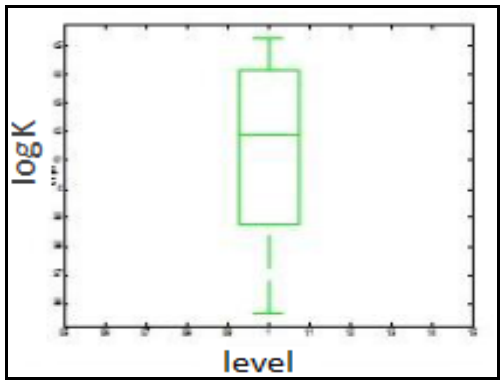	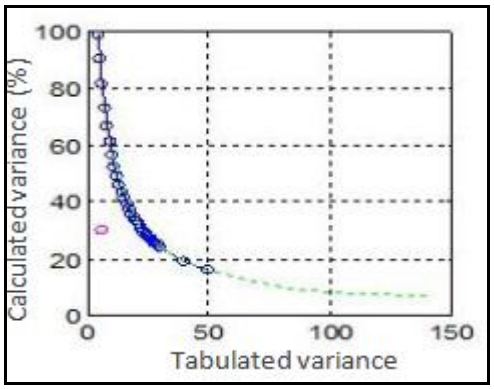
III	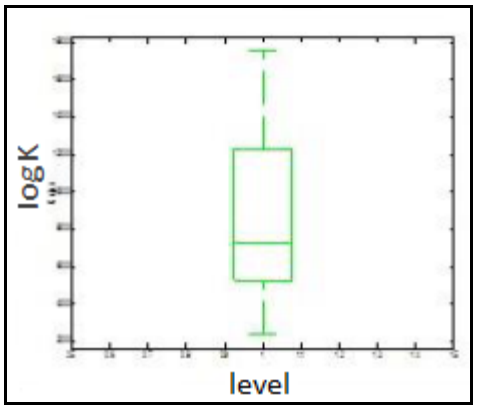	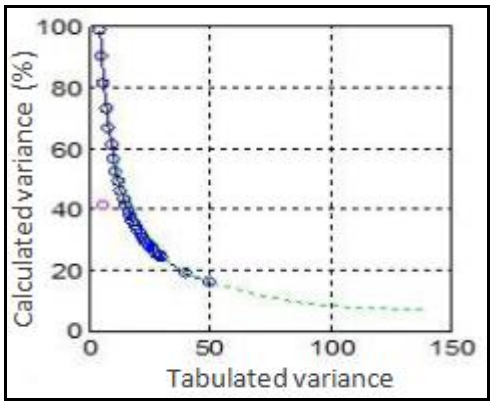

ID	Grubb's Test	
	A	B
IV	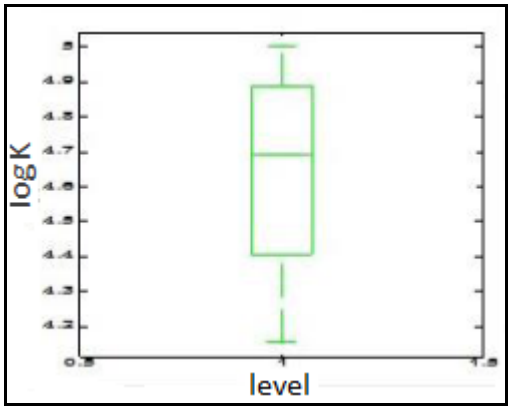	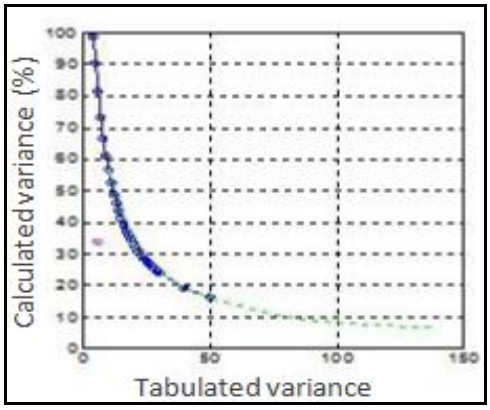
V	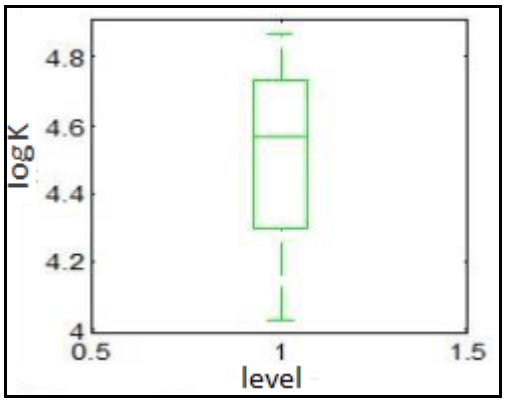	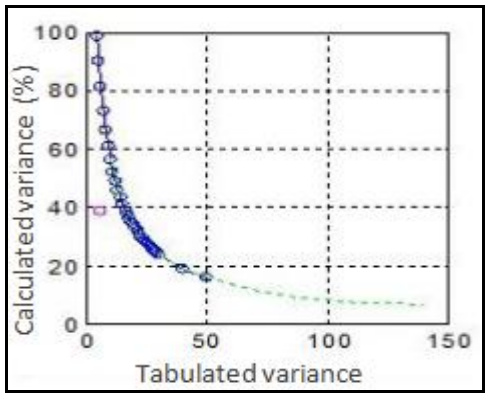

I:Fenbufen, II: Ibuprofen, III:Indoprofen, IV: Ketorolac, V: Naproxen

Appendix 1f

A shows Klotz plot for estimation of log*K*, B; shows scatchard plot, C; showing the Y-regression plot for each drug, where r is a ratio of bound drug over totalprotein and d is the free drug concentration.

	A	B	C
I	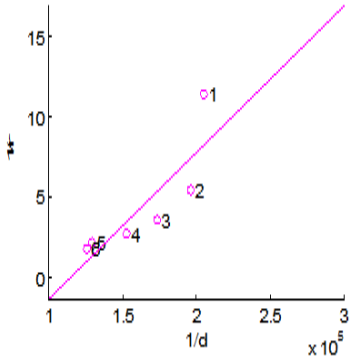	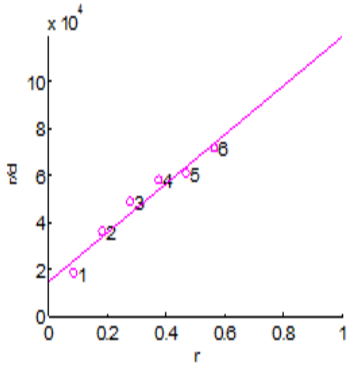	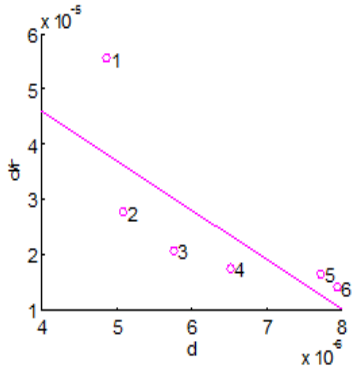
II	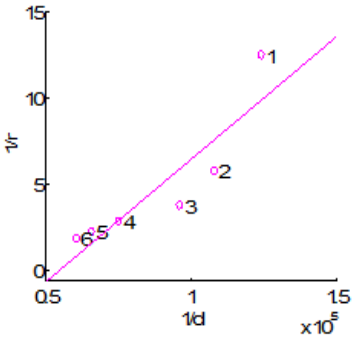	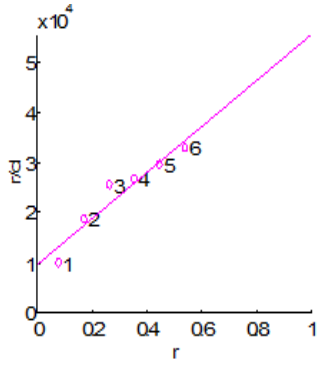	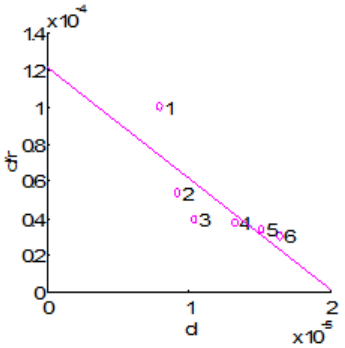
III	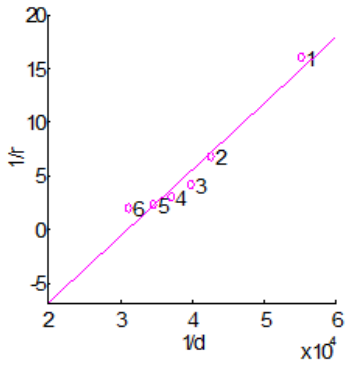	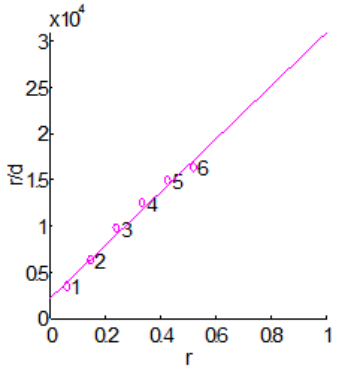	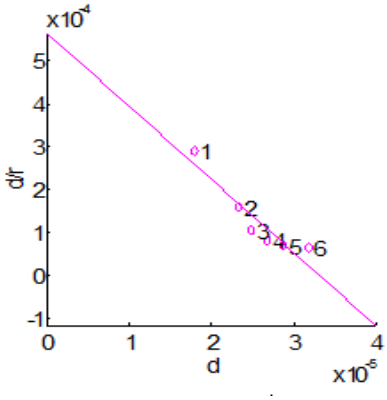

***I:Fenbufen, II: flurbiprofen, III: ibuprofen,**

Appendix 1f cont….

A shows Klotz plot for estimation of log*K*, B; shows scatchard plot, C; showing the Y-regression plot for each drug, where r is a ratio of bound drug over totalprotein and d is the free drug concentration.

	A	B	C
IV	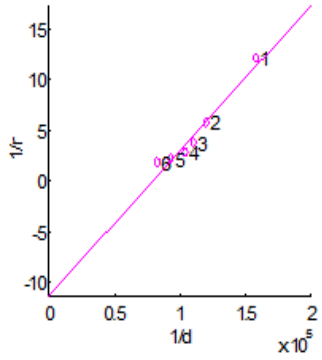	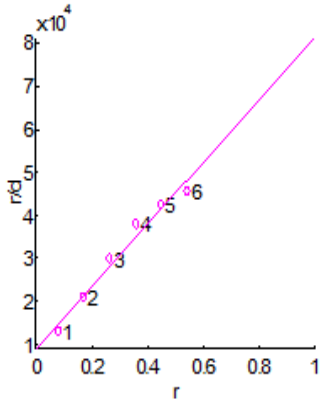	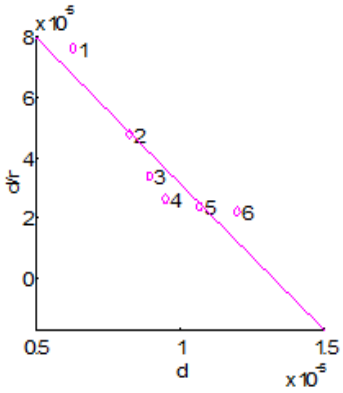
V	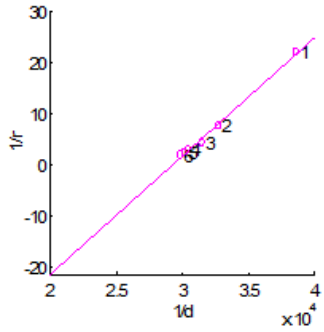	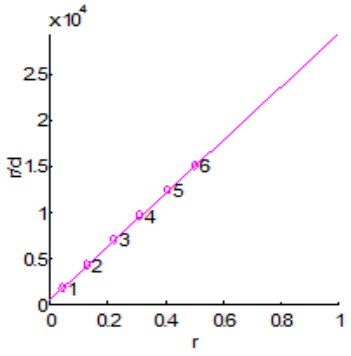	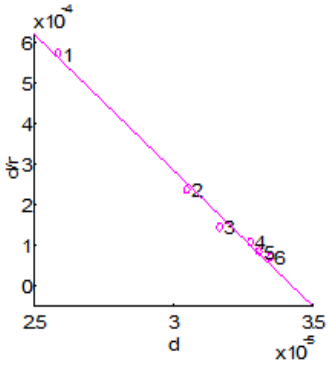
VI	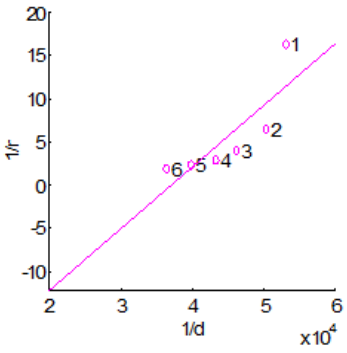	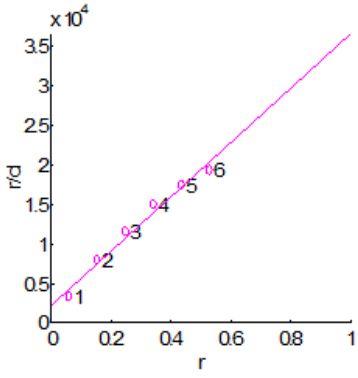	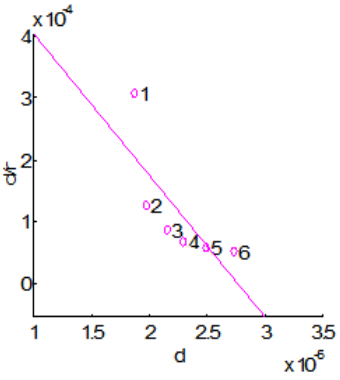

*** IV: Ketorolac, V: naproxen, VI: ketoprofen**

Appendix 2

CE-CZE drug-protein interactions (NSAIDs-HSA)

Appendix 2a

Calibration Experimental output: Graphical representation

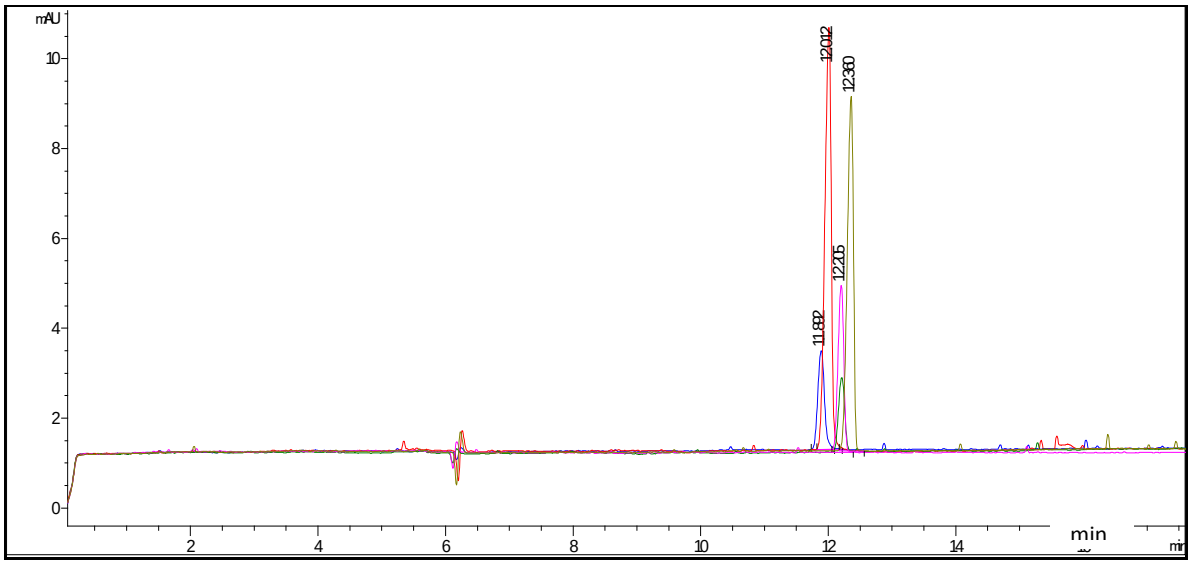

CE-CZE electropherogram showing calibration standards 50, 120, and 250µM of Ketoprofen injected by applying 50 mbar for 5s, with the capillary temperature being 36.5 °C at 220 nm.

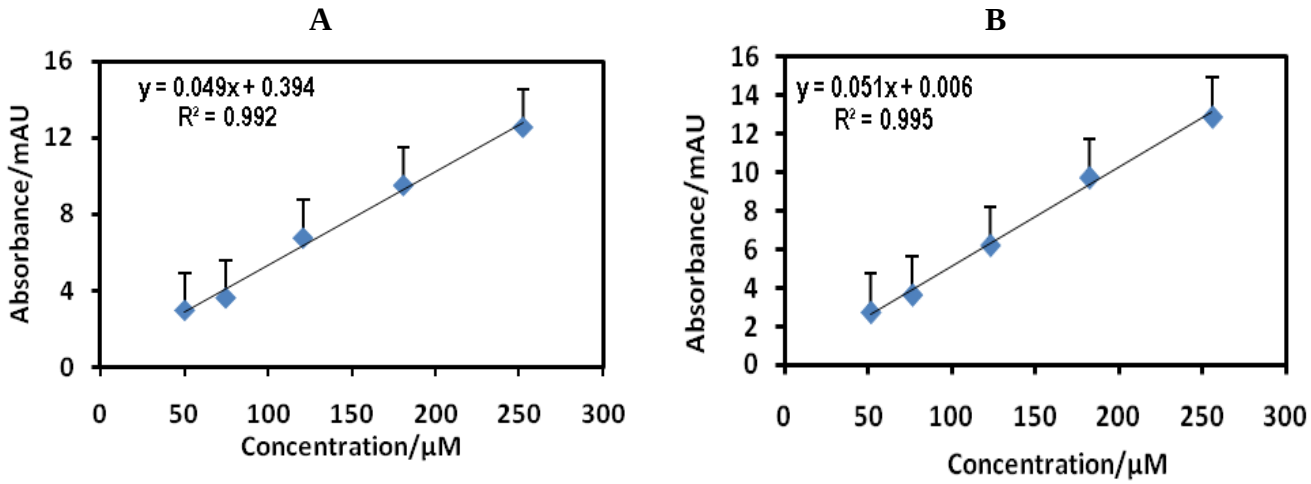

Appendix 2a cont....

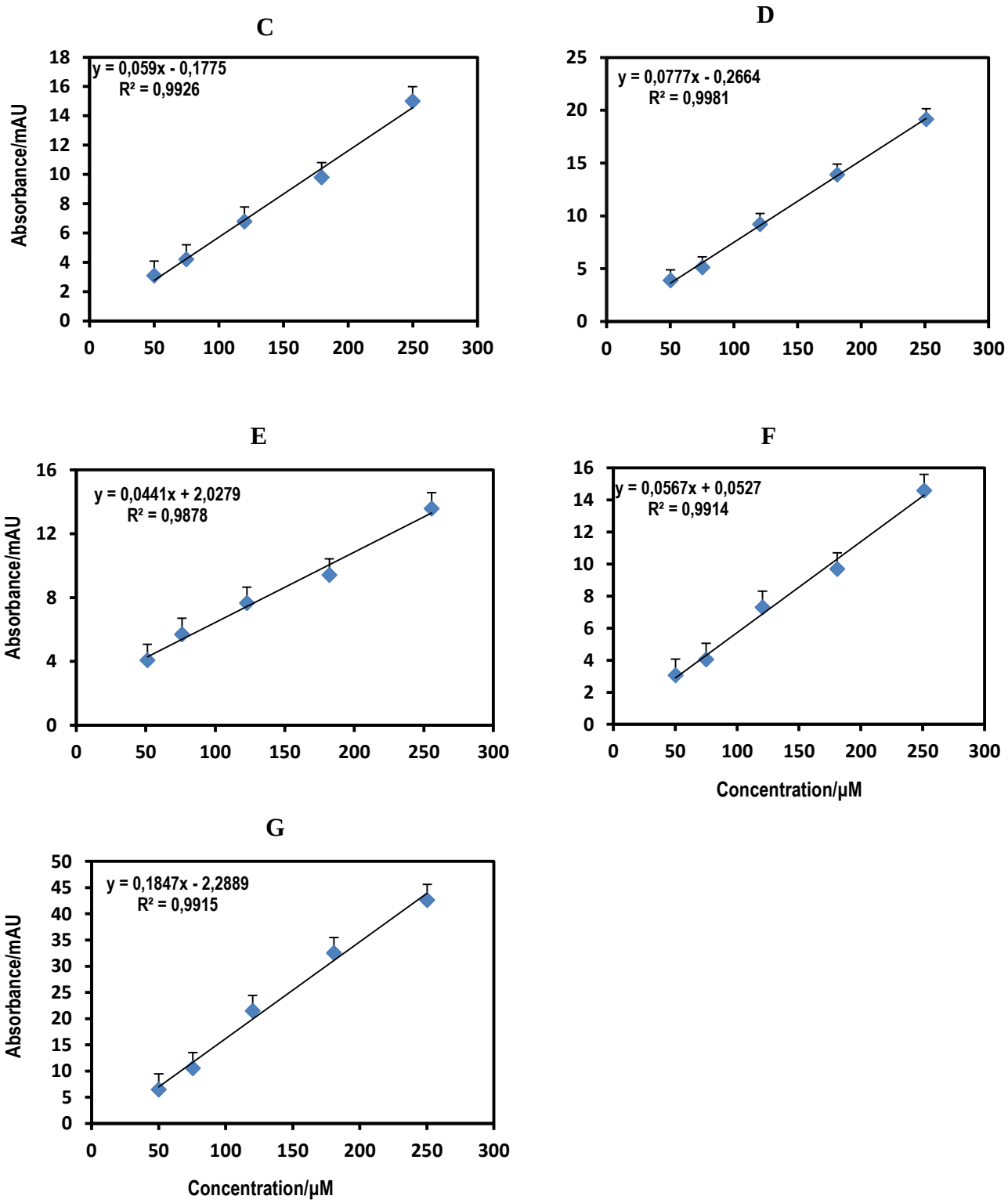

A: **ketorolac, B: ketoprofen, C: indoprofen, D: flurbiprofen, E: fenbufen, F: fenoprofen, G: naproxen**

Appendix 2b: Experimental designs

CE-CZE Experimental design for fenbufen and pharmacokinetic parameters obtained using MATLAB calculations when prepared standards were varied from 50-300 µM, and P kept constant throughout as can be seen from table.

ID	D, µM	P, µM	D_{exp}, µM	P_{exp}, µM	d,µM	d/P	K	$LogK_1$	D/P
1	50	525	51.1	527	7.6	0.014	10014.3	4.00	0.10
2	100		102.20		5.09	0.010	17802.7	4.25	0.19
3	150		153.40		5.76	0.011	21290.7	4.33	0.29
4	200		204.50		6.53	0.012	23325.5	4.37	0.39
5	250		255.60		7.72	0.015	24394.2	4.39	0.49
6	300		306.70		7.94	0.015	22188.3	4.35	0.58

CE- CZE Experimental design for naproxen and pharmacokinetic parameters obtained using MATLAB calculations.

ID	D, µM	P, µM	D_{exp}, µM	P_{exp}, µM	d,µM	d/P	K	$LogK_1$	D/P
1	50	525	50.1	526	23.8	0.045	1997.0	3.30	0.10
2	100		100.1		26.6	0.051	4509.2	3.65	0.19
3	150		150.2		29.2	0.056	6055.3	3.78	0.29
4	200		200.2		29.7	0.056	7381.9	3.87	0.38
5	250		250.3		30.1	0.057	8090.9	3.91	0.48
6	300		300.3		30.6	0.058	8169.9	3.91	0.57

CE- CZE Experimental design for ketorolac and pharmacokinetic parameters obtained using MATLAB calculations.

ID	D, µM	P, µM	D_{exp}, µM	P_{exp},µM	d,µM	d/P	K	$LogK_1$	D/P
1	50	525	50.5	526	8.93	0.017	8146.7	3.91	0.10
2	100		101.0		10.6	0.020	13421.9	4.13	0.19
3	150		151.4		11.5	0.022	16979.2	4.23	0.28
4	200		201.9		12.3	0.023	18742.6	4.27	0.38
5	250		252.4		13.4	0.025	18501.2	4.27	0.48
6	300		302.9		13.8	0.026	17937.9	4.25	0.57

CE- CZE Experimental design for ibuprofen and pharmacokinetic parameters obtained using MATLAB calculations.

ID	D, µM	P, µM	D_{exp}, µM	P_{exp}, µM	d,µM	d/P	K	$LogK_1$	D/P
1	50	525	51.1	527	17.1	0.032	3531.4	3.55	0.10
2	100		102.2		33.3	0.063	3412.8	3.53	0.19
3	150		153.4		41.5	0.079	4030.1	3.61	0.29
4	200		204.5		68.2	0.129	2811.5	3.45	0.39
5	250		255.6		71.7	0.136	3168.6	3.50	0.49
6	300		306.7		80.4	0.153	3047.5	3.48	0.58

CE- CZE Experimental design for ketoprofen and pharmacokinetic parameters obtained using MATLAB calculations.

ID	D, µM	P, µM	D_{exp}, µM	P_{exp}, µM	d,µM	d/P	K	$LogK_1$	D/P
1	50	525	50	527	23.4	0.045	2044.3	3.31	0.10
2	100		99.9		30.0	0.057	3834.5	3.58	0.19
3	150		149.8		45.0	0.086	3541.4	3.54	0.28
4	200		199.8		48.4	0.092	4230.2	3.63	0.38
5	250		249.7		51.5	0.098	4556.5	3.66	0.47
6	300		299.7		53.0	0.101	4697.8	3.67	0.57

CE-CZE Experimental design for indoprofen and pharmacokinetic parameters obtained using MATLAB calculations.

ID	D, µM	P, µM	D_{exp}, µM	P_{exp},µM	d,µM	d/P	K	$LogK_1$	D/P
1	50	525	51.0	527	28.5	0.054	1432.9	3.16	0.10
2	100		101.9		32.7	0.062	3491.3	3.54	0.19
3	150		152.9		37	0.070	4638.5	3.67	0.29
4	200		203.9		41.3	0.078	5166.6	3.71	0.39
5	250		254.9		47.2	0.090	5059.5	3.70	0.48
6	300		305.8		50.4	0.096	4955.8	3.70	0.58

CE-CZE Experimental design for fenoprofen and pharmacokinetic parameters obtained using MATLAB calculations

ID	D, µM	P, µM	D_{exp}, µM	P_{exp}, µM	d,µM	d/P	K	$LogK_1$	D/P
1	50	525	50.2	525	9.12	0.017	7909.3	3.90	0.10
2	100		100.5		9.84	0.019	14506.7	4.16	0.19
3	150		150.7		10.9	0.021	17916.7	4.25	0.29
4	200		200.9		12.4	0.024	18554.9	4.27	0.38
5	250		251.1		13.9	0.026	17817.2	4.25	0.47
6	300		301.4		14.9	0.028	16640.5	4.22	0.57

Appendix 2c: Statistical evaluation

Graphical representation of nonlinear and linear regressions obtained by GraphPad Prism for estimations of best fit values using the CE-CZE experimentally obtained data, where,b: the bound drug, P: the total protein concentration, D: total drug concentration, d: free drug concentration.

Non-linear fit	Linear fit

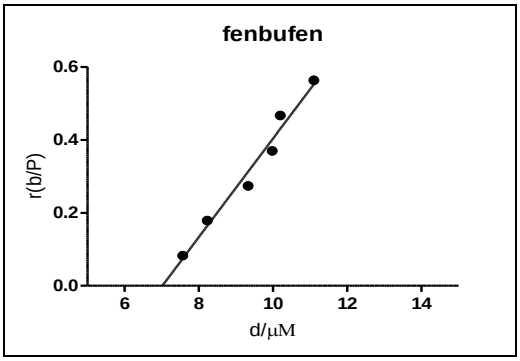

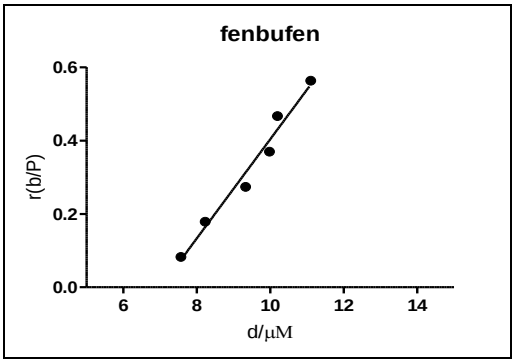

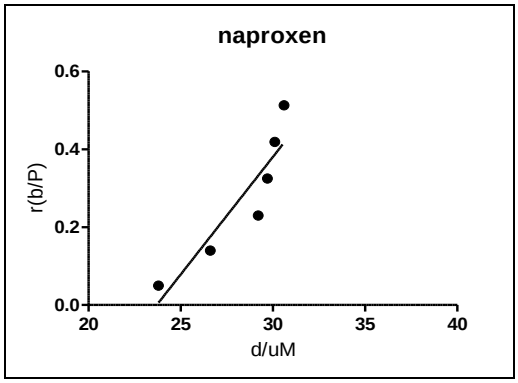

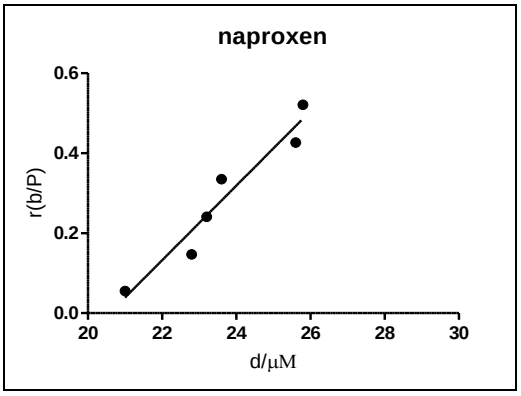

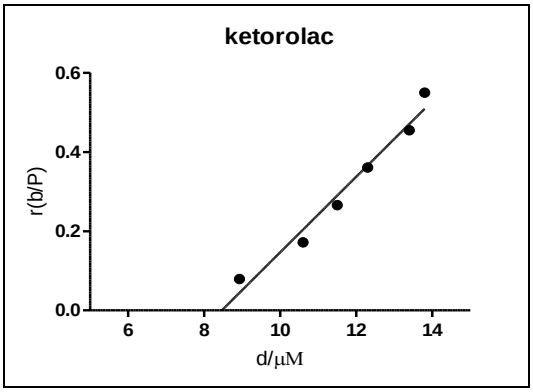

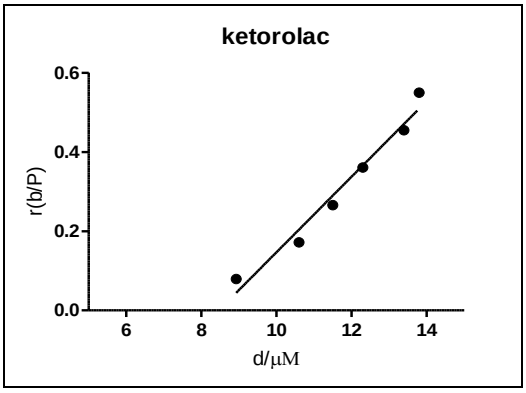

Non-linear fit	Linear fit
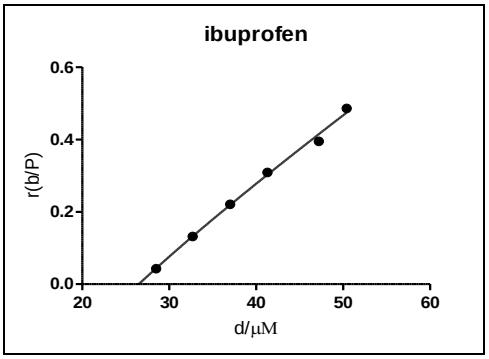	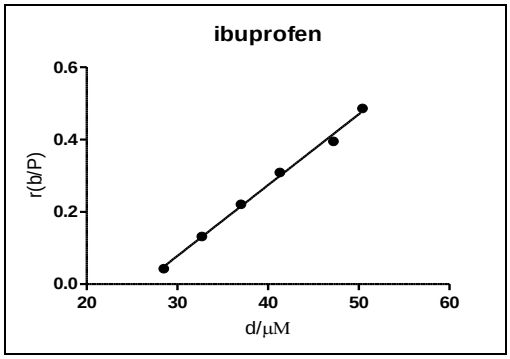
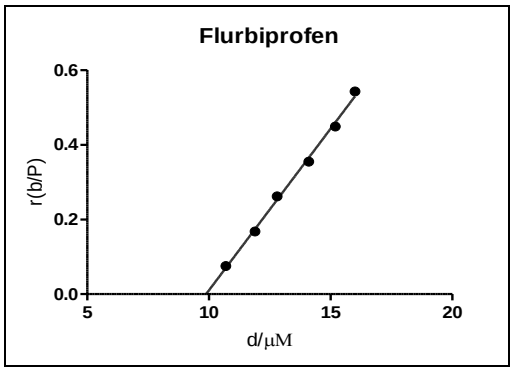	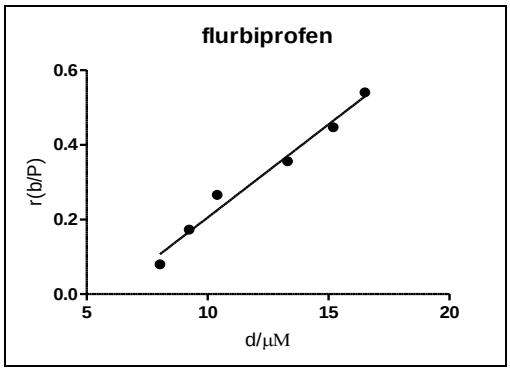
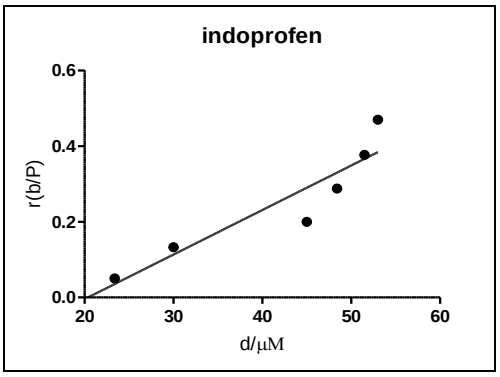	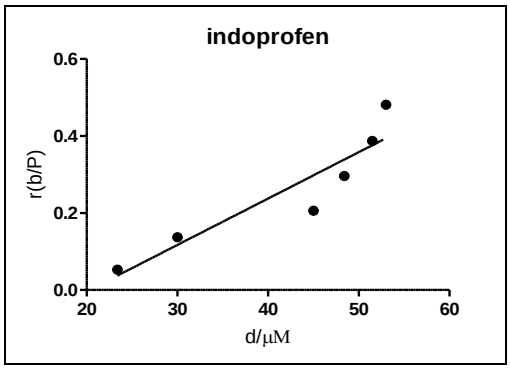
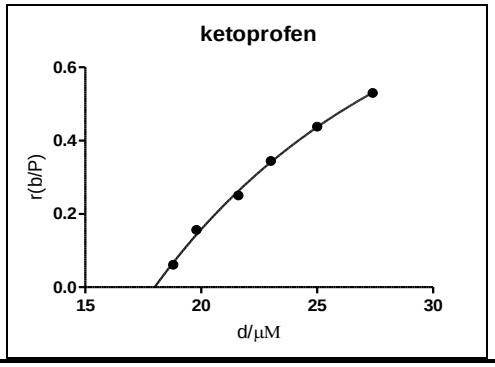	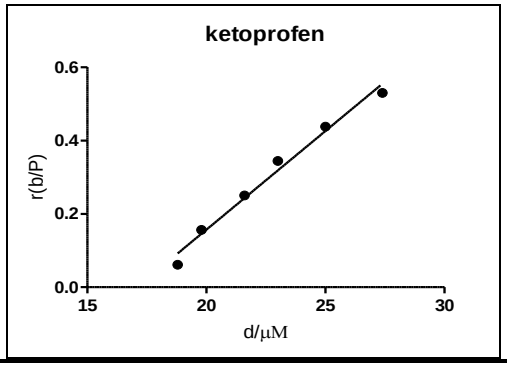

Appendix 2d

Z-score test diagrams of NSAIDs generated from MATLAB based on the data obtained via CE-CZE. A: Pink dotted lines represent the median of the data set calculated based on log at Z-score = 2 , B: shows where the data lies in a graph of Z-score=2.

ID	Z-score	
	A	B
I	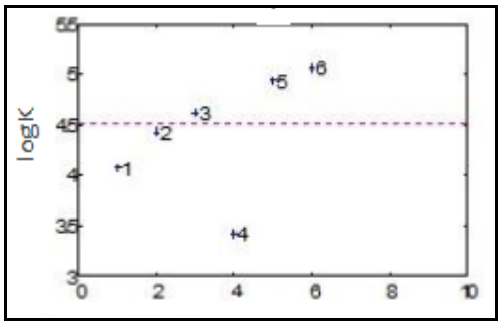	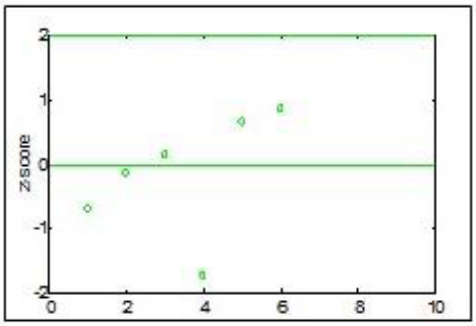
II	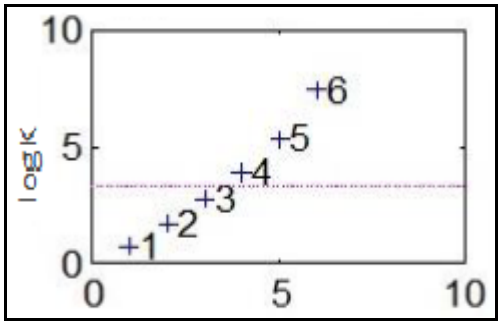	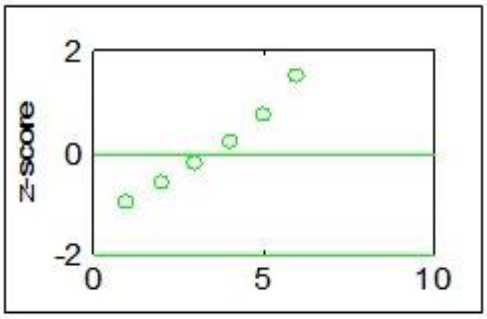
III	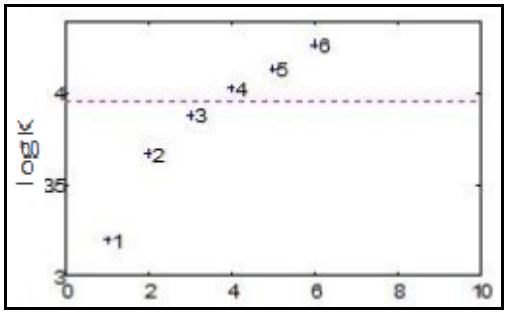	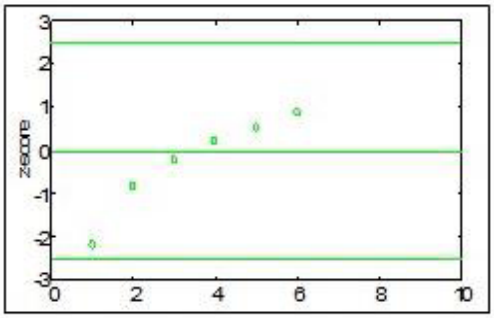
IV	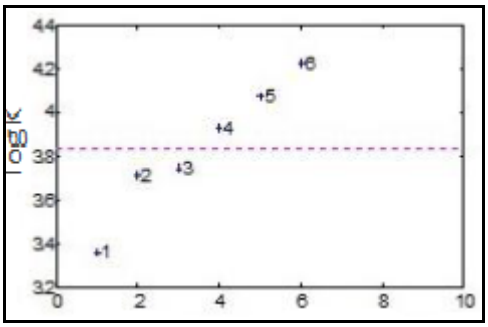	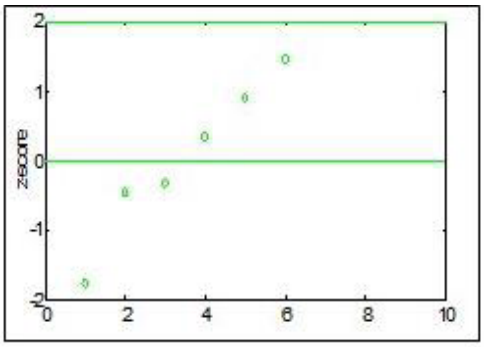

ID	Z-score	
	A	B
V	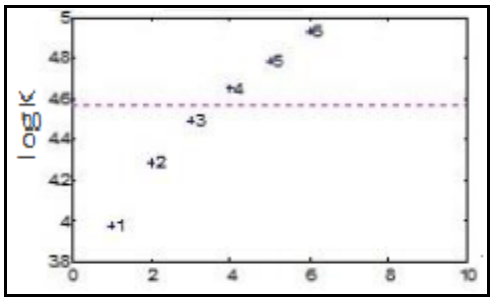	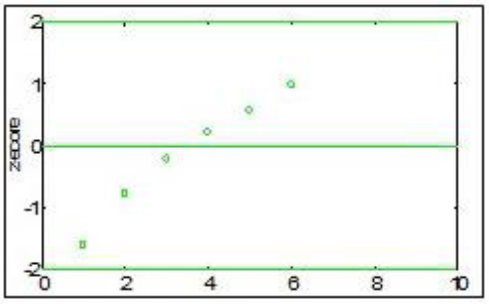
VI	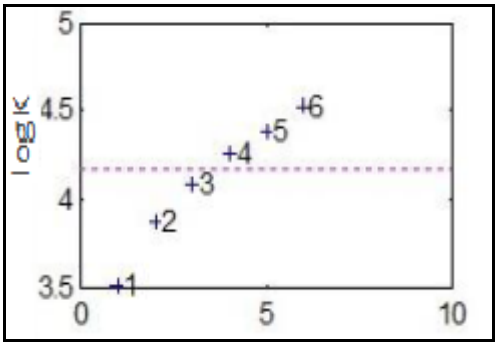	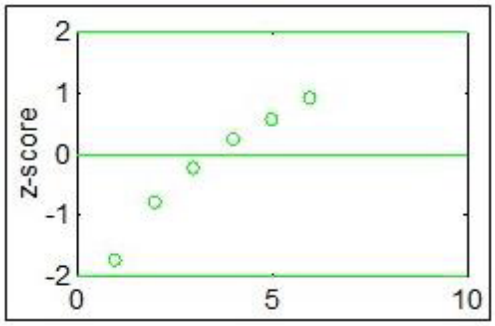
VII	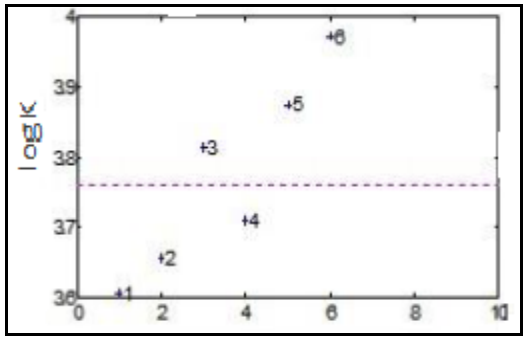	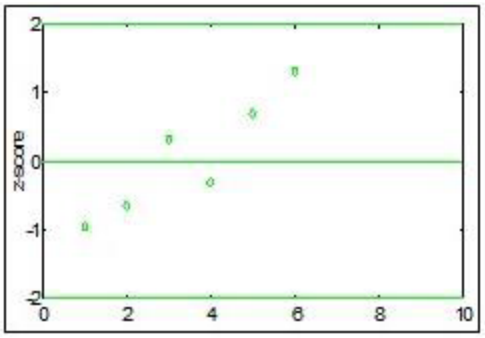

I: fenbufen, II: flurbiprofen, III: ibuprofen, IV: indoprofen, V: ketorolac, VI: naproxen, VII: ketoprofen

Appendix 2e

Grubbs' test graphical demonstration of NSAIDs generated from METLAB based on the data obtained via CE-CZE. The small pink circle in B represents the decrease in calculated variance in percentage.

ID	Grubb's Test	
	A	**B**
I	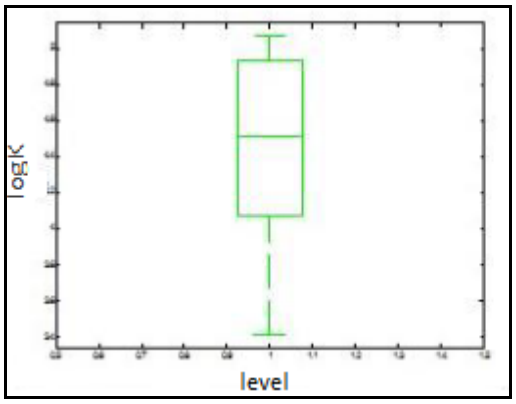	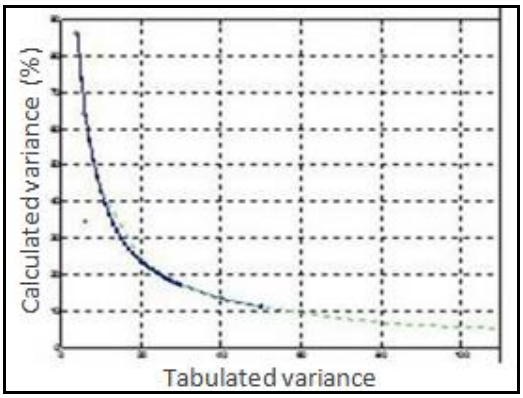
II	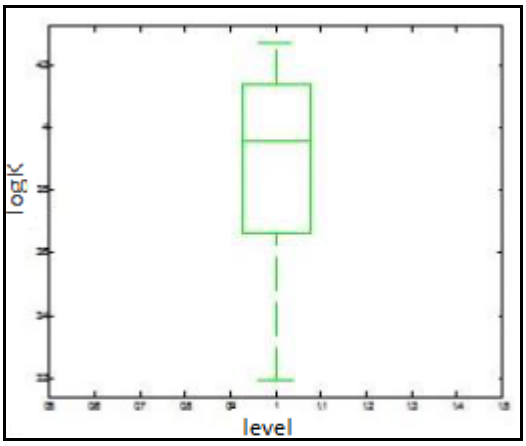	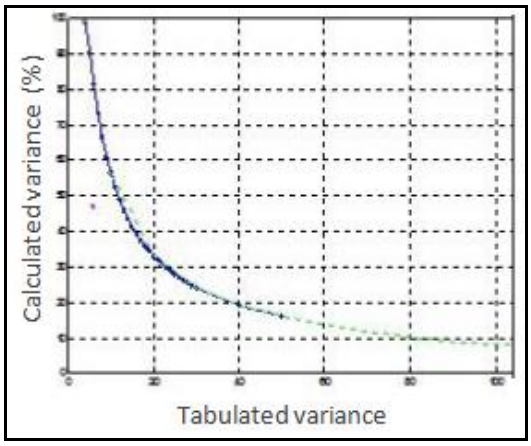
III	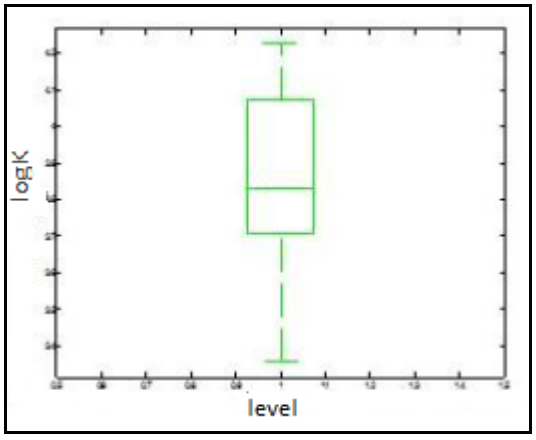	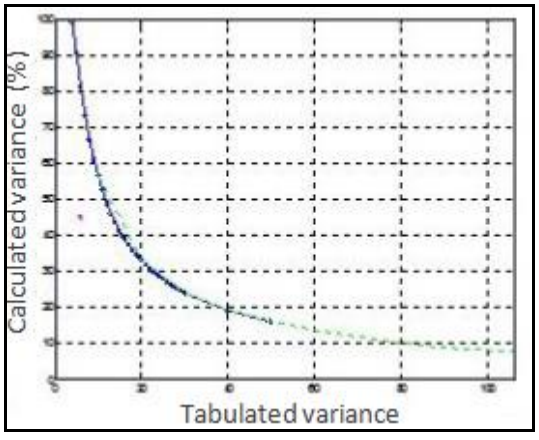

IV

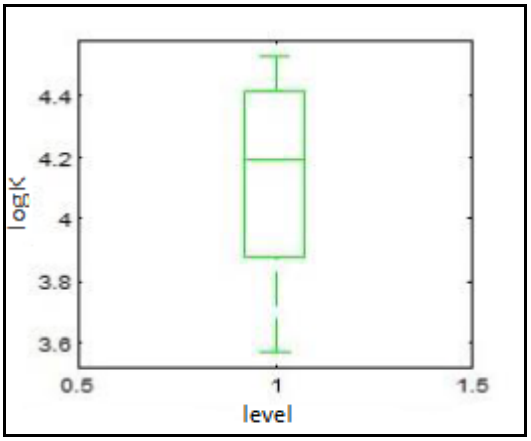

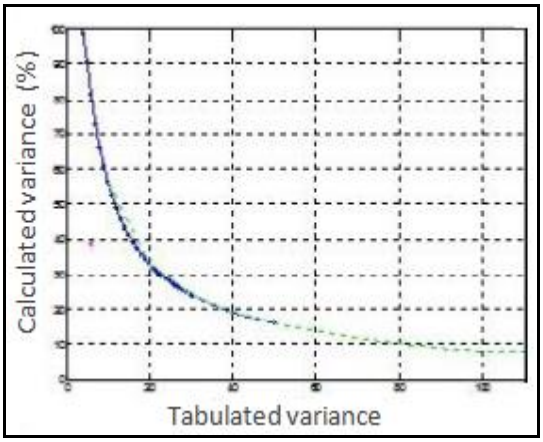

V

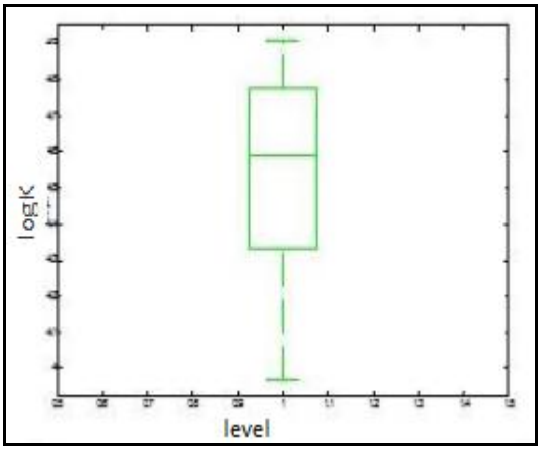

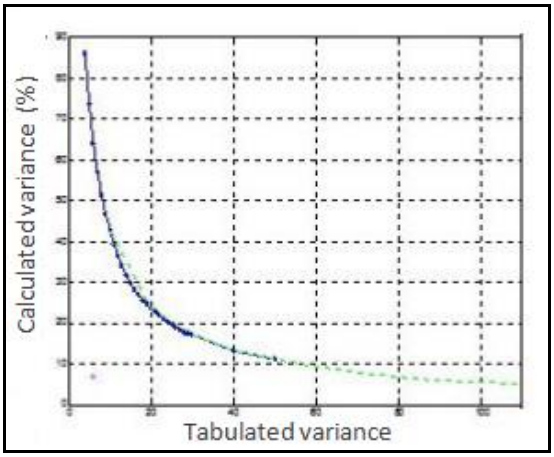

I: fenbufen, II: ibuprofen, III: indoprofen, IV: ketorolac, V: fenoprofen

Appendix 2f

A; shows Klotz plot for estimation of log*K*, B; shows scatchard plot, C; showing the Y-regression plot for each drug

	A	B	C
I	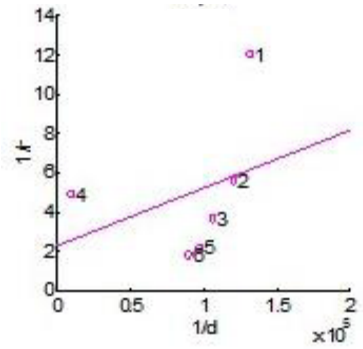	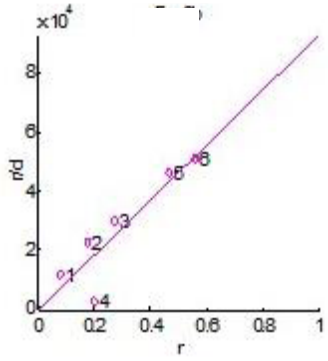	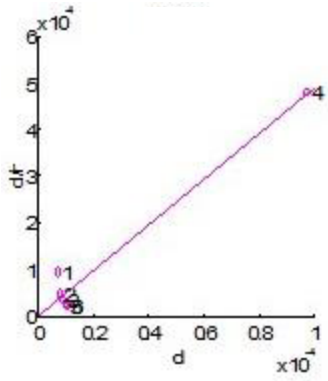
II	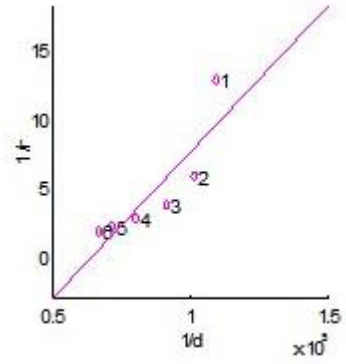	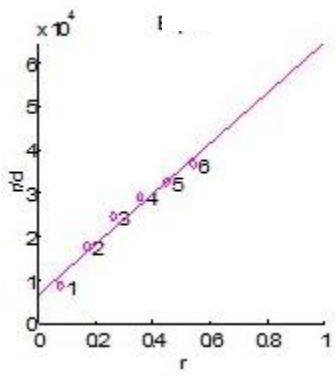	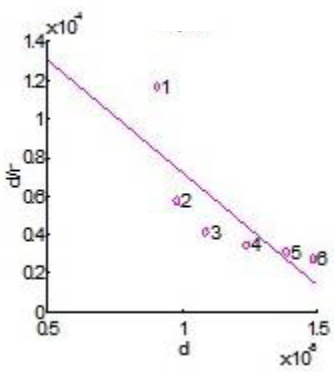
III	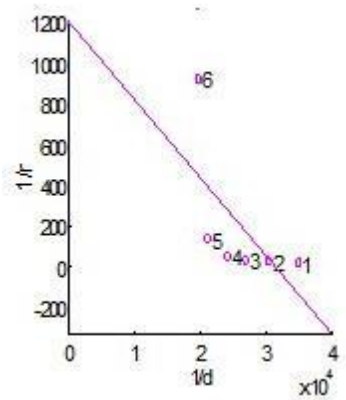	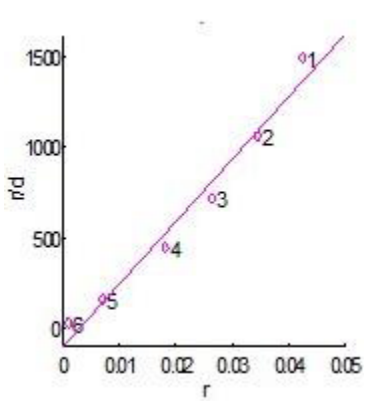	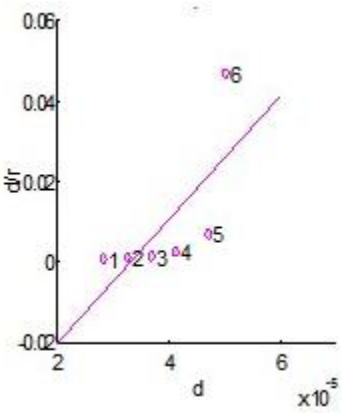

I:Fenbufen, II: fenoprofen, III: ibuprofen,

Appendix 2f cont....

	A	B	C
IV	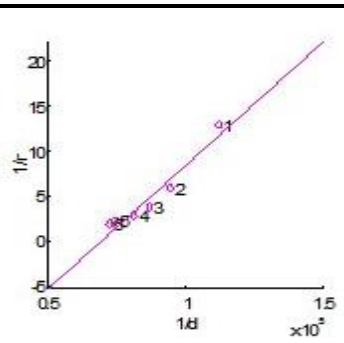	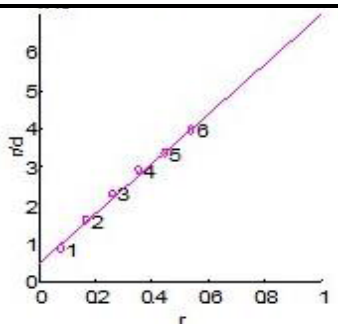	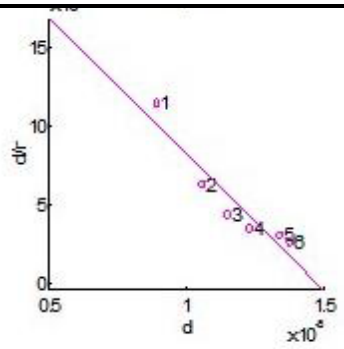
V	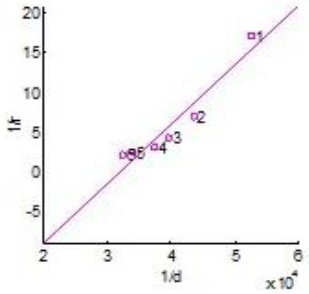	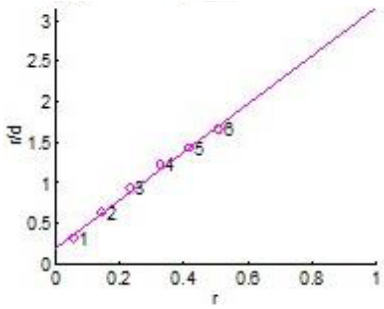	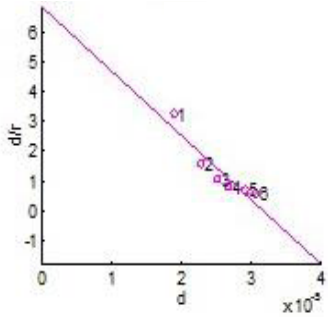
VI	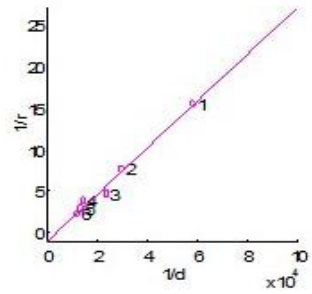	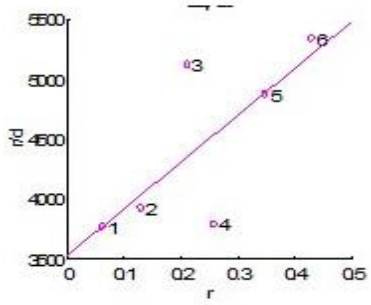	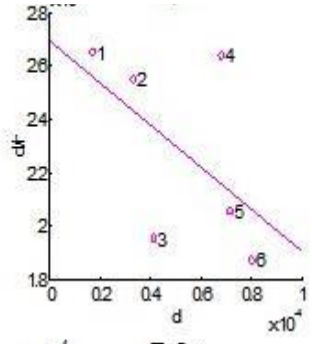
VII	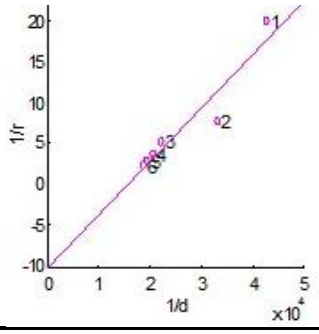	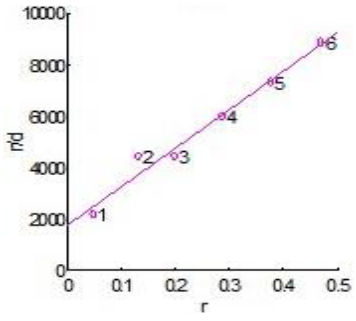	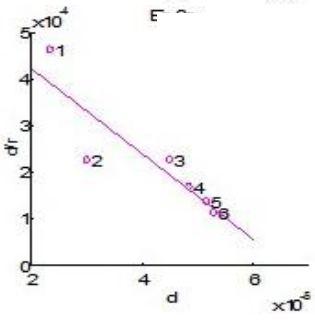

*** IV: Ketorolac, V: naproxen, VI: ketoprofen, VII: indoprofen**

Appendix 3

Appendix 3a: Protein Report for 2BXD obtained before preparation

Amino Acid Sequence from Available Structure

Chain A

SEVAHRFKDL GEENFKALVL IAFAQYLQQC PFEDHVKLVN EVTEFAKTCV
ADESAENCDK SLHTLFGDKL CTVATLRETY GEMADCCAKQ EPERNECFLQ
HKDDNPNLPR LVRPEVDVMC TAFHDNEETF LKKYLYEIAR RHPYFYAPEL
LFFAKRYKAA FTECCQAADK AACLLPKLDE LRDEGKASSA KQRLKCASLQ
KFGERAFKAW AVARLSQRFP KAEFAEVSKL VTDLTKVHTE CCHGDLLECA
DDRADLAKYI CENQDSISSK LKECCEKPLL EKSHCIAEVE NDEMPADLPS
LAADFVESKD VCKNYAEAKD VFLGMFLYEY ARRHPDYSVV LLLRLAKTYE
TTLEKCCAAA DPHECYAKVF DEFKPLVEEP QNLIKQNCEL FEQLGEYKFQ
NALLVRYTKK VPQVSTPTLV EVSRNLGKVG SKCCKHPEAK RMPCAEDYLS
VVLNQLCVLH EKTPVSDRVT KCCTESLVNR RPCFSALEVD ETYVPKEFNA
ETFTFHADIC TLSEKERQIK KQTALVELVK HKPKATKEQL KAVMDDFAAF
VEKCCKADDK ETCFAEEGKK LVAASQAA

Comparison of actual sequence versus PDB SEQRES records

Chains in SEQRES do not match structure - analysis may be faulty

Start of chain A appears to be missing - residues: ASP ALA HIS LYS

End of chain A appears to be missing - residues: LEU GLY LEU ASP ALA HIS LYS SER GLU VAL ALA HIS ARG PHE LYS ASP LEU GLY GLU GLU ASN PHE LYS ALA LEU VAL LEU ILE ALA PHE ALA GLN TYR LEU GLN GLN CYS PRO PHE GLU ASP HIS VAL LYS LEU VAL ASN GLU VAL THR GLU PHE ALA LYS THR CYS VAL ALA ASP GLU SER ALA GLU ASN CYS ASP LYS SER LEU HIS THR LEU PHE GLY ASP LYS LEU CYS THR VAL ALA THR LEU ARG GLU THR TYR GLY GLU MET ALA ASP CYS CYS ALA LYS GLN GLU PRO GLU ARG ASN GLU CYS PHE LEU GLN HIS LYS ASP ASP ASN PRO ASN LEU PRO ARG LEU VAL ARG PRO GLU VAL ASP VAL MET CYS THR ALA PHE HIS ASP ASN GLU GLU THR PHE LEU LYS LYS TYR LEU TYR GLU ILE ALA ARG ARG HIS PRO TYR PHE TYR ALA PRO GLU LEU LEU PHE PHE ALA LYS ARG TYR LYS ALA ALA PHE THR GLU CYS CYS GLN ALA ALA ASP LYS ALA ALA CYS LEU LEU PRO LYS LEU ASP GLU LEU ARG ASP GLU GLY LYS ALA SER SER ALA LYS GLN ARG LEU LYS CYS ALA SER LEU GLN LYS PHE GLY GLU ARG ALA PHE LYS ALA TRP ALA VAL ALA ARG LEU SER GLN ARG PHE PRO LYS ALA GLU PHE ALA GLU VAL SER LYS LEU VAL THR ASP LEU THR LYS VAL HIS THR GLU CYS CYS HIS GLY ASP LEU LEU GLU CYS ALA ASP ASP ARG ALA ASP LEU ALA LYS TYR ILE CYS GLU ASN GLN ASP SER ILE SER SER LYS LEU LYS GLU CYS CYS GLU LYS PRO LEU LEU GLU LYS SER HIS CYS ILE

ALA GLU VAL GLU ASN ASP GLU MET PRO ALA ASP LEU PRO SER LEU ALA ALA ASP PHE VAL GLU SER LYS ASP VAL CYS LYS ASN TYR ALA GLU ALA LYS ASP VAL PHE LEU GLY MET PHE LEU TYR GLU TYR ALA ARG ARG HIS PRO ASP TYR SER VAL VAL LEU LEULEU ARG LEU ALA LYS THR TYR GLU THR THR LEU GLU LYS CYS CYS ALA ALAALA ASP PRO HIS GLU CYS TYR ALA LYS VAL PHE ASP GLU PHE LYS PRO LEU VAL GLU GLU PRO GLN ASN LEU ILE LYS GLN ASN CYS GLU LEU PHE GLU GLN LEU GLY GLU TYR LYS PHE GLN ASN ALA LEU LEU VAL ARG TYR THR LYS LYS VAL PRO GLN VAL SER THR PRO THR LEU VAL GLU VAL SER ARG ASN LEU GLY LYS VAL GLY SER LYS CYS CYS LYS HIS PRO GLU ALA LYS ARG MET PRO CYS ALA GLU ASP TYR LEU SER VAL VAL LEU ASN GLN LEU CYS VAL LEU HIS GLU LYS THR PRO VAL SER ASP ARG VAL THR LYS CYS CYS THR GLU SER LEU VAL ASN ARG ARG PRO CYS PHE SER ALA LEU GLU VAL ASP GLU THR TYR VAL PRO LYS GLU PHE ASN ALA GLU THR PHE THR PHE HIS ALA ASP ILE CYS THR LEU SER GLU LYS GLU ARG GLN ILE LYS LYS GLN THR ALA LEU VAL GLU LEU VAL LYS HIS LYS PRO LYS ALA THR LYS GLU GLN LEU LYS ALA VAL MET ASP ASP PHE ALA ALA PHE VAL GLU LYS CYS CYS LYS ALA ASP ASP LYS GLU THR CYS PHE ALA GLU GLU GLY LYS LYS LEU VAL ALA ALA SER GLN ALA ALA LEU GLY LEU

Chain A:

SEVAHRFKDLGEENFKALVLIAFAQYLQQCPFEDHVKLVNEVTEFAKTCVADESAEN
CDKSLHTLFGDKLCTVATLRETYGEMADCCAKQEPERNECFLQHKDDNPNLPRLVR
PEVDVMCTAFHDNEETFLKKYLYEIARRHPYFYAPELLFFAKRYKAAFTECCQAADK
AACLLPKLDELRDEGKASSAKQRLKCASLQKFGERAFKAWAVARLSQRFPKAEFAE
VSKLVTDLTKVHTECCHGDLLECADDRADLAKYICENQDSISSKLKECCEKPLLEKS
HCIAEVENDEMPADLPSLAADFVESKDVCKNYAEAKDVFLGMFLYEYARRHPDYSV
VLLLRLAKTYETTLEKCCAAADPHECYAKVFDEFKPLVEEPQNLIKQNCELFEQLGE
YKFQNALLVRYTKKVPQVSTPTLVEVSRNLGKVGSKCCKHPEAKRMPCAEDYLSVV
LNQLCVLHEKTPVSDRVTKCCTESLVNRRPCFSALEVDETYVPKEFNAETFTFHADIC
TLSEKERQIKKQTALVELVKHKPKATKEQLKAVMDDFAAFVEKCCKADDKETCFAE
EGKKLVAASQA**A**

Appendix 3b. Protein properties

Electrostatic Energy (KJ/mol)	Relative Folding Energy	Electrostatic Energy (KJ/mol)	Relative Folding Energy
-13.92	-243.22	-12.32	-292.03
-13.86	-243.62	-12.29	-290.68
-13.80	-244.07	-12.26	-289.32
-13.75	-244.62	-12.23	-288.03
-13.69	-245.3	-12.20	-286.83
-13.63	-246.16	-12.17	-285.76
-13.57	-247.23	-12.14	-284.81
-13.51	-248.6	-12.11	-283.98
-13.46	-250.3	-12.08	-283.24
-13.40	-252.45	-12.06	-282.53
-13.34	-255.08	-12.03	-281.78
-13.29	-258.24	-12.00	-280.85
-13.23	-262.03	-11.98	-279.58
-13.18	-266.46	-11.95	-277.69
-13.13	-271.45	-11.92	-274.94
-13.08	-276.93	-11.90	-271.04
-13.03	-282.69	-11.88	-265.78
-12.98	-288.41	-11.85	-259.07
-12.93	-293.73	-11.83	-250.97
-12.89	-298.32	-11.81	-241.73
-12.84	-301.88	-11.79	-231.67
-12.80	-304.19	-11.77	-221.08
-12.76	-305.25	-11.75	-210.24
-12.72	-305.26	-11.73	-199.26
-12.68	-304.5	-11.72	-188.2
-12.64	-303.26	-11.70	-177.08
-12.61	-301.83	-11.69	-165.9
-12.57	-300.44	-11.67	-154.73
-12.54	-299.21	-11.66	-143.6
-12.51	-298.16	-11.65	-132.64
-12.47	-297.25	-11.64	-121.95
-12.44	-296.4	-11.63	-111.6
-12.41	-295.5	-11.62	-101.67
-12.38	-294.49	-11.61	-92.22
-12.35	-293.33		

Appendix 3b. Protein properties cont.....

3b(i): Graph of electrostatic energy and Relative Folding energy against pH

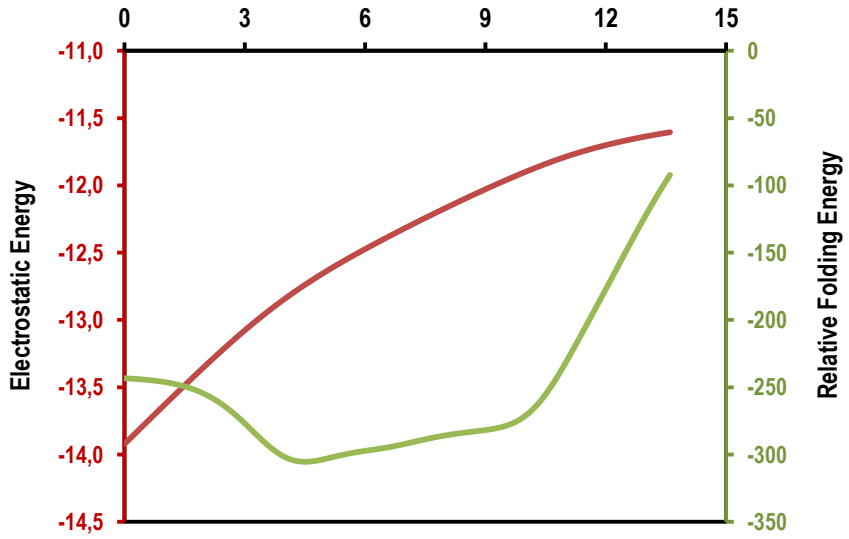

3b(ii): Graph of total charge and Relative Folding energy against pH

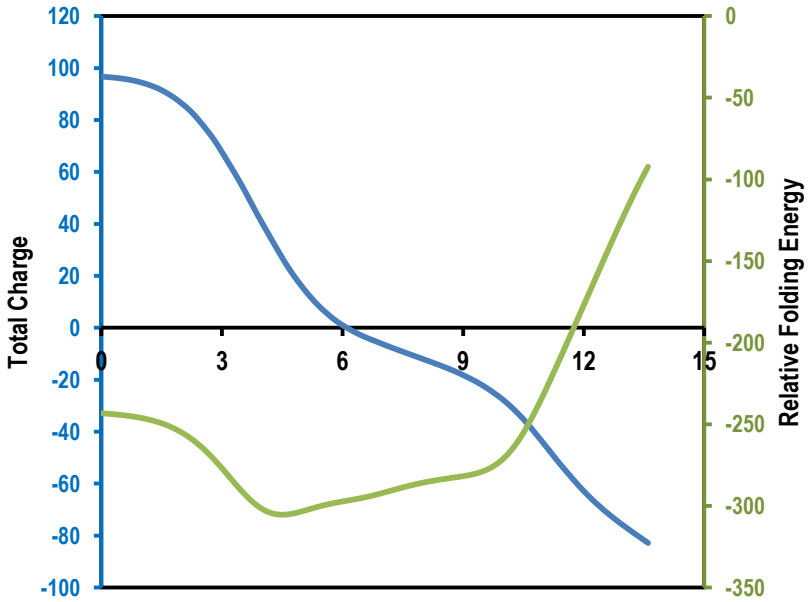

Appendix 3c. List of calculated pKa values of each residue in 2BXD protein

No.	Residues	pKa	Number	Residues	pKa	Number	Residues	pKa
1	A:SER5_NTR	8.625	36	A:ASP563	5.15	71	A:GLU321	4.901
2	A:ASP13	3.643	37	A:GLU6	3.055	72	A:GLU333	5.448
3	A:ASP38	3.226	38	A:GLU16	3.38	73	A:GLU354	4.319
4	A:ASP56	5.047	39	A:GLU17	3.713	74	A:GLU358	4.869
5	A:ASP63	3.011	40	A:GLU37	3.901	75	A:GLU368	4.283
6	A:ASP72	4.026	41	A:GLU45	4.065	76	A:GLU376	4.576
7	A:ASP89	3.037	42	A:GLU48	4.123	77	A:GLU382	4.098
8	A:ASP107	3.207	43	A:GLU57	4.227	78	A:GLU383	3.316
9	A:ASP108	1.349	44	A:GLU60	5.203	79	A:GLU393	3.942
10	A:ASP121	3.407	45	A:GLU82	4.109	80	A:GLU396	4.448
11	A:ASP129	3.314	46	A:GLU86	3.652	81	A:GLU400	3.748
12	A:ASP173	3.427	47	A:GLU95	3.342	82	A:GLU425	3.526
13	A:ASP183	3.505	48	A:GLU97	4.3	83	A:GLU442	2.992
14	A:ASP187	1.932	49	A:GLU100	4.562	84	A:GLU450	2.675
15	A:ASP237	2.951	50	A:GLU119	4.564	85	A:GLU465	3.995
16	A:ASP249	2.977	51	A:GLU131	4.526	86	A:GLU479	3.946
17	A:ASP255	4.785	52	A:GLU132	2.905	87	A:GLU492	3.613
18	A:ASP256	6.226	53	A:GLU141	4.305	88	A:GLU495	3.996
19	A:ASP259	2.76	54	A:GLU153	3.349	89	A:GLU501	4.011
20	A:ASP269	3.255	55	A:GLU167	3.761	90	A:GLU505	3.652
21	A:ASP296	3.52	56	A:GLU184	3.648	91	A:GLU518	3.844
22	A:ASP301	3.639	57	A:GLU188	3.137	92	A:GLU520	2.741
23	A:ASP308	3.603	58	A:GLU208	3.652	93	A:GLU531	4.821
24	A:ASP314	2.07	59	A:GLU227	4.066	94	A:GLU542	3.431
25	A:ASP324	2.767	60	A:GLU230	5.385	95	A:GLU556	4.185
26	A:ASP340	3.351	61	A:GLU244	0	96	A:GLU565	4.262
27	A:ASP365	3.591	62	A:GLU252	6.29	97	A:GLU570	4.392
28	A:ASP375	3.132	63	A:GLU266	4.824	98	A:GLU571	1.037
29	A:ASP451	4.846	64	A:GLU277	3.265	99	A:TYR30	14
30	A:ASP471	2.849	65	A:GLU280	4.28	100	A:TYR84	13.741
31	A:ASP494	2.008	66	A:GLU285	2.868	101	A:TYR138	14
32	A:ASP512	1.135	67	A:GLU292	2.43	102	A:TYR140	14
33	A:ASP549	3.303	68	A:GLU294	2.929	103	A:TYR148	12.007
34	A:ASP550	3.72	69	A:GLU297	3.421	104	A:TYR150	12.851
35	A:ASP562	3.644	70	A:GLU311	4.195	105	A:TYR161	14

Appendix 3c. List of calculated pKa values of each residue in 2BXD protein continued

Number	Residues	pKa	Number	Residues	pKa	Number	Residues	pKa
106	A:TYR263	13.294	143	A:LYS159	11.538	179	A:LYS524	9.893
107	A:TYR319	14	144	A:LYS162	11.392	180	A:LYS525	10.57
108	A:TYR332	13.507	145	A:LYS174	10.826	181	A:LYS534	12.673
109	A:TYR334	14	146	A:LYS181	11.571	182	A:LYS536	9.908
110	A:TYR341	13.402	147	A:LYS190	9.505	183	A:LYS538	10.793
111	A:TYR353	14	148	A:LYS195	10.732	184	A:LYS541	9.719
112	A:TYR370	14	149	A:LYS199	10.316	185	A:LYS545	10.847
113	A:TYR401	12.043	150	A:LYS205	9.807	186	A:LYS557	10.54
114	A:TYR411	12.001	151	A:LYS212	11.483	187	A:LYS560	11.321
115	A:TYR452	14	152	A:LYS225	11.471	188	A:LYS564	11.01
116	A:TYR497	14	153	A:LYS233	12.133	189	A:LYS573	10.819
117	A:CYS34	11.774	154	A:LYS240	14	190	A:LYS574	12.602
118	A:HIS9	6.847	155	A:LYS262	12.142	191	A:ARG10	14
119	A:HIS39	8.034	156	A:LYS274	11.707	192	A:ARG81	14
120	A:HIS67	6.276	157	A:LYS276	11.064	193	A:ARG98	14
121	A:HIS105	8.495	158	A:LYS281	11.509	194	A:ARG114	14
122	A:HIS128	7.038	159	A:LYS286	11.289	195	A:ARG117	14
123	A:HIS146	3.731	160	A:LYS313	10.967	196	A:ARG144	14
124	A:HIS242	6.218	161	A:LYS317	12.329	197	A:ARG145	14
125	A:HIS247	8.617	162	A:LYS323	11.396	198	A:ARG160	14
126	A:HIS288	7.837	163	A:LYS351	9.673	199	A:ARG186	13.377
127	A:HIS338	7.568	164	A:LYS359	10.793	200	A:ARG197	14
128	A:HIS367	7.167	165	A:LYS372	11.402	201	A:ARG209	14
129	A:HIS440	5.647	166	A:LYS378	11.089	202	A:ARG218	14
130	A:HIS464	5.928	167	A:LYS389	10.764	203	A:ARG222	14
131	A:HIS510	7.711	168	A:LYS402	8.757	204	A:ARG257	14
132	A:HIS535	6.347	169	A:LYS413	11.2	205	A:ARG336	14
133	A:LYS12	11.865	170	A:LYS414	11.93	206	A:ARG337	14
134	A:LYS20	12.005	171	A:LYS432	10.787	207	A:ARG348	14
135	A:LYS41	11.584	172	A:LYS436	9.693	208	A:ARG410	14
136	A:LYS51	12.134	173	A:LYS439	11.253	209	A:ARG428	14
137	A:LYS64	11.11	174	A:LYS444	10.825	210	A:ARG445	14
138	A:LYS73	10.534	175	A:LYS466	9.865	211	A:ARG472	14
139	A:LYS93	11.319	176	A:LYS475	10.501	212	A:ARG484	14
140	A:LYS106	13.409	177	A:LYS500	10.759	213	A:ARG485	14
141	A:LYS136	11.403	178	A:LYS519	9.38	214	A:ARG521	14
142	A:LYS137	10.759						

Appendix 3d: List of 72 residues for which side chain were completed.

Number	Residue	Number	Residue	Number	Residue
1	A:LYS12	26	A:LYS205	51	A:GLU505
2	A:GLN33	27	A:ARG209	52	A:PHE509
3	A:ASP56	28	A:LYS240	53	A:HIS510
4	A:GLU60	29	A:LYS276	54	A:ILE513
5	A:LEU69	30	A:GLU277	55	A:LEU516
6	A:LYS73	31	A:GLU294	56	A:LYS519
7	A:ARG81	32	A:GLU297	57	A:GLU520
8	A:GLU82	33	A:ASP301	58	A:LYS524
9	A:TYR84	34	A:LYS313	59	A:LYS536
10	A:GLU86	35	A:LYS317	60	A:LYS538
11	A:GLN94	36	A:GLU321	61	A:LYS541
12	A:GLU95	37	A:LYS351	62	A:LYS545
13	A:GLU97	38	A:LYS359	63	A:LYS560
14	A:GLN104	39	A:LYS372	64	A:ASP562
15	A:ASN111	40	A:LYS378	65	A:LYS564
16	A:ARG114	41	A:GLU382	66	A:GLU565
17	A:GLU119	42	A:LYS389	67	A:PHE568
18	A:ASP121	43	A:GLN390	68	A:GLU570
19	A:GLU132	44	A:GLN397	69	A:LYS573
20	A:LYS137	45	A:LYS402	70	A:LYS574
21	A:LYS159	46	A:LYS432	71	A:LEU575
22	A:GLN170	47	A:LYS436	72	A:GLN580
23	A:LYS174	48	A:LYS439		
24	A:LEU178	49	A:LYS444		
25	A:LYS190	50	A:LYS466		

Appendix 3e: properties of ligands

Index	Name	#PHAC	$PADSC	MMFF94_energy	Shape-Self Ovelap	Shape_Volume	
1	3335	19	0	52.29	801.52	205.80	Prepared
2	3342	18	0	56.42	757.16	194.00	Prepared
3	3394	18	0	50.02	759.57	193.40	Prepared
4	3826	19	0	56.35	816.46	199.40	Prepared
5	3825	19	0	58.87	805.42	204.00	Prepared
6	156391	17	1	54.48	715.96	183.50	Prepared
7	114864	15	1	33.43	605.09	172.20	Prepared
8	181818	19	1	55.81	816.33	199.50	Rejected
9	180540	19	1	58.86	805.33	204.00	Rejected
10	3672	15	0	33.43	605.09	172.20	Rejected
11	3718	21	0	67.02	901.28	220.10	Prepared
12	3718	21	0	67.02	901.28	220.10	Prepared
13	39912	15	1	32.43	603.78	172.70	Prepared
14	68700	21	1	66.87	901.21	220.10	Prepared
15	181817	19	1	55.80	816.26	199.50	Prepared
16	667550	19	1	58.93	805.91	204.10	Prepared

#PHAC: Pubchem Heavy Atom Count; $PADSC: Pubchem Atom Dif Stereo Count

Index	Name	ALogP	Molecular Weight	H-Acceptors	Rotatable Bonds	Rings	Aromatic Rings	*MFPSA
1	3335	1.459	253.273	3	5	2	2	0.216
2	3342	2.043	241.262	3	4	2	2	0.195
3	3394	2.206	243.253	2	3	2	2	0.158
4	3826	1.358	254.261	3	3	3	2	0.246
5	3825	1.887	253.273	3	4	2	2	0.214
6	156391	1.375	229.251	3	3	2	2	0.2
7	114864	2.133	205.273	2	4	1	1	0.164
8	3718	1.227	280.298	3	3	3	2	0.212
9	39912	2.133	205.273	2	4	1	1	0.164
10	68700	1.227	280.298	3	3	3	2	0.212
11	181817	1.358	254.261	3	3	3	2	0.246
12	667550	1.887	253.273	3	4	2	2	0.214

***MFPSA: Molecular Fraction Polar Surface Area**

Ligand Scoring results

Index	Name	Ligscore 1	Ligscore 2	PLP	PLP	Jain	PMF	PMF04
1	3335	-999.9	-999.9	-774.45	-537.35	0.22	-321.13	-382.86
2	3342	-999.9	-999.9	-695.97	-472.59	0.72	-294.35	-328.04
3	3394	-999.9	-999.9	-773.29	-515.33	0.03	-339.53	-349.72
4	3826	-999.9	-999.9	-754.87	-501.25	1.73	-333.63	-340.5
5	3825	-999.9	-999.9	-757.4	-522.44	-0.28	-326.91	-355.58
6	156391	-999.9	-999.9	-579.61	-399.26	-2.46	-275.75	-251.11
7	114864	-999.9	-999.9	-615.47	-387.74	-1.03	-310.19	-299.43
8	3718	-999.9	-999.9	-465.31	-307.6	2.81	-233.69	-261.7
9	39912	-999.9	-999.9	-587.52	-400.57	-0.39	-307.71	-278.23
10	68700	-999.9	-999.9	-490.18	-325.77	2.52	-244.05	-261.55
11	181817	-999.9	-999.9	-572.89	-377.94	2.14	-272.58	-261.66
12	667550	-999.9	-999.9	-715.24	-486.46	1.66	-325.07	-346.29

Appendix 3f: Frequency Data Obtained For Atom

Residue	Favorable	Unfavorable	Hydrogen bonds	Charge	Hydrophibic	Halogen	Other
A:ASP108:OD1	1	0	1	0	0	0	0
A:LYS190:O	0	7	0	0	0	0	0
A:LYS190:CB	2	0	0	0	2	0	0
A:LYS190:CG	2	0	0	0	2	0	0
A:LYS190:CD	2	0	0	0	2	0	0
A:ALA191:O	1	6	0	0	0	1	0
A:ALA191:CB	5	0	0	0	5	0	0
A:ALA191:CA	0	1	0	0	0	0	0
A:ALA191:HA	3	1	3	0	0	0	0
A:ALA191:C	0	2	0	0	0	0	0
A:SER192:C	2	0	0	0	2	0	0
A:SER192:O	3	0	0	0	2	1	0
A:SER192:HA	1	0	1	0	0	0	0
A:SER193:N	2	0	0	0	2	0	0
A:SER193:HG	1	0	1	0	0	0	0
A:SER193:O	3	4	0	0	0	0	3
A:SER193:C	1	4	0	0	0	1	0
A:ALA194:HN	0	7	0	0	0	0	0
A:ALA194:O	0	12	0	0	0	0	0
A:ALA194:C	0	12	0	0	0	0	0
A:ALA194:HB3	0	11	0	0	0	0	0
A:ALA194:HB2	0	12	0	0	0	0	0
A:ALA194:HB1	0	12	0	0	0	0	0
A:ALA194:CB	10	12	0	0	10	0	0
A:ALA194:HA	0	12	0	0	0	0	0
A:ALA194:CA	0	12	0	0	0	0	0
A:ALA194:N	0	12	0	0	0	0	0
A:LYS195:HG2	0	3	0	0	0	0	0
A:LYS195:CB	5	4	0	0	5	0	0
A:LYS195:CG	5	4	0	0	5	0	0
A:LYS195:CD	5	1	0	0	5	0	0
A:LYS195:HD2	0	1	0	0	0	0	0
A:LYS195:N	0	11	0	0	0	0	0
A:LYS195:HD1	0	1	0	0	0	0	0
A:LYS195:HG1	0	4	0	0	0	0	0
A:LYS195:HB2	0	2	0	0	0	0	0
A:LYS195:HB1	0	1	0	0	0	0	0
A:LYS195:HA	0	7	0	0	0	0	0
A:LYS195:NZ	1	0	0	1	0	0	0
A:LYS195:HN	0	7	0	0	0	0	0
A:LYS195:O	1	7	0	0	1	0	0
A:LYS195:C	1	10	0	0	1	0	0
A:LYS195:CA	0	10	0	0	0	0	0
A:GLN196:HN	0	1	0	0	0	0	0
A:GLN196:CA	0	1	0	0	0	0	0
A:GLN196:N	1	4	0	0	1	0	0

Appendix 3f. cont...

Residue	Favorable	Unfavorable	Hydrogen bonds	Charge	Hydrophibic	Halogen	Other
A:GLN196:C	0	5	0	0	0	0	0
A:GLN196:O	1	3	0	0	0	0	1
A:ARG197:CG	9	7	0	0	9	0	0
A:ARG197:CB	9	10	0	0	9	0	0
A:ARG197:HD1	0	2	0	0	0	0	0
A:ARG197:HB2	0	4	0	0	0	0	0
A:ARG197:N	0	7	0	0	0	0	0
A:ARG197:HN	0	5	0	0	0	0	0
A:ARG197:CA	0	7	0	0	0	0	0
A:ARG197:HA	0	3	0	0	0	0	0
A:ARG197:HB1	0	11	0	0	0	0	0
A:ARG197:C	0	8	0	0	0	0	0
A:ARG197:HG1	0	2	0	0	0	0	0
A:ARG197:HG2	0	6	0	0	0	0	0
A:ARG197:CD	0	3	0	0	0	0	0
A:ARG197:O	0	5	0	0	0	0	0
A:LEU198:HB2	0	2	0	0	0	0	0
A:LEU198:HB1	0	4	0	0	0	0	0
A:LEU198:HA	0	1	0	0	0	0	0
A:LEU198:CB	3	5	0	0	3	0	0
A:LEU198:CD2	3	0	0	0	3	0	0
A:LEU198:CD1	3	0	0	0	3	0	0
A:LEU198:CG	3	1	0	0	3	0	0
A:LEU198:N	0	8	0	0	0	0	0
A:LEU198:HN	0	8	0	0	0	0	0
A:LEU198:CA	0	6	0	0	0	0	0
A:LEU198:C	0	4	0	0	0	0	0
A:LYS199:N	0	3	0	0	0	0	0
A:LYS199:HN	0	3	0	0	0	0	0
A:LYS199:CB	4	0	0	0	4	0	0
A:LYS199:CD	4	0	0	0	4	0	0
A:LYS199:NZ	2	0	0	2	0	0	0
A:LYS199:CG	4	0	0	0	4	0	0
A:CYS200:SG	2	0	0	0	2	0	0
A:CYS200:CB	2	0	0	0	2	0	0
A:ALA201:CB	1	0	0	0	1	0	0
A:LYS432:NZ	2	0	0	2	0	0	0
A:LYS436:NZ	1	0	0	1	0	0	0
A:VAL455:HG23	0	2	0	0	0	0	0
A:VAL455:HG22	0	2	0	0	0	0	0
A:VAL455:CB	10	0	0	0	10	0	0
A:VAL455:CG1	10	4	0	0	10	0	0
A:VAL455:CG2	10	2	0	0	10	0	0
A:VAL455:HG11	0	4	0	0	0	0	0
A:VAL455:HG12	0	1	0	0	0	0	0
A:VAL455:HG13	0	4	0	0	0	0	0

Appendix 3g. Frequency Data Obtained For Residue

Amino Acid	Favorable	Unfavorable	Hydrogen bonds	Charge	Hydrophibic	Halogen	Other
A:ASP108	1	0	1	0	0	0	0
A:LYS190	2	7	0	0	2	0	0
A:ALA191	8	6	3	0	5	1	0
A:SER192	4	0	1	0	2	1	0
A:SER193	4	5	1	0	0	1	3
A:ALA194	10	12	0	0	10	0	0
A:LYS195	6	11	0	1	6	0	0
A:GLN196	1	7	0	0	0	0	1
A:ARG197	9	12	0	0	9	0	0
A:LEU198	3	8	0	0	3	0	0
A:LYS199	6	3	0	2	4	0	0
A:CYS200	2	0	0	0	2	0	0
A:ALA201	1	0	0	0	1	0	0
A:LYS432	2	0	0	2	0	0	0
A:LYS436	1	0	0	1	0	0	0
A:VAL455	10	6	0	0	10	0	0
A:ASN458	0	1	0	0	0	0	0
A:GLN459	0	1	0	0	0	0	0

Appendix 3h: Statistical Residue Analysis

Statistical Residue Analysis

Total Interaction Count

Favorable	Unfavorable	HydrogenBond	Charge	Hydrophobic	Halogen	Other
70	79	6	6	54	3	4

Top 5 Residues with Favorable Interactions (6)

Residue	Favorable	Unfavorable	HydrogenBond	Charge	Hydrophobic	Halogen	Other
A:VAL455	10	6	0	0	10	0	0
A:ALA194	10	12	0	0	10	0	0
A:ARG197	9	12	0	0	9	0	0
A:ALA191	8	6	3	0	5	1	0
A:LYS195	6	11	0	1	6	0	0
A:LYS199	6	3	0	2	4	0	0

Top 5 Residues with Unfavorable Interactions (6)

Residue	Unfavorable	Favorable	HydrogenBond	Charge	Hydrophobic	Halogen	Other
A:ALA194	12	10	0	0	10	0	0
A:ARG197	12	9	0	0	9	0	0
A:LYS195	11	6	0	1	6	0	0
A:LEU198	8	3	0	0	3	0	0
A:LYS190	7	2	0	0	2	0	0
A:GLN196	7	1	0	0	0	0	1

Top 5 Residues with HydrogenBond Interactions (4)

Residue	HydrogenBond	Unfavorable	Favorable	Charge	Hydrophobic	Halogen	Other
A:ALA191	3	6	8	0	5	1	0
A:ASP108	1	0	1	0	0	0	0
A:SER192	1	0	4	0	2	1	0
A:SER193	1	5	4	0	0	1	3

Top 5 Residues with Charge Interactions (4)

Residue	Charge	Unfavorable	HydrogenBond	Favorable	Hydrophobic	Halogen	Other
A:LYS432	2	0	0	2	0	0	0
A:LYS199	2	3	0	6	4	0	0
A:LYS436	1	0	0	1	0	0	0
A:LYS195	1	11	0	6	6	0	0

Top 5 Residues with Hydrophobic Interactions (5)

Residue	Hydrophobic	Unfavorable	HydrogenBond	Charge	Favorable	Halogen	Other
A:ALA194	10	12	0	0	10	0	0
A:VAL455	10	6	0	0	10	0	0
A:ARG197	9	12	0	0	9	0	0
A:LYS195	6	11	0	1	6	0	0
A:ALA191	5	6	3	0	8	1	0

Top 5 Residues with Halogen Interactions (3)

Residue	Halogen	Unfavorable	HydrogenBond	Charge	Hydrophobic	Favorable	Other
A:ALA191	1	6	3	0	5	8	0
A:SER192	1	0	1	0	2	4	0
A:SER193	1	5	1	0	0	4	3

Top 5 Residues with Other Interactions (2)

Residue	Other	Unfavorable	HydrogenBond	Charge	Hydrophobic	Halogen	Favorable
A:SER193	3	5	1	0	0	1	4
A:GLN196	1	7	0	0	0	0	1